Constraints on Gravitational Waves from the 2024 Vela Pulsar Glitch

Downloaded from: https://research.chalmers.se, 2026-11-10 05:56 UTC

Citation for the original published paper (version of record):
Abac, A., Abouelfettouh, I., Acernese, F. et al (2026). Constraints on Gravitational Waves from the 2024 Vela Pulsar Glitch. Astrophysical Journal, 1005(1). http://dx.doi.org/10.3847/1538-4357/ae63bc

N.B. When citing this work, cite the original published paper.

research.chalmers.se offers the possibility of retrieving research publications produced at Chalmers University of Technology. It covers all kind of research output: articles, dissertations, conference papers, reports etc. since 2004. research.chalmers.se is administrated and maintained by Chalmers Library

(article starts on next page)

The Astrophysical Journal, 1005:12 (40pp), 2026 July 1 https://doi.org/10.3847/1538-4357/ae63bc
© 2026. The Author(s). Published by the American Astronomical Society.
OPEN ACCESS

Constraints on Gravitational Waves from the 2024 Vela Pulsar Glitch

A. G. Abac[1], I. Abouelfettouh[2], F. Acernese[3,4], K. Ackley[5], C. Adamcewicz[6], S. Adhicary[7], D. Adhikari[8,9], N. Adhikari[10], R. X. Adhikari[11], V. K. Adkins[12], S. Afroz[13], A. Agapito[14], D. Agarwal[15], M. Agathos[16], N. Aggarwal[17], S. Aggarwal[18], O. D. Aguiar[19], I.-L. Ahrend[20], L. Aiello[21,22], A. Ain[23], P. Ajith[24], T. Akutsu[25,26], S. Albanesi[27,28], W. Ali[29,30], S. Al-Kershi[8,9], C. Alléné[31], A. Allocca[4,32], S. Al-Shammari[33], P. A. Altin[34], S. Alvarez-Lopez[35], O. Amarasinghe[33], A. Amato[36,37], F. Amicucci[38,39], C. Amra[40], A. Ananyeva[11], S. B. Anderson[11], W. G. Anderson[11], M. Andia[41], M. Ando[42], M. Andrés-Carcasona[43], T. Andrić[8,9,44,45], J. Anglin[46], S. Ansoldi[47,48], J. M. Antelis[49], S. Antier[41], M. Aoumi[50], E. Z. Appavuravther[51,52], S. Appert[11], S. K. Apple[53], K. Arai[11], A. Araya[42], M. C. Araya[11], M. Arca Sedda[44,45], J. S. Areeda[54], N. Aritomi[2], F. Armato[29,30], S. Armstrong[55], N. Arnaud[56], M. Arogeti[57], S. M. Aronson[12], G. Ashton[58], Y. Aso[25,59], L. Asprea[28], M. Assiduo[60,61], S. Assis de Souza Melo[62], S. M. Aston[63], P. Astone[38], F. Attadio[38,39], F. Aubin[64], K. AultONeal[65], G. Avallone[66], E. A. Avila[49], S. Babak[20], C. Badger[67], S. Bae[68], S. Bagnasco[28], L. Baiotti[69], R. Bajpai[70], T. Baka[37,71], A. M. Baker[6], K. A. Baker[72], T. Baker[73], G. Baldi[74,75], N. Baldicchi[51,76], M. Ball[77], G. Ballardin[62], S. W. Ballmer[78], S. Banagiri[6], B. Banerjee[44], D. Bankar[79], T. M. Baptiste[12], P. Baral[10], M. Baratti[80,81], J. C. Barayoga[11], B. C. Barish[11], D. Barker[2], N. Barman[79], P. Barneo[82,83,84], F. Barone[4,85], B. Barr[86], L. Barsotti[35], M. Barsuglia[20], D. Barta[87], A. M. Bartoletti[88], M. A. Barton[86], I. Bartos[46], A. Basalaev[8,9], R. Bassiri[89], A. Basti[80,81], M. Bawaj[51,76], P. Baxi[90], J. C. Bayley[86], A. C. Baylor[10], P. A. Baynard II[57], M. Bazzan[91,92], V. M. Bedakihale[93], F. Beirnaert[94], M. Bejger[95], D. Belardinelli[22], A. S. Bell[86], D. S. Bellie[96], L. Bellizzi[80,81], W. Benoit[18], I. Bentara[56], J. D. Bentley[97], M. Ben Yaala[55], S. Bera[98,99], F. Bergamin[33], B. K. Berger[89], S. Bernuzzi[27], M. Beroiz[11], D. Bersanetti[29], T. Bertheas[100], A. Bertolini[36,37], J. Betzwieser[63], D. Beveridge[72], G. Bevilacqua[101], N. Bevins[102], R. Bhandare[103], R. Bhatt[11], D. Bhattacharjee[104,105], S. Bhattacharyya[106], S. Bhaumik[46], V. Biancalana[101], A. Bianchi[37,107], I. A. Bilenko[108], G. Billingsley[11], A. Binetti[109], S. Bini[11,74,75], C. Binu[110], S. Biot[111], O. Birnholtz[112], S. Biscoveanu[96], A. Bisht[9], M. Bitossi[62,80], M.-A. Bizouard[113], S. Blaber[114], J. K. Blackburn[11], L. A. Blagg[77], C. D. Blair[63,72], D. G. Blair[72], N. Bode[8,9], N. Boettner[97], G. Boileau[113], M. Boldrini[38], G. N. Bolingbroke[115], A. Bolliand[40,116], L. D. Bonavena[46], R. Bondarescu[82], F. Bondu[117], E. Bonilla[89], M. S. Bonilla[54], A. Bonino[118], R. Bonnand[31,116], A. Borchers[8,9], V. Boschi[80], S. Bose[119], V. Bossilkov[63], Y. Bothra[37,107], A. Boudon[56], L. Bourg[57], M. Boyle[120], A. Bozzi[62], C. Bradaschia[80], P. R. Brady[10], A. Branch[63], M. Branchesi[44,45], I. Braun[104], T. Briant[121], A. Brillet[113,327], M. Brinkmann[8,9], P. Brockill[10], E. Brockmueller[8,9], A. F. Brooks[11], B. C. Brown[46], D. D. Brown[115], M. L. Brozzetti[51,76], S. Brunett[11], G. Bruno[15], R. Bruntz[122], J. Bryant[118], Y. Bu[123], F. Bucci[61], J. Buchanan[122], O. Bulashenko[82,83], T. Bulik[124], H. J. Bulten[37], A. Buonanno[1,125], K. Burtnyk[2], R. Buscicchio[126,127], D. Buskulic[31], C. Buy[100], R. L. Byer[89], G. S. Cabourn Davies[73], R. Cabrita[15], V. Cáceres-Barbosa[7], L. Cadonati[57], G. Cagnoli[128], C. Cahillane[78], A. Calafat[98], T. A. Callister[129], E. Calloni[4,32], S. R. Callos[77], M. Canepa[29,30], G. Caneva Santoro[43], K. C. Cannon[42], H. Cao[35], L. A. Capistran[130], E. Capocasa[20], E. Capote[2,11], G. Capurri[80,81], G. Carapella[66,131], F. Carbognani[62], M. Carlassara[8,9], J. B. Carlin[123], T. K. Carlson[132], M. F. Carney[104], M. Carpinelli[62,126], G. Carrillo[77], J. J. Carter[8,9], G. Carullo[118,133], A. Casallas-Lagos[134], J. Casanueva Diaz[62], C. Casentini[22,135], S. Y. Castro-Lucas[136], S. Caudill[132], M. Cavaglià[105], R. Cavalieri[62], A. Ceja[54], G. Cella[80], P. Cerdá-Durán[137,138], E. Cesarini[22], N. Chabbra[34], W. Chaibi[113], A. Chakraborty[13], P. Chakraborty[8,9], S. Chakraborty[103], S. Chalathadka Subrahmanya[97], J. C. L. Chan[139], M. Chan[114], K. Chang[140], S. Chao[140,141], P. Charlton[142], E. Chassande-Mottin[20], C. Chatterjee[143], Debarati Chatterjee[79], Deep Chatterjee[35], M. Chaturvedi[103], S. Chaty[20], A. Chen[144], A. H.-Y. Chen[145], D. Chen[146], H. Chen[141], H. Y. Chen[147], S. Chen[143], Yanbei Chen[148], Yitian Chen[120], H. P. Cheng[149], P. Chessa[51,76], H. T. Cheung[90], S. Y. Cheung[6], F. Chiadini[131,150], G. Chiarini[8,9,92], A. Chiba[151], A. Chincarini[29], M. L. Chiofalo[80,81], A. Chiummo[4,62], C. Chou[145], S. Choudhary[72], N. Christensen[113,152], S. S. Y. Chua[34], G. Ciani[74,75], P. Ciecielag[95], M. Cieślar[124], M. Cifaldi[22], B. Cirok[153], F. Clara[2], J. A. Clark[11,57], T. A. Clarke[6], P. Clearwater[154], S. Clesse[111], F. Cleva[113,116], E. Coccia[43,44,45], E. Codazzo[155,156], P.-F. Cohadon[121], S. Colace[30], E. Colangeli[73], M. Colleoni[98], C. G. Collette[157], J. Collins[63], S. Colloms[86], A. Colombo[127,158], C. M. Compton[2], G. Connolly[77], L. Conti[92], T. R. Corbitt[12], I. Cordero-Carrión[159], S. Corezzi[51,76], N. J. Cornish[160], I. Coronado[161], A. Corsi[162], R. Cottingham[63], M. W. Coughlin[18], A. Couineaux[38], P. Couvares[11,57], D. M. Coward[72], R. Coyne[163], A. Cozzumbo[44], J. D. E. Creighton[10], T. D. Creighton[164], P. Cremonese[98], S. Crook[63], R. Crouch[2], J. Csizmazia[2], J. R. Cudell[165], T. J. Cullen[11], A. Cumming[86], E. Cuoco[166,167], M. Cusinato[137], L. V. Da Conceição[168], T. Dal Canton[41], S. Dal Pra[169], G. Dálya[100], B. D'Angelo[29], S. Danilishin[36,37], S. D'Antonio[38], K. Danzmann[8,9], K. E. Darroch[122], L. P. Dartez[63], R. Das[106], A. Dasgupta[93], V. Dattilo[62], A. Daumas[20], N. Davari[170,171], I. Dave[103], A. Davenport[136], M. Davier[41], T. F. Davies[72], D. Davis[11], L. Davis[72], M. C. Davis[18], P. Davis[172,173], E. J. Daw[174], M. Dax[1], J. De Bolle[94], M. Deenadayalan[79], J. Degallaix[175], M. De Laurentis[4,32], F. De Lillo[23], S. Della Torre[127], W. Del Pozzo[80,81], A. Demagny[31], F. De Marco[38,39], G. Demasi[61,176], F. De Matteis[21,22], N. Demos[35], T. Dent[177], A. Depasse[15], N. DePergola[102], R. De Pietri[178,179], R. De Rosa[4,32],

C. De Rossi[62], M. Desai[35], R. DeSalvo[180], A. DeSimone[181], R. De Simone[131,150], A. Dhani[1], R. Diab[46], M. C. Díaz[164], M. Di Cesare[4,32], G. Dideron[182], T. Dietrich[1], L. Di Fiore[4], C. Di Fronzo[72], M. Di Giovanni[38,39], T. Di Girolamo[4,32], D. Diksha[36,37], J. Ding[20,183], S. Di Pace[38,39], I. Di Palma[38,39], D. Di Piero[48,184], F. Di Renzo[56], Divyajyoti[33], A. Dmitriev[118], J. P. Docherty[86], Z. Doctor[96], N. Doerksen[168], E. Dohmen[2], A. Doke[132], A. Domiciano De Souza[185], L. D'Onofrio[38], F. Donovan[35], K. L. Dooley[33], T. Dooney[71], S. Doravari[79], O. Dorosh[186], W. J. D. Doyle[122], M. Drago[38,39], J. C. Driggers[2], L. Dunn[123], U. Dupletsa[44], P.-A. Duverne[20], D. D'Urso[155,170], P. Dutta Roy[46], H. Duval[187], S. E. Dwyer[2], C. Eassa[2], M. Ebersold[31,188], T. Eckhardt[97], G. Eddolls[78], A. Effler[63], J. Eichholz[34], H. Einsle[113], M. Eisenmann[25], M. Emma[58], K. Endo[151], R. Enficiaud[1], L. Errico[4,32], R. Espinosa[164], M. Esposito[4,32], R. C. Essick[189], H. Estellés[1], T. Etzel[11], M. Evans[35], T. Evstafyeva[182], B. E. Ewing[7], J. M. Ezquiaga[139], F. Fabrizi[60,61], V. Fafone[21,22], S. Fairhurst[33], A. M. Farah[129], B. Farr[77], W. M. Farr[190,191], G. Favaro[91], M. Favata[192], M. Fays[165], M. Fazio[55], J. Feicht[11], M. M. Fejer[89], R. Felicetti[48,184], E. Fenyvesi[87,193], J. Fernandes[194], T. Fernandes[137,195], D. Fernando[110], S. Ferraiuolo[38,39,196], T. A. Ferreira[12], M. Ferrer[98], F. Fidecaro[80,81], P. Figura[95], A. Fiori[80,81], I. Fiori[62], M. Fishbach[189], R. P. Fisher[122], R. Fittipaldi[131,197], V. Fiumara[131,198], R. Flaminio[31], S. M. Fleischer[199], L. S. Fleming[200], E. Floden[18], H. Fong[114], J. A. Font[137,138], F. Fontinele-Nunes[18], C. Foo[1], B. Fornal[201], K. Franceschetti[178], F. Frappez[31], S. Frasca[38,39], F. Frasconi[80], J. P. Freed[65], Z. Frei[202], A. Freise[37,107], O. Freitas[137,195], R. Frey[77], W. Frischhertz[63], P. Fritschel[35], V. V. Frolov[63], G. G. Fronzé[28], M. Fuentes-Garcia[11], S. Fujii[203], T. Fujimori[204], P. Fulda[46], M. Fyffe[63], B. Gadre[71], J. R. Gair[1], S. Galaudage[185], V. Galdi[205], R. Gamba[7], A. Gamboa[1], S. Gamoji[180], D. Ganapathy[206], A. Ganguly[79], B. Garaventa[29], J. García-Bellido[207], C. García-Quirós[188], J. W. Gardner[34], K. A. Gardner[114], S. Garg[42], J. Gargiulo[62], X. Garrido[41], A. Garron[98], F. Garufi[4,32], P. A. Garver[89], C. Gasbarra[21,22], B. Gateley[2], F. Gautier[208], V. Gayathri[10], T. Gayer[78], G. Gemme[29], A. Gennai[80], V. Gennari[100], J. George[103], R. George[147], O. Gerberding[97], L. Gergely[153], Archisman Ghosh[94], Sayantan Ghosh[194], Shaon Ghosh[192], Shrobana Ghosh[8,9], Suprovo Ghosh[209], Tathagata Ghosh[79], J. A. Giaime[12,63], K. D. Giardina[63], D. R. Gibson[200], C. Gier[55], S. Gkaitatzis[80,81], J. Glanzer[11], F. Glotin[41], J. Godfrey[77], R. V. Godley[8,9], P. Godwin[11], A. S. Goettel[33], E. Goetz[114], J. Golomb[11], S. Gomez Lopez[38,39], B. Goncharov[44], G. González[12], P. Goodarzi[210], S. Goode[6], A. W. Goodwin-Jones[15], M. Gosselin[62], R. Gouaty[31], D. W. Gould[34], K. Govorkova[35], A. Grado[51,76], V. Graham[86], A. E. Granados[18], M. Granata[175], V. Granata[131,211], S. Gras[35], P. Grassia[11], J. Graves[57], C. Gray[2], R. Gray[86], G. Greco[51], A. C. Green[37,107], L. Green[212], S. M. Green[73], S. R. Green[213], C. Greenberg[132], A. M. Gretarsson[65], H. K. Griffin[18], D. Griffith[11], H. L. Griggs[57], G. Grignani[51,76], C. Grimaud[31], H. Grote[33], S. Grunewald[1], D. Guerra[137], D. Guetta[214], G. M. Guidi[60,61], A. R. Guimaraes[12], H. K. Gulati[93], F. Gulminelli[172,173], H. Guo[144], W. Guo[72], Y. Guo[36,37], Anuradha Gupta[215], I. Gupta[7], N. C. Gupta[93], S. K. Gupta[46], V. Gupta[18], N. Gupte[1], J. Gurs[97], N. Gutierrez[175], N. Guttman[6], F. Guzman[130], D. Haba[216], M. Haberland[1], S. Haino[217], E. D. Hall[35], E. Z. Hamilton[98], G. Hammond[86], M. Haney[37], J. Hanks[2], C. Hanna[7], M. D. Hannam[33], O. A. Hannuksela[218], A. G. Hanselman[129], H. Hansen[2], J. Hanson[63], S. Hanumasagar[57], R. Harada[42], A. R. Hardison[181], S. Harikumar[186], K. Haris[37,71], I. Harley-Trochimczyk[130], T. Harmark[133], J. Harms[44,45], G. M. Harry[219], I. W. Harry[73], J. Hart[104], B. Haskell[95,220,221], C.-J. Haster[212], K. Haughian[86], H. Hayakawa[50], K. Hayama[222], M. C. Heintze[63], J. Heinze[118], J. Heinzel[35], H. Heitmann[113], F. Hellman[206], A. F. Helmling-Cornell[77], G. Hemming[62], O. Henderson-Sapir[115], M. Hendry[86], I. S. Heng[86], M. H. Hennig[86], C. Henshaw[57], M. Heurs[8,9], A. L. Hewitt[223,224], J. Heynen[15], J. Heyns[35], S. Higginbotham[33], S. Hild[36,37], S. Hill[86], Y. Himemoto[225], N. Hirata[25], C. Hirose[226], W. C. G. Ho[227], D. Hofman[175], B. E. Hogan[65], N. A. Holland[37,107], K. Holley-Bockelmann[143], I. J. Hollows[174], D. E. Holz[129], L. Honet[111], D. J. Horton-Bailey[206], J. Hough[86], S. Hourihane[11], N. T. Howard[143], E. J. Howell[72], C. G. Hoy[73], C. A. Hrishikesh[21], P. Hsi[35], H.-F. Hsieh[141], H.-Y. Hsieh[141], C. Hsiung[228], S.-H. Hsu[145], W.-F. Hsu[109], Q. Hu[86], H. Y. Huang[140], Y. Huang[7], Y. T. Huang[78], A. D. Huddart[229], B. Hughey[65], V. Hui[31], S. Husa[98], R. Huxford[7], L. Iampieri[38,39], G. A. Iandolo[36], M. Ianni[21,22], G. Iannone[131], J. Iascau[77], K. Ide[230], R. Iden[216], A. Ierardi[44,45], S. Ikeda[146], H. Imafuku[42], Y. Inoue[140], G. Iorio[91], P. Iosif[48,184], M. H. Iqbal[34], J. Irwin[86], R. Ishikawa[230], M. Isi[190,191], K. S. Isleif[231], Y. Itoh[204,232], M. Iwaya[203], B. R. Iyer[24], C. Jacquet[100], P.-E. Jacquet[121], T. Jacquot[41], S. J. Jadhav[233], S. P. Jadhav[154], M. Jain[132], T. Jain[223], A. L. James[11], K. Jani[143], J. Janquart[15], N. N. Janthalur[233], S. Jaraba[234], P. Jaranowski[235], R. Jaume[98], W. Javed[33], A. Jennings[2], M. Jensen[2], W. Jia[35], J. Jiang[149], H.-B. Jin[236,237], G. R. Johns[122], N. A. Johnson[46], M. C. Johnston[212], R. Johnston[86], N. Johny[8,9], D. H. Jones[34], D. I. Jones[209], R. Jones[86], H. E. Jose[77], P. Joshi[7], S. K. Joshi[79], G. Joubert[56], J. Ju[238], L. Ju[72], K. Jung[239], J. Junker[34], V. Juste[111], H. B. Kabagoz[35,63], T. Kajita[240], I. Kaku[204], V. Kalogera[96], M. Kalomenopoulos[212], M. Kamiizumi[50], N. Kanda[204,232], S. Kandhasamy[79], G. Kang[241], N. C. Kannachel[6], J. B. Kanner[11], S. A. KantiMahanty[18], S. J. Kapadia[79], D. P. Kapasi[54], M. Karthikeyan[132], M. Kasprzack[11], H. Kato[151], T. Kato[203], E. Katsavounidis[35], W. Katzman[63], R. Kaushik[103], K. Kawabe[2], R. Kawamoto[204], D. Keitel[98], L. J. Kemperman[115], J. Kennington[7], F. A. Kerkow[18], R. Kesharwani[79], J. S. Key[242], R. Khadela[8,9], S. Khadka[89], S. S. Khadkikar[7], F. Y. Khalili[108], F. Khan[8,9], T. Khanam[162], M. Khursheed[103], N. M. Khusid[190,191], W. Kiendrebeogo[113,243], N. Kijbunchoo[115], C. Kim[244], J. C. Kim[245], K. Kim[246], M. H. Kim[238], S. Kim[247], Y.-M. Kim[246], C. Kimball[96], K. Kimes[54], M. Kinnear[33], J. S. Kissel[2], S. Klimenko[46], A. M. Knee[114], E. J. Knox[77], N. Knust[8,9], K. Kobayashi[203], S. M. Koehlenbeck[89], G. Koekoek[36,37], K. Kohri[248,249], K. Kokeyama[33,250],

S. Koley[44,165], P. Kolitsidou[118], A. E. Koloniari[251], K. Komori[42], A. K. H. Kong[141], A. Kontos[252], L. M. Koponen[118], M. Korobko[97], X. Kou[18], A. Koushik[23], N. Kouvatsos[67], M. Kovalam[72], T. Koyama[151], D. B. Kozak[11], S. L. Kranzhoff[36,37], V. Kringel[8,9], N. V. Krishnendu[118], S. Kroker[253], A. Królak[186,254], K. Kruska[8,9], J. Kubisz[255], G. Kuehn[8,9], S. Kulkarni[215], A. Kulur Ramamohan[34], Achal Kumar[46], Anil Kumar[233], Praveen Kumar[177], Prayush Kumar[24], Rahul Kumar[2], Rakesh Kumar[93], J. Kume[42,256,257], K. Kuns[35], N. Kuntimaddi[33], S. Kuroyanagi[207,258], S. Kuwahara[42], K. Kwak[239], K. Kwan[34], S. Kwon[42], G. Lacaille[86], D. Laghi[100,188], A. H. Laity[163], E. Lalande[259], M. Lalleman[23], P. C. Lalremruati[260], M. Landry[2], B. B. Lane[35], R. N. Lang[35], J. Lange[147], R. Langgin[212], B. Lantz[89], I. L. Rosa[98], J. Larsen[199], A. Lartaux-Vollard[41], P. D. Lasky[6], J. Lawrence[164], M. Laxen[63], C. Lazarte[137], A. Lazzarini[11], C. Lazzaro[155,156], P. Leaci[38,39], L. Leali[18], Y. K. Lecoeuche[114], H. M. Lee[261], H. W. Lee[262], J. Lee[78], K. Lee[238], R.-K. Lee[141], R. Lee[35], Sungho Lee[246], Sunjae Lee[238], Y. Lee[140], I. N. Legred[11], J. Lehmann[8,9], L. Lehner[182], M. Le Jean[116,175], A. Lemai^tre[263], M. Lenti[61,176], M. Leonardi[74,75,264], M. Lequime[40], N. Leroy[41], M. Lesovsky[11], N. Letendre[31], M. Lethuillier[56], Y. Levin[6], K. Leyde[73], A. K. Y. Li[11], K. L. Li[265], T. G. F. Li[109], X. Li[148], Y. Li[96], Z. Li[86], A. Lihos[122], E. T. Lin[141], F. Lin[140], L. C.-C. Lin[265], Y.-C. Lin[141], C. Lindsay[200], S. D. Linker[180], A. Liu[218], G. C. Liu[228], Jian Liu[72], F. Llamas Villarreal[164], J. Llobera-Querol[98], R. K. L. Lo[139], J.-P. Locquet[109], S. C. G. Loggins[266], M. R. Loizou[132], L. T. London[67], A. Longo[60,61], D. Lopez[165], M. Lopez Portilla[71], M. Lorenzini[21,22], A. Lorenzo-Medina[177], V. Loriette[41], M. Lormand[63], G. Losurdo[80,267], E. Lotti[132], T. P. Lott IV[57], J. D. Lough[8,9], H. A. Loughlin[35], C. O. Lousto[110], N. Low[123], N. Lu[34], L. Lucchesi[80], H. Lück[8,9], D. Lumaca[22], A. P. Lundgren[268,269], A. W. Lussier[259], R. Macas[73], M. MacInnis[35], D. M. Macleod[33], I. A. O. MacMillan[11], A. Macquet[41], K. Maeda[151], S. Maenaut[109], S. S. Magare[79], R. M. Magee[11], E. Maggio[1], R. Maggiore[37,107], M. Magnozzi[29,30], M. Mahesh[97], M. Maini[163], S. Majhi[79], E. Majorana[38,39], C. N. Makarem[11], D. Malakar[105], J. A. Malaquias-Reis[19], U. Mali[189], S. Maliakal[11], A. Malik[103], L. Mallick[168,189], A.-K. Malz[58], N. Man[113], M. Mancarella[99], V. Mandic[18], V. Mangano[155,170], B. Mannix[77], G. L. Mansell[78], M. Manske[10], M. Mantovani[62], M. Mapelli[91,92,270], C. Marinelli[101], F. Marion[31], A. S. Markosyan[89], A. Markowitz[11], E. Maros[11], S. Marsat[100], F. Martelli[60,61], I. W. Martin[86], R. M. Martin[192], B. B. Martinez[130], D. A. Martinez[54], M. Martinez[43,271], V. Martinez[128], A. Martini[74,75], J. C. Martins[19], D. V. Martynov[118], E. J. Marx[35], L. Massaro[36,37], A. Masserot[31], M. Masso-Reid[86], S. Mastrogiovanni[38], T. Matcovich[51], M. Matiushechkina[8,9], L. Maurin[208], N. Mavalvala[35], N. Maxwell[2], G. McCarrol[63], R. McCarthy[2], D. E. McClelland[34], S. McCormick[63], L. McCuller[11], S. McEachin[122], C. McElhenny[122], G. I. McGhee[86], K. B. M. McGowan[143], J. McIver[114], A. McLeod[72], I. McMahon[188], T. McRae[34], R. McTeague[86], D. Meacher[10], B. N. Meagher[78], R. Mechum[110], Q. Meijer[71], A. Melatos[123], C. S. Menoni[136], F. Mera[2], R. A. Mercer[10], L. Mereni[175], K. Merfeld[162], E. L. Merilh[63], J. R. Mérou[98], J. D. Merritt[77], M. Merzougui[113], C. Messick[10], B. Mestichelli[44], Z. Metzler[125,272,273], M. Meyer-Conde[274], F. Meylahn[8,9], A. Mhaske[79], A. Miani[74,75], H. Miao[275], C. Michel[175], Y. Michimura[42], H. Middleton[118], D. P. Mihaylov[104], S. J. Miller[11], M. Millhouse[57], E. Milotti[48,184], V. Milotti[91], Y. Minenkov[22], E. M. Minihan[65], Ll. M. Mir[43], L. Mirasola[155,156], M. Miravet-Tenés[137], C.-A. Miritescu[43], A. Mishra[24], C. Mishra[106], T. Mishra[46], A. L. Mitchell[37,107], J. G. Mitchell[65], S. Mitra[79], V. P. Mitrofanov[108], K. Mitsuhashi[25], R. Mittleman[35], O. Miyakawa[50], S. Miyoki[50], A. Miyoko[65], G. Mo[35], L. Mobilia[60,61], S. R. P. Mohapatra[11], S. R. Mohite[7], M. Molina- Ruiz[206], M. Mondin[180], M. Montani[60,61], C. J. Moore[223], D. Moraru[2], A. More[79], S. More[79], C. Moreno[134], E. A. Moreno[35], G. Moreno[2], A. Moreso Serra[82], S. Morisaki[42,203], Y. Moriwaki[151], G. Morras[207], A. Moscatello[91], M. Mould[35], B. Mours[64], C. M. Mow-Lowry[37,107], L. Muccillo[61,176], F. Muciaccia[38,39], D. Mukherjee[118], Samanwaya Mukherjee[24], Soma Mukherjee[164], Subroto Mukherjee[93], Suvodip Mukherjee[13], N. Mukund[35], A. Mullavey[63], H. Mullock[114], J. Mundi[219], C. L. Mungioli[72], M. Murakoshi[230], P. G. Murray[86], D. Nabari[74,75], S. L. Nadji[8,9], A. Nagar[28,276], N. Nagarajan[86], K. Nakagaki[50], K. Nakamura[25], H. Nakano[277], M. Nakano[11], D. Nanadoumgar-Lacroze[43], D. Nandi[12], V. Napolano[62], P. Narayan[215], I. Nardecchia[22], T. Narikawa[203], H. Narola[71], L. Naticchioni[38], R. K. Nayak[260], L. Negri[71], A. Nela[86], C. Nelle[77], A. Nelson[130], T. J. N. Nelson[63], M. Nery[8,9], A. Neunzert[2], S. Ng[54], L. Nguyen Quynh[278], S. A. Nichols[12], A. B. Nielsen[279], Y. Nishino[25,42], A. Nishizawa[280], S. Nissanke[37,281], W. Niu[7], F. Nocera[62], J. Noller[282], M. Norman[33], C. North[33], J. Novak[116,234,283], R. Nowicki[143], J. F. Nuño Siles[207], L. K. Nuttall[73], K. Obayashi[230], J. Oberling[2], J. O'Dell[229], E. Oelker[35], M. Oertel[116,234,283,284], G. Oganesyan[44,45], T. O'Hanlon[63], M. Ohashi[50], F. Ohme[8,9], R. Oliveri[116,283,284], R. Omer[18], B. O'Neal[122], M. Onishi[151], K. Oohara[285], B. O'Reilly[63], M. Orselli[51,76], R. O'Shaughnessy[110], S. O'Shea[86], S. Oshino[50], C. Osthelder[11], I. Ota[12], D. J. Ottaway[115], A. Ouzriat[56], H. Overmier[63], B. J. Owen[286], R. Ozaki[230], A. E. Pace[7], R. Pagano[12], M. A. Page[25], A. Pai[194], L. Paiella[44], A. Pal[287], S. Pal[260], M. A. Palaia[80,81], M. Pálfi[202], P. P. Palma[21,22,39], C. Palomba[38], P. Palud[20], H. Pan[141], J. Pan[72], K. C. Pan[141], P. K. Panda[233], Shiksha Pandey[7], Swadha Pandey[35], P. T. H. Pang[37,71], F. Pannarale[38,39], K. A. Pannone[54], B. C. Pant[103], F. H. Panther[72], M. Panzeri[60,61], F. Paoletti[80], A. Paolone[38,288], A. Papadopoulos[86], E. E. Papalexakis[210], L. Papalini[80,81], G. Papigkiotis[251], A. Paquis[41], A. Parisi[51,76], B.-J. Park[246], J. Park[289], W. Parker[63], G. Pascale[8,9], D. Pascucci[94], A. Pasqualetti[62], R. Passaquieti[80,81], L. Passenger[6], D. Passuello[80], O. Patane[2], A. V. Patel[140], D. Pathak[79], A. Patra[33], B. Patricelli[80,81], B. G. Patterson[33], K. Paul[106], S. Paul[77], E. Payne[11], T. Pearce[33], M. Pedraza[11], A. Pele[11], F. E. Peña Arellano[290], X. Peng[118], Y. Peng[57], S. Penn[291], M. D. Penuliar[54], A. Perego[74,75], Z. Pereira[132],

C. Périgois[91,92,292], G. Perna[91], A. Perreca[44,74,75], J. Perret[20], S. Perriès[56], J. W. Perry[37,107], D. Pesios[251], S. Peters[165], S. Petracca[205], C. Petrillo[76], H. P. Pfeiffer[1], H. Pham[63], K. A. Pham[18], K. S. Phukon[118], H. Phurailatpam[218], M. Piarulli[100], L. Piccari[38,39], O. J. Piccinni[34], M. Pichot[113], M. Piendibene[80,81], F. Piergiovanni[60,61], L. Pierini[38], G. Pierra[38], V. Pierro[131,293], M. Pietrzak[95], M. Pillas[165], F. Pilo[80], L. Pinard[175], I. M. Pinto[32,131,293,294], M. Pinto[62], B. J. Piotrzkowski[10], M. Pirello[2], M. D. Pitkin[86,223], A. Placidi[51], E. Placidi[38,39], M. L. Planas[98], W. Plastino[22,211], C. Plunkett[35], R. Poggiani[80,81], E. Polini[35], J. Pomper[80,81], L. Pompili[1], J. Poon[218], E. Porcelli[37], E. K. Porter[20], C. Posnansky[7], R. Poulton[62], J. Powell[154], G. S. Prabhu[79], M. Pracchia[165], B. K. Pradhan[79], T. Pradier[64], A. K. Prajapati[93], K. Prasai[295], R. Prasanna[233], P. Prasia[79], G. Pratten[118], G. Principe[48,184], G. A. Prodi[74,75], P. Prosperi[80], P. Prosposito[21,22], A. C. Providence[65], A. Puecher[1], J. Pullin[12], P. Puppo[38], M. Pürrer[163], H. Qi[16], J. Qin[34], G. Quéméner[116,173], V. Quetschke[164], P. J. Quinonez[65], N. Qutob[57], R. Rading[231], I. Rainho[137], S. Raja[103], C. Rajan[103], B. Rajbhandari[110], K. E. Ramirez[63], F. A. Ramis Vidal[98], M. Ramos Arevalo[164], A. Ramos-Buades[37,98], S. Ranjan[57], K. Ransom[63], P. Rapagnani[38,39], B. Ratto[65], A. Ravichandran[132], A. Ray[96], V. Raymond[33], M. Razzano[80,81], J. Read[54], T. Regimbau[31], S. Reid[55], C. Reissel[35], D. H. Reitze[11], A. I. Renzini[11,126], B. Revenu[41,296], A. Revilla Peña[82], R. Reyes[180], L. Ricca[15], F. Ricci[38,39], M. Ricci[38,39], A. Ricciardone[80,81], J. Rice[78], J. W. Richardson[210], M. L. Richardson[115], A. Rijal[65], K. Riles[90], H. K. Riley[33], S. Rinaldi[270], J. Rittmeyer[97], C. Robertson[229], F. Robinet[41], M. Robinson[2], A. Rocchi[22], L. Rolland[31], J. G. Rollins[11], A. E. Romano[297], R. Romano[3,4], A. Romero[31], I. M. Romero-Shaw[223], J. H. Romie[63], S. Ronchini[7], T. J. Roocke[115], L. Rosa[4,32], T. J. Rosauer[210], C. A. Rose[57], D. Rosińska[124], M. P. Ross[53], M. Rossello-Sastre[98], S. Rowan[86], S. K. Roy[190,191], S. Roy[15], D. Rozza[126,127], P. Ruggi[62], N. Ruhama[239], E. Ruiz Morales[207,298], K. Ruiz-Rocha[143], S. Sachdev[57], T. Sadecki[2], P. Saffarieh[37,107], S. Safi-Harb[168], M. R. Sah[13], S. Saha[141], T. Sainrat[64], S. Sajith Menon[38,39,214], K. Sakai[299], Y. Sakai[274], M. Sakellariadou[67], S. Sakon[7], O. S. Salafia[126,127,158], F. Salces-Carcoba[11], L. Salconi[62], M. Saleem[147], F. Salemi[38,39], M. Sallé[37], S. U. Salunkhe[79], S. Salvador[172,173], A. Salvarese[147], A. Samajdar[37,71], A. Sanchez[2], E. J. Sanchez[11], L. E. Sanchez[11], N. Sanchis-Gual[137], J. R. Sanders[181], E. M. Sänger[1], F. Santoliquido[44,45], F. Sarandrea[28], T. R. Saravanan[79], N. Sarin[6], P. Sarkar[8,9], A. Sasli[251], P. Sassi[51,76], B. Sassolas[175], R. Sato[226], S. Sato[151], Yukino Sato[151], Yu Sato[151], O. Sauter[46], R. L. Savage[2], T. Sawada[50], H. L. Sawant[79], S. Sayah[175], V. Scacco[21,22], D. Schaetzl[11], M. Scheel[148], A. Schiebelbein[189], M. G. Schiworski[78], P. Schmidt[118], S. Schmidt[71], R. Schnabel[97], M. Schneewind[8,9], R. M. S. Schofield[77], K. Schouteden[109], B. W. Schulte[8,9], B. F. Schutz[8,9,33], E. Schwartz[300], M. Scialpi[301], J. Scott[86], S. M. Scott[34], R. M. Sedas[63], T. C. Seetharamu[86], M. Seglar-Arroyo[43], Y. Sekiguchi[302], D. Sellers[63], N. Sembo[204], A. S. Sengupta[303], E. G. Seo[86], J. W. Seo[109], V. Sequino[4,32], M. Serra[38], A. Sevrin[187], T. Shaffer[2], U. S. Shah[57], M. A. Shaikh[261], L. Shao[304], A. K. Sharma[98], Preeti Sharma[12], Prianka Sharma[103], Ritwik Sharma[18], S. Sharma Chaudhary[105], P. Shawhan[125], N. S. Shcheblanov[263,305], E. Sheridan[143], Z.-H. Shi[141], M. Shikauchi[42], R. Shimomura[306], H. Shinkai[306], S. Shirke[79], D. H. Shoemaker[35], D. M. Shoemaker[147], R. W. Short[2], S. ShyamSundar[103], A. Sider[157], H. Siegel[190,191], D. Sigg[2], L. Silenzi[36,37], L. Silvestri[39,169], M. Simmonds[115], L. P. Singer[272], Amitesh Singh[215], Anika Singh[11], D. Singh[206], N. Singh[98], S. Singh[59,216], A. M. Sintes[98], V. Sipala[155,170], V. Skliris[33], B. J. J. Slagmolen[34], D. A. Slater[199], T. J. Slaven-Blair[72], J. Smetana[118], J. R. Smith[54], L. Smith[48,86,184], R. J. E. Smith[6], W. J. Smith[143], S. Soares de Albuquerque Filho[60], M. Soares- Santos[188], K. Somiya[216], I. Song[141], S. Soni[35], V. Sordini[56], F. Sorrentino[29], H. Sotani[307], F. Spada[80], V. Spagnuolo[37], A. P. Spencer[86], P. Spinicelli[62], A. K. Srivastava[93], F. Stachurski[86], C. J. Stark[122], D. A. Steer[308], N. Steinle[168], J. Steinlechner[36,37], S. Steinlechner[36,37], N. Stergioulas[251], P. Stevens[41], M. StPierre[163], M. D. Strong[12], A. Strunk[2], A. L. Stuver[102,328], M. Suchenek[95], S. Sudhagar[95], Y. Sudo[230], N. Sueltmann[97], L. Suleiman[54], K. D. Sullivan[12], J. Sun[241], L. Sun[34], S. Sunil[93], J. Suresh[113], B. J. Sutton[67], P. J. Sutton[33], K. Suzuki[216], M. Suzuki[203], B. L. Swinkels[37], A. Syx[116], M. J. Szczepańczyk[309], P. Szewczyk[124], M. Tacca[37], H. Tagoshi[203], S. C. Tait[11], K. Takada[203], H. Takahashi[274], R. Takahashi[25], A. Takamori[42], S. Takano[310], H. Takeda[311,312], K. Takeshita[216], I. Takimoto Schmiegelow[44,45], M. Takou-Ayaoh[78], C. Talbot[129], M. Tamaki[203], N. Tamanini[100], D. Tanabe[140], K. Tanaka[50], S. J. Tanaka[230], S. Tanioka[33], D. B. Tanner[46], W. Tanner[8,9], L. Tao[210], R. D. Tapia[7], E. N. Tapia San Martín[37], C. Taranto[21,22], A. Taruya[313], J. D. Tasson[152], J. G. Tau[110], D. Tellez[54], R. Tenorio[98], H. Themann[180], A. Theodoropoulos[137], M. P. Thirugnanasambandam[79], L. M. Thomas[11], M. Thomas[63], P. Thomas[2], J. E. Thompson[209], S. R. Thondapu[103], K. A. Thorne[63], E. Thrane[6], J. Tissino[44,45], A. Tiwari[79], Pawan Tiwari[44], Praveer Tiwari[194], S. Tiwari[188], V. Tiwari[118], M. R. Todd[78], M. Toffano[91], A. M. Toivonen[18], K. Toland[86], A. E. Tolley[73], T. Tomaru[25], V. Tommasini[11], T. Tomura[50], H. Tong[6], C. Tong-Yu[140], A. Torres-Forné[137,138], C. I. Torrie[11], I. Tosta e Melo[314], E. Tournefier[31], M. Trad Nery[113], K. Tran[122], A. Trapananti[51,52], R. Travaglini[167], F. Travasso[51,52], G. Traylor[63], M. Trevor[125], M. C. Tringali[62], A. Tripathee[90], G. Troian[48,184], A. Trovato[48,184], L. Trozzo[4], R. J. Trudeau[11], T. Tsang[33], S. Tsuchida[315], L. Tsukada[212], K. Turbang[23,187], M. Turconi[113], C. Turski[94], H. Ubach[82,83], N. Uchikata[203], T. Uchiyama[50], R. P. Udall[11], T. Uehara[316], K. Ueno[42], V. Undheim[279], L. E. Uronen[218], T. Ushiba[50], M. Vacatello[80,81], H. Vahlbruch[8,9], N. Vaidya[11], G. Vajente[11], A. Vajpeyi[6], J. Valencia[98], M. Valentini[37,107], S. A. Vallejo-Peña[297], S. Vallero[28], V. Valsan[10], M. van Dael[37,317], E. Van den Bossche[187], J. F. J. van den Brand[36,37,107], C. Van Den Broeck[37,71], M. van der Sluys[37,71], A. Van de Walle[41], J. van Dongen[37,107],

K. Vandra[102], M. VanDyke[119], H. van Haevermaet[23], J. V. van Heijningen[37,107], P. Van Hove[64], J. Vanier[259], M. VanKeuren[104], J. Vanosky[2], N. van Remortel[23], M. Vardaro[36,37], A. F. Vargas[123], V. Varma[132], A. N. Vazquez[89], A. Vecchio[118], G. Vedovato[92], J. Veitch[86], P. J. Veitch[115], S. Venikoudis[15], R. C. Venterea[18], P. Verdier[56], M. Vereecken[15], D. Verkindt[31], B. Verma[132], Y. Verma[103], S. M. Vermeulen[11], F. Vetrano[60], A. Veutro[38,39], A. Viceré[60,61], S. Vidyant[78], A. D. Viets[88], A. Vijaykumar[189], A. Vilkha[110], N. Villanueva Espinosa[137], V. Villa-Ortega[177], E. T. Vincent[57], J.-Y. Vinet[113], S. Viret[56], S. Vitale[35], H. Vocca[51,76], D. Voigt[97], E. R. G. von Reis[2], J. S. A. von Wrangel[8,9], W. E. Vossius[231], L. Vujeva[139], S. P. Vyatchanin[108], J. Wack[11], L. E. Wade[104], M. Wade[104], K. J. Wagner[110], L. Wallace[11], E. J. Wang[89], H. Wang[216], J. Z. Wang[90], W. H. Wang[164], Y. F. Wang[1], G. Waratkar[194], J. Warner[2], M. Was[31], T. Washimi[25], N. Y. Washington[11], D. Watarai[42], B. Weaver[2], S. A. Webster[86], N. L. Weickhardt[97], M. Weinert[8,9], A. J. Weinstein[11], R. Weiss[35,329], L. Wen[72], K. Wette[34], J. T. Whelan[110], B. F. Whiting[46], C. Whittle[11], E. G. Wickens[73], D. Wilken[8,9], A. T. Wilkin[210], B. M. Williams[119], D. Williams[86], M. J. Williams[73], N. S. Williams[1], J. L. Willis[11], B. Willke[8,9], M. Wils[109], L. Wilson[104], C. W. Winborn[105], J. Winterflood[72], C. C. Wipf[11], G. Woan[86], J. Woehler[36,37], N. E. Wolfe[35], H. T. Wong[140], I. C. F. Wong[109,218], K. Wong[189], T. Wouters[37,71], J. L. Wright[2], M. Wright[71,86], B. Wu[78], C. Wu[141], D. S. Wu[8,9], H. Wu[141], K. Wu[119], Q. Wu[53], Y. Wu[96], Z. Wu[100], E. Wuchner[54], D. M. Wysocki[10], V. A. Xu[206], Y. Xu[98], N. Yadav[28], H. Yamamoto[11], K. Yamamoto[151], T. S. Yamamoto[42], T. Yamamoto[50], R. Yamazaki[230], T. Yan[118], K. Z. Yang[18], Y. Yang[145], Z. Yarbrough[12], J. Yebana[98], S.-W. Yeh[141], A. B. Yelikar[143], X. Yin[35], J. Yokoyama[42,318], T. Yokozawa[50], S. Yuan[72], H. Yuzurihara[50], M. Zanolin[65], M. Zeeshan[110], T. Zelenova[62], J.-P. Zendri[92], M. Zeoli[15], M. Zerrad[40], M. Zevin[96], L. Zhang[11], N. Zhang[57], R. Zhang[149], T. Zhang[118], C. Zhao[72], Yue Zhao[161], Yuhang Zhao[20], Z.-C. Zhao[319], Y. Zheng[105], H. Zhong[18], H. Zhou[78], H. O. Zhu[72], Z.-H. Zhu[319,320], A. B. Zimmerman[147], L. Zimmermann[56], M. E. Zucker[11,35], J. Zweizig[11],

(The LIGO Scientific Collaboration, the Virgo Collaboration, and the KAGRA Collaboration),

Jim Palfreyman[321], S.B. Araujo Furlan[322,323], S. del Palacio[324,325], G. Gancio[324], F. García[324,326], G. E. Romero[324,326], and E. Zubieta[324,326]

[1] Max Planck Institute for Gravitational Physics (Albert Einstein Institute), D-14476 Potsdam, Germany
[2] LIGO Hanford Observatory, Richland, WA 99352, USA
[3] Dipartimento di Farmacia, Università di Salerno, I-84084 Fisciano, Salerno, Italy
[4] INFN, Sezione di Napoli, I-80126 Napoli, Italy
[5] University of Warwick, Coventry, CV 4 7AL, UK
[6] OzGrav, School of Physics & Astronomy, Monash University, Clayton 3800, Victoria, Australia
[7] The Pennsylvania State University, University Park, PA 16802, USA
[8] Max Planck Institute for Gravitational Physics (Albert Einstein Institute), D-30167 Hannover, Germany
[9] Leibniz Universität Hannover, D-30167 Hannover, Germany
[10] University of Wisconsin-Milwaukee, Milwaukee, WI 53201, USA
[11] LIGO Laboratory, California Institute of Technology, Pasadena, CA 91125, USA
[12] Louisiana State University, Baton Rouge, LA 70803, USA
[13] Tata Institute of Fundamental Research, Mumbai 400005, India
[14] Centre de Physique Théorique, Aix-Marseille Université, Campus de Luminy, 163 Avenue de Luminy, 13009 Marseille, France
[15] Université catholique de Louvain, B-1348 Louvain-la-Neuve, Belgium
[16] Queen Mary University of London, London, E1 4NS, UK
[17] University of California, Davis, CA 95616, USA
[18] University of Minnesota, Minneapolis, MN 55455, USA
[19] Instituto Nacional de Pesquisas Espaciais, 12227-010 São José dos Campos, São Paulo, Brazil
[20] Université Paris Cité, CNRS, Astroparticule et Cosmologie, F-75013 Paris, France
[21] Università di Roma Tor Vergata, I-00133 Roma, Italy
[22] INFN, Sezione di Roma Tor Vergata, I-00133 Roma, Italy
[23] Universiteit Antwerpen, 2000 Antwerpen, Belgium
[24] International Centre for Theoretical Sciences, Tata Institute of Fundamental Research, Bengaluru 560089, India
[25] Gravitational Wave Science Project, National Astronomical Observatory of Japan, 2-21-1 Osawa, Mitaka City, Tokyo 181-8588, Japan
[26] Advanced Technology Center, National Astronomical Observatory of Japan, 2-21-1 Osawa, Mitaka City, Tokyo 181-8588, Japan
[27] Theoretisch-Physikalisches Institut, Friedrich-Schiller-Universität Jena, D-07743 Jena, Germany
[28] INFN Sezione di Torino, I-10125 Torino, Italy
[29] INFN, Sezione di Genova, I-16146 Genova, Italy
[30] Dipartimento di Fisica, Università degli Studi di Genova, I-16146 Genova, Italy
[31] Univ. Savoie Mont Blanc, CNRS, Laboratoire d'Annecy de Physique des Particules—IN2P3, F-74000 Annecy, France
[32] Università di Napoli "Federico II", I-80126 Napoli, Italy
[33] Cardiff University, Cardiff, CF24 3AA, UK
[34] OzGrav, Australian National University, Canberra, Australian Capital Territory 0200, Australia
[35] LIGO Laboratory, Massachusetts Institute of Technology, Cambridge, MA 02139, USA
[36] Maastricht University, 6200 MD Maastricht, The Netherlands
[37] Nikhef, 1098 XG Amsterdam, The Netherlands
[38] INFN, Sezione di Roma, I-00185 Roma, Italy
[39] Università di Roma "La Sapienza", I-00185 Roma, Italy
[40] Aix Marseille Univ, CNRS, Centrale Med, Institut Fresnel, F-13013 Marseille, France
[41] Université Paris-Saclay, CNRS/IN2P3, IJCLab, 91405 Orsay, France
[42] University of Tokyo, Tokyo, 113-0033, Japan
[43] Institut de Física d'Altes Energies (IFAE), The Barcelona Institute of Science and Technology, Campus UAB, E-08193 Bellaterra (Barcelona), Spain
[44] Gran Sasso Science Institute (GSSI), I-67100 L'Aquila, Italy
[45] INFN, Laboratori Nazionali del Gran Sasso, I-67100 Assergi, Italy

[46] University of Florida, Gainesville, FL 32611, USA
[47] Dipartimento di Scienze Matematiche, Informatiche e Fisiche, Università di Udine, I-33100 Udine, Italy
[48] INFN, Sezione di Trieste, I-34127 Trieste, Italy
[49] Tecnologico de Monterrey, Escuela de Ingeniería y Ciencias, 64849, Monterrey, Nuevo León, Mexico
[50] Institute for Cosmic Ray Research, KAGRA Observatory, The University of Tokyo, 238 Higashi-Mozumi, Kamioka-cho, Hida City, Gifu 506-1205, Japan
[51] INFN, Sezione di Perugia, I-06123 Perugia, Italy
[52] Università di Camerino, I-62032 Camerino, Italy
[53] University of Washington, Seattle, WA 98195, USA
[54] California State University Fullerton, Fullerton, CA 92831, USA
[55] SUPA, University of Strathclyde, Glasgow G1 1XQ, UK
[56] Université Claude Bernard Lyon 1, CNRS, IP2I Lyon/IN2P3, UMR 5822, F-69622 Villeurbanne, France
[57] Georgia Institute of Technology, Atlanta, GA 30332, USA
[58] Royal Holloway, University of London, London, TW20 0EX, UK
[59] Astronomical course, The Graduate University for Advanced Studies (SOKENDAI), 2-21-1 Osawa, Mitaka City, Tokyo 181-8588, Japan
[60] Università degli Studi di Urbino "Carlo Bo", I-61029 Urbino, Italy
[61] INFN, Sezione di Firenze, I-50019 Sesto Fiorentino, Firenze, Italy
[62] European Gravitational Observatory (EGO), I-56021 Cascina, Pisa, Italy
[63] LIGO Livingston Observatory, Livingston, LA 70754, USA
[64] Université de Strasbourg, CNRS, IPHC UMR 7178, F-67000 Strasbourg, France
[65] Embry-Riddle Aeronautical University, Prescott, AZ 86301, USA
[66] Dipartimento di Fisica "E.R. Caianiello", Università di Salerno, I-84084 Fisciano, Salerno, Italy
[67] King's College London, University of London, London, WC2R 2LS, UK
[68] Korea Institute of Science and Technology Information, Daejeon 34141, Republic of Korea
[69] International College, Osaka University, 1-1 Machikaneyama-cho, Toyonaka City, Osaka 560-0043, Japan
[70] Accelerator Laboratory, High Energy Accelerator Research Organization (KEK), 1-1 Oho, Tsukuba City, Ibaraki 305-0801, Japan
[71] Institute for Gravitational and Subatomic Physics (GRASP), Utrecht University, 3584 CC Utrecht, The Netherlands
[72] OzGrav, University of Western Australia, Crawley, Western Australia 6009, Australia
[73] University of Portsmouth, Portsmouth, PO1 3FX, UK
[74] Università di Trento, Dipartimento di Fisica, I-38123 Povo, Trento, Italy
[75] INFN, Trento Institute for Fundamental Physics and Applications, I-38123 Povo, Trento, Italy
[76] Università di Perugia, I-06123 Perugia, Italy
[77] University of Oregon, Eugene, OR 97403, USA
[78] Syracuse University, Syracuse, NY 13244, USA
[79] Inter-University Centre for Astronomy and Astrophysics, Pune 411007, India
[80] INFN, Sezione di Pisa, I-56127 Pisa, Italy
[81] Università di Pisa, I-56127 Pisa, Italy
[82] Institut de Ciències del Cosmos (ICCUB), Universitat de Barcelona (UB), c. Martí i Franquès, 1, 08028 Barcelona, Spain
[83] Departament de Física Quàntica i Astrofísica (FQA), Universitat de Barcelona (UB), c. Martí i Franqués, 1, 08028 Barcelona, Spain
[84] Institut d'Estudis Espacials de Catalunya, c. Gran Capità, 2-4, 08034 Barcelona, Spain
[85] Dipartimento di Medicina, Chirurgia e Odontoiatria "Scuola Medica Salernitana," Università di Salerno, I-84081 Baronissi, Salerno, Italy
[86] IGR, University of Glasgow, Glasgow, G12 8QQ, UK
[87] HUN-REN Wigner Research Centre for Physics, H-1121 Budapest, Hungary
[88] Concordia University Wisconsin, Mequon, WI 53097, USA
[89] Stanford University, Stanford, CA 94305, USA
[90] University of Michigan, Ann Arbor, MI 48109, USA
[91] Università di Padova, Dipartimento di Fisica e Astronomia, I-35131 Padova, Italy
[92] INFN, Sezione di Padova, I-35131 Padova, Italy
[93] Institute for Plasma Research, Bhat, Gandhinagar 382428, India
[94] Universiteit Gent, B-9000 Gent, Belgium
[95] Nicolaus Copernicus Astronomical Center, Polish Academy of Sciences, 00-716, Warsaw, Poland
[96] Northwestern University, Evanston, IL 60208, USA
[97] Universität Hamburg, D-22761 Hamburg, Germany
[98] IAC3–IEEC, Universitat de les Illes Balears, E-07122 Palma de Mallorca, Spain
[99] Aix-Marseille Université, Université de Toulon, CNRS, CPT, Marseille, France
[100] Laboratoire des 2 Infinis - Toulouse (L2IT-IN2P3), F-31062 Toulouse Cedex 9, France
[101] Università di Siena, Dipartimento di Scienze Fisiche, della Terra e dell'Ambiente, I-53100 Siena, Italy
[102] Villanova University, Villanova, PA 19085, USA
[103] RRCAT, Indore, Madhya Pradesh 452013, India
[104] Kenyon College, Gambier, OH 43022, USA
[105] Missouri University of Science and Technology, Rolla, MO 65409, USA
[106] Indian Institute of Technology Madras, Chennai 600036, India
[107] Department of Physics and Astronomy, Vrije Universiteit Amsterdam, 1081 HV Amsterdam, The Netherlands
[108] Lomonosov Moscow State University, Moscow 119991, Russia
[109] Katholieke Universiteit Leuven, Oude Markt 13, 3000 Leuven, Belgium
[110] Rochester Institute of Technology, Rochester, NY 14623, USA
[111] Université libre de Bruxelles, 1050 Bruxelles, Belgium
[112] Bar-Ilan University, Ramat Gan, 5290002, Israel
[113] Université Côte d'Azur, Observatoire de la Côte d'Azur, CNRS, Artemis, F-06304 Nice, France
[114] University of British Columbia, Vancouver, BC V6T 1Z4, Canada
[115] OzGrav, University of Adelaide, Adelaide, South Australia 5005, Australia
[116] Centre national de la recherche scientifique, 75016 Paris, France
[117] Univ Rennes, CNRS, Institut FOTON—UMR 6082, F-35000 Rennes, France
[118] University of Birmingham, Birmingham, B15 2TT, UK
[119] Washington State University, Pullman, WA 99164, USA
[120] Cornell University, Ithaca, NY 14850, USA
[121] Laboratoire Kastler Brossel, Sorbonne Université, CNRS, ENS-Université PSL, Collège de France, F-75005 Paris, France

[122] Christopher Newport University, Newport News, VA 23606, USA
[123] OzGrav, University of Melbourne, Parkville, Victoria 3010, Australia
[124] Astronomical Observatory Warsaw University, 00-478 Warsaw, Poland
[125] University of Maryland, College Park, MD 20742, USA
[126] Università degli Studi di Milano-Bicocca, I-20126 Milano, Italy
[127] INFN, Sezione di Milano-Bicocca, I-20126 Milano, Italy
[128] Université de Lyon, Université Claude Bernard Lyon 1, CNRS, Institut Lumière Matière, F-69622 Villeurbanne, France
[129] University of Chicago, Chicago, IL 60637, USA
[130] University of Arizona, Tucson, AZ 85721, USA
[131] INFN, Sezione di Napoli, Gruppo Collegato di Salerno, I-80126 Napoli, Italy
[132] University of Massachusetts Dartmouth, North Dartmouth, MA 02747, USA
[133] Niels Bohr Institute, Copenhagen University, 2100 København, Denmark
[134] Universidad de Guadalajara, 44430, Guadalajara, Jalisco, Mexico
[135] Istituto di Astrofisica e Planetologia Spaziali di Roma, 00133 Roma, Italy
[136] Colorado State University, Fort Collins, CO 80523, USA
[137] Departamento de Astronomía y Astrofísica, Universitat de València, E-46100 Burjassot, València, Spain
[138] Observatori Astronòmic, Universitat de València, E-46980 Paterna, València, Spain
[139] Niels Bohr Institute, University of Copenhagen, 2100 Kóbenhavn, Denmark
[140] National Central University, Taoyuan City 320317, Taiwan
[141] National Tsing Hua University, Hsinchu City 30013, Taiwan
[142] OzGrav, Charles Sturt University, Wagga Wagga, New South Wales 2678, Australia
[143] Vanderbilt University, Nashville, TN 37235, USA
[144] University of Chinese Academy of Sciences/International Centre for Theoretical Physics Asia-Pacific, Bejing 100190, People's Republic of China
[145] Department of Electrophysics, National Yang Ming Chiao Tung University, 101 University Street, Hsinchu, Taiwan
[146] Kamioka Branch, National Astronomical Observatory of Japan, 238 Higashi-Mozumi, Kamioka-cho, Hida City, Gifu 506-1205, Japan
[147] University of Texas, Austin, TX 78712, USA
[148] CaRT, California Institute of Technology, Pasadena, CA 91125, USA
[149] Northeastern University, Boston, MA 02115, USA
[150] Dipartimento di Ingegneria Industriale (DIIN), Università di Salerno, I-84084 Fisciano, Salerno, Italy
[151] Faculty of Science, University of Toyama, 3190 Gofuku, Toyama City, Toyama 930-8555, Japan
[152] Carleton College, Northfield, MN 55057, USA
[153] University of Szeged, Dóm tér 9, Szeged 6720, Hungary
[154] OzGrav, Swinburne University of Technology, Hawthorn VIC 3122, Australia
[155] INFN Cagliari, Physics Department, Università degli Studi di Cagliari, Cagliari 09042, Italy
[156] Università degli Studi di Cagliari, Via Università 40, 09124 Cagliari, Italy
[157] Université Libre de Bruxelles, Brussels 1050, Belgium
[158] INAF, Osservatorio Astronomico di Brera sede di Merate, I-23807 Merate, Lecco, Italy
[159] Departamento de Matemáticas, Universitat de València, E-46100 Burjassot, València, Spain
[160] Montana State University, Bozeman, MT 59717, USA
[161] The University of Utah, Salt Lake City, UT 84112, USA
[162] Johns Hopkins University, Baltimore, MD 21218, USA
[163] University of Rhode Island, Kingston, RI 02881, USA
[164] The University of Texas Rio Grande Valley, Brownsville, TX 78520, USA
[165] Université de Liège, B-4000 Liège, Belgium
[166] DIFA—Alma Mater Studiorum Università di Bologna, Via Zamboni, 33 - 40126 Bologna, Italy
[167] Istituto Nazionale Di Fisica Nucleare—Sezione di Bologna, viale Carlo Berti Pichat 6/2 - 40127 Bologna, Italy
[168] University of Manitoba, Winnipeg, MB R3T 2N2, Canada
[169] INFN-CNAF—Bologna, Viale Carlo Berti Pichat, 6/2, 40127, Bologna BO, Italy
[170] Università degli Studi di Sassari, I-07100 Sassari, Italy
[171] INFN, Laboratori Nazionali del Sud, I-95125 Catania, Italy
[172] Université de Normandie, ENSICAEN, UNICAEN, CNRS/IN2P3, LPC Caen, F-14000 Caen, France
[173] Laboratoire de Physique Corpusculaire Caen, 6 boulevard du maréchal Juin, F-14050 Caen, France
[174] The University of Sheffield, Sheffield, S10 2TN, UK
[175] Université Claude Bernard Lyon 1, CNRS, Laboratoire des Matériaux Avancés (LMA), IP2I Lyon/IN2P3, UMR 5822, F-69622 Villeurbanne, France
[176] Università di Firenze, Sesto Fiorentino I-50019, Italy
[177] IGFAE, Universidade de Santiago de Compostela, E-15782 Santiago de Compostela, Spain
[178] Dipartimento di Scienze Matematiche, Fisiche e Informatiche, Università di Parma, I-43124 Parma, Italy
[179] INFN, Sezione di Milano Bicocca, Gruppo Collegato di Parma, I-43124 Parma, Italy
[180] California State University, Los Angeles, Los Angeles, CA 90032, USA
[181] Marquette University, Milwaukee, WI 53233, USA
[182] Perimeter Institute, Waterloo, ON N2L 2Y5, Canada
[183] Corps des Mines, Mines Paris, Université PSL, 60 Boulevard Saint-Michel, 75272 Paris, France
[184] Dipartimento di Fisica, Università di Trieste, I-34127 Trieste, Italy
[185] Université Côte d'Azur, Observatoire de la Côte d'Azur, CNRS, Lagrange, F-06304 Nice, France
[186] National Center for Nuclear Research, 05-400 Świerk-Otwock, Poland
[187] Vrije Universiteit Brussel, 1050 Brussel, Belgium
[188] University of Zurich, Winterthurerstrasse 190, 8057 Zurich, Switzerland
[189] Canadian Institute for Theoretical Astrophysics, University of Toronto, Toronto, ON M5S 3H8, Canada
[190] Stony Brook University, Stony Brook, NY 11794, USA
[191] Center for Computational Astrophysics, Flatiron Institute, New York, NY 10010, USA
[192] Montclair State University, Montclair, NJ 07043, USA
[193] HUN-REN Institute for Nuclear Research, H-4026 Debrecen, Hungary
[194] Indian Institute of Technology Bombay, Powai, Mumbai 400 076, India
[195] Centro de Física das Universidades do Minho e do Porto, Universidade do Minho, PT-4710-057 Braga, Portugal
[196] Aix Marseille Univ, CNRS/IN2P3, CPPM, Marseille, France
[197] CNR-SPIN, I-84084 Fisciano, Salerno, Italy

[198] Scuola di Ingegneria, Università della Basilicata, I-85100 Potenza, Italy
[199] Western Washington University, Bellingham, WA 98225, USA
[200] SUPA, University of the West of Scotland, Paisley PA1 2BE, UK
[201] Barry University, Miami Shores, FL 33168, USA
[202] Eötvös University, Budapest 1117, Hungary
[203] Institute for Cosmic Ray Research, KAGRA Observatory, The University of Tokyo, 5-1-5 Kashiwa-no-Ha, Kashiwa City, Chiba 277-8582, Japan
[204] Department of Physics, Graduate School of Science, Osaka Metropolitan University, 3-3-138 Sugimoto-cho, Sumiyoshi-ku, Osaka City, Osaka 558-8585, Japan
[205] University of Sannio at Benevento, I-82100 Benevento, Italy and INFN, Sezione di Napoli, I-80100 Napoli, Italy
[206] University of California, Berkeley, CA 94720, USA
[207] Instituto de Fisica Teorica UAM-CSIC, Universidad Autonoma de Madrid, 28049 Madrid, Spain
[208] Laboratoire d'Acoustique de l'Université du Mans, UMR CNRS 6613, F-72085 Le Mans, France
[209] University of Southampton, Southampton, SO17 1BJ, UK
[210] University of California, Riverside, Riverside, CA 92521, USA
[211] Dipartimento di Ingegneria Industriale, Elettronica e Meccanica, Università degli Studi Roma Tre, I-00146 Roma, Italy
[212] University of Nevada, Las Vegas, NV 89154, USA
[213] University of Nottingham NG7 2RD, UK
[214] Ariel University, Ramat HaGolan St 65, Ari'el, Israel
[215] The University of Mississippi, University, MS 38677, USA
[216] Graduate School of Science, Institute of Science Tokyo, 2-12-1 Ookayama, Meguro-ku, Tokyo 152-8551, Japan
[217] Institute of Physics, Academia Sinica, 128 Sec. 2, Academia Road, Nankang, Taipei 11529, Taiwan
[218] The Chinese University of Hong Kong, Shatin, NT, Hong Kong
[219] American University, Washington, DC 20016, USA
[220] Dipartimento di Fisica, Università degli studi di Milano, Via Celoria 16, I-20133, Milano, Italy
[221] INFN, sezione di Milano, Via Celoria 16, I-20133, Milano, Italy
[222] Department of Applied Physics, Fukuoka University, 8-19-1 Nanakuma, Jonan, Fukuoka City, Fukuoka 814-0180, Japan
[223] University of Cambridge, Cambridge, CB2 1TN, UK
[224] University of Lancaster, Lancaster, LA1 4YW, UK
[225] College of Industrial Technology, Nihon University, 1-2-1 Izumi, Narashino City, Chiba 275-8575, Japan
[226] Faculty of Engineering, Niigata University, 8050 Ikarashi-2-no-cho, Nishi-ku, Niigata City, Niigata 950-2181, Japan
[227] Department of Physics and Astronomy, Haverford College, 370 Lancaster Avenue, Haverford, PA 19041, USA
[228] Department of Physics, Tamkang University, No. 151, Yingzhuan Road, Danshui Dist., New Taipei City 25137, Taiwan
[229] Rutherford Appleton Laboratory, Didcot, OX11 0DE, UK
[230] Department of Physical Sciences, Aoyama Gakuin University, 5-10-1 Fuchinobe, Sagamihara City, Kanagawa 252-5258, Japan
[231] Helmut Schmidt University, D-22043 Hamburg, Germany
[232] Nambu Yoichiro Institute of Theoretical and Experimental Physics (NITEP), Osaka Metropolitan University, 3-3-138 Sugimoto-cho, Sumiyoshi-ku, Osaka City, Osaka 558-8585, Japan
[233] Directorate of Construction, Services & Estate Management, Mumbai 400094, India
[234] Observatoire Astronomique de Strasbourg, 11 Rue de l'Université, 67000 Strasbourg, France
[235] Faculty of Physics, University of Białystok, 15-245 Białystok, Poland
[236] National Astronomical Observatories, Chinese Academic of Sciences, 20A Datun Road, Chaoyang District, Beijing, People's Republic of China
[237] School of Astronomy and Space Science, University of Chinese Academy of Sciences, 20A Datun Road, Chaoyang District, Beijing, People's Republic of China
[238] Sungkyunkwan University, Seoul 03063, Republic of Korea
[239] Department of Physics, Ulsan National Institute of Science and Technology (UNIST), 50 UNIST-gil, Ulju-gun, Ulsan 44919, Republic of Korea
[240] Institute for Cosmic Ray Research, The University of Tokyo, 5-1-5 Kashiwa-no-Ha, Kashiwa City, Chiba 277-8582, Japan
[241] Chung-Ang University, Seoul 06974, Republic of Korea
[242] University of Washington Bothell, Bothell, WA 98011, USA
[243] Laboratoire de Physique et de Chimie de l'Environnement, Université Joseph KI-ZERBO, 9GH2+3V5, Ouagadougou, Burkina Faso
[244] Ewha Womans University, Seoul 03760, Republic of Korea
[245] National Institute for Mathematical Sciences, Daejeon 34047, Republic of Korea
[246] Korea Astronomy and Space Science Institute, Daejeon 34055, Republic of Korea
[247] Department of Astronomy and Space Science, Chungnam National University, 9 Daehak-ro, Yuseong-gu, Daejeon 34134, Republic of Korea
[248] Institute of Particle and Nuclear Studies (IPNS), High Energy Accelerator Research Organization (KEK), 1-1 Oho, Tsukuba City, Ibaraki 305-0801, Japan
[249] Division of Science, National Astronomical Observatory of Japan, 2-21-1 Osawa, Mitaka City, Tokyo 181-8588, Japan
[250] Nagoya University, Nagoya, 464-8601, Japan
[251] Department of Physics, Aristotle University of Thessaloniki, 54124 Thessaloniki, Greece
[252] Bard College, Annandale-On-Hudson, NY 12504, USA
[253] Technical University of Braunschweig, D-38106 Braunschweig, Germany
[254] Institute of Mathematics, Polish Academy of Sciences, 00656 Warsaw, Poland
[255] Astronomical Observatory, Jagiellonian University, 31-007 Cracow, Poland
[256] Department of Physics and Astronomy, University of Padova, Via Marzolo, 8-35151 Padova, Italy
[257] Sezione di Padova, Istituto Nazionale di Fisica Nucleare (INFN), Via Marzolo, 8-35131 Padova, Italy
[258] Department of Physics, Nagoya University, ES building, Furocho, Chikusa-ku, Nagoya, Aichi 464-8602, Japan
[259] Université de Montréal/Polytechnique, Montreal, Quebec H3T 1J4, Canada
[260] Indian Institute of Science Education and Research, Kolkata, Mohanpur, West Bengal 741252, India
[261] Seoul National University, Seoul 08826, Republic of Korea
[262] Department of Computer Simulation, Inje University, 197 Inje-ro, Gimhae, Gyeongsangnam-do 50834, Republic of Korea
[263] NAVIER, École des Ponts, Univ Gustave Eiffel, CNRS, Marne-la-Vallée, France
[264] Gravitational Wave Science Project, National Astronomical Observatory of Japan (NAOJ), Mitaka City, Tokyo 181-8588, Japan
[265] Department of Physics, National Cheng Kung University, No.1, University Road, Tainan City 701, Taiwan
[266] St. Thomas University, Miami Gardens, FL 33054, USA
[267] Scuola Normale Superiore, I-56126 Pisa, Italy
[268] Institució Catalana de Recerca i Estudis Avançats, E-08010 Barcelona, Spain
[269] Institut de Física d'Altes Energies, E-08193 Barcelona, Spain
[270] Institut fuer Theoretische Astrophysik, Zentrum fuer Astronomie Heidelberg, Universitaet Heidelberg, Albert Ueberle Str. 2, 69120 Heidelberg, Germany
[271] Institucio Catalana de Recerca i Estudis Avançats (ICREA), Passeig de Lluís Companys, 23, 08010 Barcelona, Spain
[272] NASA Goddard Space Flight Center, Greenbelt, MD 20771, USA

[273] Center for Research and Exploration in Space Science and Technology, NASA/GSFC, Greenbelt, MD 20771, USA
[274] Research Center for Space Science, Advanced Research Laboratories, Tokyo City University, 3-3-1 Ushikubo-Nishi, Tsuzuki-Ku, Yokohama, Kanagawa 224-8551, Japan
[275] Tsinghua University, Beijing 100084, People's Republic of China
[276] Institut des Hautes Etudes Scientifiques, F-91440 Bures-sur-Yvette, France
[277] Faculty of Law, Ryukoku University, 67 Fukakusa Tsukamoto-cho, Fushimi-ku, Kyoto City, Kyoto 612-8577, Japan
[278] Phenikaa Institute for Advanced Study (PIAS), Phenikaa University, Yen Nghia, Ha Dong, Hanoi, Vietnam
[279] University of Stavanger, 4021 Stavanger, Norway
[280] Physics Program, Graduate School of Advanced Science and Engineering, Hiroshima University, 1-3-1 Kagamiyama, Higashihiroshima City, Hiroshima 739-8526, Japan
[281] GRAPPA, Anton Pannekoek Institute for Astronomy and Institute for High-Energy Physics, University of Amsterdam, 1098 XH Amsterdam, Netherlands
[282] University College London, London, WC1E 6BT, UK
[283] Observatoire de Paris, 75014 Paris, France
[284] Laboratoire Univers et Théories, Observatoire de Paris, 92190 Meudon, France
[285] Graduate School of Science and Technology, Niigata University, 8050 Ikarashi-2-no-cho, Nishi-ku, Niigata City, Niigata 950-2181, Japan
[286] University of Maryland, Baltimore County, Baltimore, MD 21250, USA
[287] CSIR-Central Glass and Ceramic Research Institute, Kolkata, West Bengal 700032, India
[288] Consiglio Nazionale delle Ricerche—Istituto dei Sistemi Complessi, I-00185 Roma, Italy
[289] Department of Astronomy, Yonsei University, 50 Yonsei-Ro, Seodaemun-Gu, Seoul 03722, Republic of Korea
[290] Department of Physics, University of Guadalajara, Av. Revolucion 1500, Colonia Olimpica C.P. 44430, Guadalajara, Jalisco, Mexico
[291] Hobart and William Smith Colleges, Geneva, NY 14456, USA
[292] INAF, Osservatorio Astronomico di Padova, I-35122 Padova, Italy
[293] Dipartimento di Ingegneria, Università del Sannio, I-82100 Benevento, Italy
[294] Museo Storico della Fisica e Centro Studi e Ricerche "Enrico Fermi", I-00184 Roma, Italy
[295] Kennesaw State University, Kennesaw, GA 30144, USA
[296] Subatech, CNRS/IN2P3—IMT Atlantique—Nantes Université, 4 rue Alfred Kastler BP 20722 44307 Nantes CÉDEX 03, France
[297] Universidad de Antioquia, Medellín, Colombia
[298] Departamento de Física—ETSIDI, Universidad Politécnica de Madrid, 28012 Madrid, Spain
[299] Department of Electronic Control Engineering, National Institute of Technology, Nagaoka College, 888 Nishikatakai, Nagaoka City, Niigata 940-8532, Japan
[300] Trinity College, Hartford, CT 06106, USA
[301] Dipartimento di Fisica e Scienze della Terra, Università Degli Studi di Ferrara, Via Saragat, 1, 44121, Ferrara FE, Italy
[302] Faculty of Science, Toho University, 2-2-1 Miyama, Funabashi City, Chiba 274-8510, Japan
[303] Indian Institute of Technology, Palaj, Gandhinagar, Gujarat 382355, India
[304] Kavli Institute for Astronomy and Astrophysics, Peking University, Yiheyuan Road 5, Haidian District, Beijing 100871, People's Republic of China
[305] Laboratoire MSME, Cité Descartes, 5 Boulevard Descartes, Champs-sur-Marne, 77454, Marne-la-Vallée Cedex 2, France
[306] Faculty of Information Science and Technology, Osaka Institute of Technology, 1-79-1 Kitayama, Hirakata City, Osaka 573-0196, Japan
[307] Faculty of Science and Technology, Kochi University, 2-5-1 Akebono-cho, Kochi-shi, Kochi 780-8520, Japan
[308] Laboratoire de Physique de l'École Normale Supérieure, ENS, (CNRS, Université PSL, Sorbonne Université, Université Paris Cité), F-75005 Paris, France
[309] Faculty of Physics, University of Warsaw, Ludwika Pasteura 5, 02-093 Warszawa, Poland
[310] Laser Interferometry and Gravitational Wave Astronomy, Max Planck Institute for Gravitational Physics, Callinstrasse 38, 30167 Hannover, Germany
[311] The Hakubi Center for Advanced Research, Kyoto University, Yoshida-honmachi, Sakyou-ku, Kyoto City, Kyoto 606-8501, Japan
[312] Department of Physics, Kyoto University, Kita-Shirakawa Oiwake-cho, Sakyou-ku, Kyoto City, Kyoto 606-8502, Japan
[313] Yukawa Institute for Theoretical Physics (YITP), Kyoto University, Kita-Shirakawa Oiwake-cho, Sakyou-ku, Kyoto City, Kyoto 606-8502, Japan
[314] University of Catania, Department of Physics and Astronomy, Via S. Sofia, 64, 95123, Catania CT, Italy
[315] National Institute of Technology, Fukui College, Geshi-cho, Sabae-shi, Fukui 916-8507, Japan
[316] Department of Communications Engineering, National Defense Academy of Japan, 1-10-20 Hashirimizu, Yokosuka City, Kanagawa 239-8686, Japan
[317] Eindhoven University of Technology, 5600 MB Eindhoven, Netherlands
[318] Kavli Institute for the Physics and Mathematics of the Universe (Kavli IPMU), WPI, The University of Tokyo, 5-1-5 Kashiwa-no-Ha, Kashiwa City, Chiba 277-8583, Japan
[319] Department of Astronomy, Beijing Normal University, Xinjiekouwai Street 19, Haidian District, Beijing 100875, People's Republic of China
[320] School of Physics and Technology, Wuhan University, Bayi Road 299, Wuchang District, Wuhan, Hubei 430072, People's Republic of China
[321] School of Natural Sciences, University of Tasmania, Hobart, Australia
[322] Instituto de Astronomía Teórica y Experimental, CONICET-UNC, Laprida 854, X5000BGR—Córdoba, Argentina
[323] Facultad de Matemática, Astronomía, Física y Computación, UNC. Av. Medina Allende s/n, Ciudad Universitaria, CP:X5000HUA—Córdoba, Argentina
[324] Instituto Argentino de Radioastronomía (CCT La Plata, CONICET; CICPBA; UNLP), C.C.5, (1894) Villa Elisa, Buenos Aires, Argentina
[325] Department of Space, Earth and Environment, Chalmers University of Technology, SE-412 96 Gothenburg, Sweden
[326] Facultad de Ciencias Astronómicas y Geofísicas, Universidad Nacional de La Plata, Paseo del Bosque, B1900FWA La Plata, Argentina
Received 2026 January 20; revised 2026 April 1; accepted 2026 April 4; published 2026 June 19

Abstract

Among known neutron stars, the Vela pulsar is one of the best targets for gravitational-wave searches. It is also one of the most prolific in terms of glitches, which are sudden frequency changes in a pulsar's rotation. Such glitches could cause a variety of transient gravitational-wave signals. Here, we search for signals associated with a Vela glitch on 2024 April 29 in data of the two LIGO detectors from the fourth LIGO–Virgo–KAGRA observing

[327] Deceased, March 2026.
[328] Deceased, September 2024.
[329] Deceased, August 2025.

Original content from this work may be used under the terms of the Creative Commons Attribution 4.0 licence. Any further distribution of this work must maintain attribution to the author(s) and the title of the work, journal citation and DOI.

run. We search both for seconds-scale burst-like emission, primarily from fundamental (f-)mode oscillations, and for longer quasi-monochromatic transients up to 4 months in duration, primarily from quasi-static quadrupolar deformations. We find no significant detection candidates, but for the first time we set direct observational upper limits on gravitational strain amplitude that are stricter than what can be indirectly inferred from the overall glitch energy scale. We discuss the short- and long-duration observational constraints in the context of specific emission models. These results demonstrate the potential of gravitational-wave probes of glitching pulsars as detector sensitivity continues to improve.

Unified Astronomy Thesaurus concepts: Pulsars (1306); Gravitational wave astronomy (675); Interdisciplinary astronomy (804); Neutron stars (1108)

1. Introduction

Pulsar glitches are sudden, enigmatic jumps in a pulsar's spin frequency, which have been observed so far in over 200 pulsars (C. M. Espinoza et al. 2011; M. Yu et al. 2013; A. Basu et al. 2022). They generally involve an initial rapid change in frequency and frequency derivative (on timescales of less than a minute) followed by a more gradual (on timescales of up to months) relaxation toward the previous spin-down state (D. Antonopoulou et al. 2022). While the common view is that glitches are linked to an exchange of angular momentum between an interior superfluid component and the crust of a neutron star (NS), the quantitative details are still an open question. Diverse mechanisms such as vortex avalanches, fluid instabilities, and crust-quakes have been invoked as possible triggers (see B. Haskell & A. Melatos 2015; S. Zhou et al. 2022, for reviews).

Glitches are key tools for studying NS interiors (B. Link et al. 1992, 2000; B. Haskell 2018) and could also trigger various types of gravitational-wave (GW) emission: both transient signals linked to the initial jump and longer-lived signals linked to the relaxation (N. Andersson & K. D. Kokkotas 1998; C. A. van Eysden & A. Melatos 2008; M. F. Bennett et al. 2010; R. Prix et al. 2011; L. Keer & D. I. Jones 2015; A. Melatos et al. 2015; A. Singh 2017; W. C. G. Ho et al. 2020; G. Yim & D. I. Jones 2020, 2023; T. Cheunchitra et al. 2024; B. Haskell & D. I. Jones 2024; O. H. Wilson & W. C. G. Ho 2024; G. Yim et al. 2024). Studying these signals can constrain the NS mass and radius, and hence the nuclear matter equation of state.

Among the known pulsar population, the Vela pulsar has some of the largest and most frequent glitches (J. R. Fuentes et al. 2017). It is also relatively close to Earth at a distance of 287^{+19}_{-17} pc (R. Dodson et al. 2003). For these reasons, it has been identified in several studies (D. Lopez et al. 2022; J. Moragues et al. 2023; G. Yim et al. 2024) as a priority target to search for glitch-associated transient GWs.

Here, we present a set of searches for GW emission associated with the 2024 April 29 glitch of the Vela pulsar, first observed (E. Zubieta et al. 2024a, 2025) by the Argentine Institute of Radio Astronomy (IAR; E. Zubieta et al. 2023) and subsequently confirmed by several other observatories and precisely timed (J. Palfreyman 2024) by the Mount Pleasant Radio Observatory (MPRO) of the University of Tasmania. This glitch happened during the LIGO–Virgo–KAGRA (LVK) fourth observing run (O4), shortly after the two LIGO detectors (J. Aasi et al. 2015) had restarted observations for the second part (O4b) of the run and were joined also by Virgo (F. Acernese et al. 2015). The electromagnetic (EM) observations of the glitch are summarized in Section 2 and the GW dataset is described in Section 3.

To cover a range of glitch-related GW emission scenarios (see B. Haskell & D. I. Jones 2024 for a review), our searches fall into two categories. First, we search for transient GW bursts that may be triggered by the initial rapid rise in frequency, on dynamical timescales of milliseconds to seconds, primarily from f-mode oscillations at kHz frequencies, in Section 4. Second, we cover longer-duration (up to 4 months) quasi-monochromatic signals at lower frequencies, coupled with the pulsar spin frequency and associated with the postglitch relaxation, in Section 5. Even longer signals are well covered by standard continuous wave (CW) searches (for latest O4a+b results see A. G. Abac et al. 2026a). Details of the emission models are included in each of these sections.

Previous searches for GWs from pulsar glitches have included an f-mode burst search on the 2006 August Vela glitch using initial LIGO data (J. Abadie et al. 2011), various all-sky burst searches (latest O4a results: A. G. Abac et al. 2026, 2025c), and long-duration searches on O2 data (D. Keitel et al. 2019; L. M. Modafferi et al. 2023), including the 2016 Vela glitch (J. Palfreyman et al. 2018), and O3 data (L. M. Modafferi et al. 2021; R. Abbott et al. 2022a, not including a Vela glitch). However, matching the studies of detection prospects for the two cases by D. Lopez et al. (2022) and J. Moragues et al. (2023), none of these searches has yet been able to make a GW detection or to place physically constraining observational upper limits below the energy scale indirectly set by the glitch size. Searches for NS f-modes have also been performed on bursting magnetars, with no detection yet either (e.g., A. G. Abac et al. 2024; R. Abbott et al. 2024).

The improved sensitivity of the LIGO O4 data (D. Ganapathy et al. 2023; W. Jia et al. 2024; E. Capote et al. 2025) now gives us for the first time the opportunity to reach physically constraining results on GWs from a pulsar glitch. We discuss their implications for pulsar glitch models and GW emission channels in Section 6 and present our conclusions in Section 7.

2. The Vela Pulsar and its 2024 Glitch

The Vela Pulsar (PSR B0833−45/J0835−4510), discovered by M. I. Large et al. (1968), was the first pulsar known to glitch (V. Radhakrishnan & R. N. Manchester 1969). It is young ($\sim 10^4$ yr) and one of the most active pulsars in terms of glitching, with 23 large glitches (often considered as those with relative frequency changes $\Delta f_{\rm rot}/f_{\rm rot} > 10^{-7}$, C. M. Espinoza et al. 2011; M. Yu et al. 2013; A. Basu et al. 2022) reported so far—approximately once every two to three years (P. E. Reichley & G. S. Downs 1969; R. Dodson et al. 2007). It also exhibits microglitches sporadically (J. M. Cordes et al. 1988; C. M. Espinoza et al. 2021; L. Dunn et al. 2023; E. Zubieta et al. 2024b).

During O4, the Vela pulsar has been monitored with almost daily combined cadence by the IAR and MPRO.

2.1. IAR Observations

The IAR[330] was founded in 1962 as a pioneer radio observatory in South America. Located near the city of La Plata, Buenos Aires, it is located at 34°51′57″.35 S 58°08′25″.04 W. It has two 30 m diameter single-dish antennas, aligned on a north–south direction, separated by 120 m. Observing around 1400 MHz with 56 MHz and 400 MHz bandwidths simultaneously, the data is obtained with a time resolution of 146 μs.

A summary of IAR pulsar observation work and future projects is given in G. Gancio et al. (2020) and C. O. Lousto et al. (2024), and references therein. The IAR has reported the observation of the last three large Vela glitches: on 2019 February 1 with a relative frequency change of 2.7×10^{-6} (F. G. Lopez Armengol et al. 2019; G. Gancio et al. 2020), on 2021 July 22 with relative change of 1.2×10^{-6} (V. Sosa-Fiscella et al. 2021), and the 2024 April 29 glitch of interest for this paper (counted as large Vela glitch #23) first reported in E. Zubieta et al. (2024a) with $(\Delta f_{\rm rot}/f_{\rm rot}) = 2.4 \times 10^{-6}$ and a more detailed analysis given in E. Zubieta et al. (2025).

For the data used in this paper, we used the PRESTO (S. Ransom 2011) package to remove radio-frequency interference (RFI) and fold the observations. We cross-correlated the folded profile with a noise-free template profile in order to obtain the times of arrival (TOAs). We obtained the template with the tool psrsmooth in PSRCHIVE (A. W. Hotan et al. 2004) on a pulse profile with high signal-to-noise ratio (S/N).

2.2. MPRO Observations

The University of Tasmania's MPRO 26 m radio telescope is located at Mt. Pleasant, near Hobart, Australia at 42°48′12″.90 S 147°26′25″.87 E. It has previously detected several Vela glitches, including the real-time observation of the 2016 glitch with associated magnetospheric changes (J. Palfreyman et al. 2018), which suggest a connection between the magnetosphere and the internal dynamics of the pulsar that probably provokes glitches.

The center frequency of the observations used here is 2250 MHz with bandwidth 64 MHz. Processing was done using the software packages DSPSR (W. van Straten & M. Bailes 2011), TEMPO2 (G. B. Hobbs et al. 2006; R. T. Edwards et al. 2006), and PSRCHIVE, which perform phase-coherent dedispersion using 16 frequency channels and 8192 pulse phase bins over the 89.3 ms pulse period. This gives a time resolution of 10.9 μs.

2.3. Timing Model

We collected the TOAs from both observatories between Modified Julian Date (MJD) 60402.28 and MJD 60493.53 and characterized the rotation of the Vela pulsar with TEMPO2 by fitting a Taylor series

$$\phi(t) = f_{\rm rot}\,(t - T_{\rm ref}) + \frac{1}{2}\dot{f}_{\rm rot}\,(t - T_{\rm ref})^2 + \ldots. \quad (1)$$

[330] https://www.iar.unlp.edu.ar

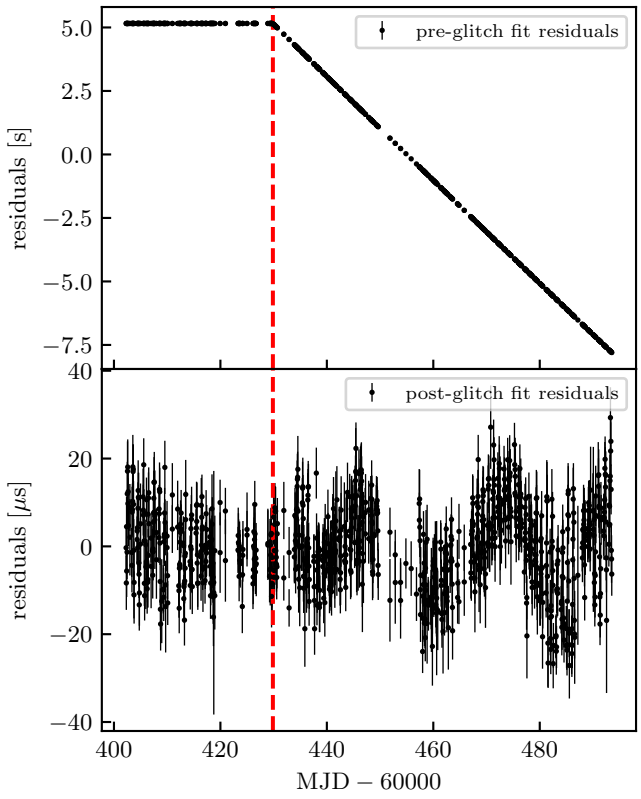

Figure 1. Top panel: Vela pulsar radio timing residuals before fitting for the 2024 April 29 glitch. Bottom panel: Timing residuals after fitting for the glitch with the parameters shown in Table 1.

The pulsar's rotation frequency is $f_{\rm rot}$, its derivatives are $\dot{f}_{\rm rot}$, $\ddot{f}_{\rm rot}$, etc., and $T_{\rm ref}$ is the reference epoch.

To characterize the glitch, we added a glitch-induced change in the rotational phase (R. T. Edwards et al. 2006; M. Yu et al. 2013) to this model

$$\phi_{\rm g}(t) = \Delta\phi + \Delta f_{\rm rot}\,(t - T_{\rm gl}) + \frac{1}{2}\Delta\dot{f}_{\rm rot}\,(t - T_{\rm gl})^2 + \sum_i \left[1 - \exp\left(-\frac{t - T_{\rm gl}}{\tau_{\rm d}^i}\right)\right]\Delta f_{\rm rot}^{d,i}\ \tau_{\rm d}^i. \quad (2)$$

Here, $T_{\rm gl}$ is the epoch of the glitch, with its uncertainty counteracted by $\Delta\phi$, while $\Delta f_{\rm rot}$ and $\Delta\dot{f}_{\rm rot}$ are the permanent parts of the changes in $f_{\rm rot}$ and $\dot{f}_{\rm rot}$ at $T_{\rm gl}$. In addition, $\Delta f_{\rm rot}^{d,i}$ are the temporary increases (recovery terms) in the rotational frequency of the pulsar that decay exponentially on a timescale $\tau_{\rm d}^i$ days.

The 2024 April 29 Vela glitch is evident from the residuals of a preglitch fit in Figure 1. We characterized the preglitch timing model by fitting Equation (1) to TOAs from 1 month of observations before the glitch. By combining the IAR and MPRO data, we found preference for three transient increase terms in the frequency of the pulsar in addition to the permanent changes $\Delta f_{\rm rot}$ and $\Delta\dot{f}_{\rm rot}$. The postfit residuals can be seen in the bottom panel of Figure 1. We then extended the data span to MJD 60357–60551, which is the full range of interest for the GW search here. With this data span, we fitted $f_{\rm rot}$, $\dot{f}_{\rm rot}$, $\ddot{f}_{\rm rot}$, and $\dddot{f}_{\rm rot}$, keeping the glitch parameters frozen. The full timing solution covering the extended range of observations is shown in Table 1. This is valid within the listed

Table 1
Parameters of the Vela Pulsar and Its 2024 Glitch

Parameter	Value
R.A.	08:35:20.61993 ± 0.00002
Decl.	−45:10:33.7232 ± 0.0003
d [pc]	287^{+19}_{-17}[a]
$T_{\rm ref}$ [days] (MJD)	60408
$T_{\rm ref}$ [s] (GPS)	1396569549
START (MJD)	60357
FINISH (MJD)	60551
$f_{\rm rot}$ [Hz]	(11.182888898688 ± 0.000000000002)
$\dot{f}_{\rm rot}$ [Hz s^{-1}]	$(-1.5541536 \pm 0.000001) \times 10^{-11}$
$\ddot{f}_{\rm rot}$ [Hz s^{-2}]	$(3.82 \pm 0.03) \times 10^{-22}$
$\dddot{f}_{\rm rot}$ [Hz s^{-3}]	$(1.283 \pm 0.07) \times 10^{-28}$
$T_{\rm gl}$ [d] (MJD)	60429.86975 ± 0.00139
$T_{\rm gl}$ [s] (GPS)	1398459095.216 ± 120.096
$\Delta\phi$	−0.00034 ± 0.00017
$\Delta f_{\rm rot}$ [Hz]	$(2.65854 \pm 0.00005) \times 10^{-5}$
$\Delta\dot{f}_{\rm rot}$ [Hz s^{-1}]	$(-1.0298 \pm 0.0009) \times 10^{-13}$
$\Delta\ddot{f}_{\rm rot}$ [Hz s^{-2}]	…
τ_d^1 [d]	15.1 ± 0.1
$\Delta f_{\rm rot}^{d,1}$ [Hz]	$(1.501 \pm 0.004) \times 10^{-7}$
τ_d^2 [d]	2.45 ± 0.06
$\Delta f_{\rm rot}^{d,2}$ [Hz]	$(1.24 \pm 0.03) \times 10^{-7}$
τ_d^3 [d]	0.39 ± 0.03
$\Delta f_{\rm rot}^{d,3}$ [Hz]	$(1.8 \pm 0.1) \times 10^{-7}$

Notes. All other values were derived from IAR and MPRO observations, as described in Section 2. Reference time and glitch epoch (at the solar system barycenter) are given in both MJD (terrestrial time standard), as is conventional in radio astronomy, and in GPS seconds (UTC standard) for LVK data analysis. $T_{\rm gl}$ is given to the precision ingested by burst analyses.
[a] R. Dodson et al. (2003).

START and FINISH dates, and hence the listed $\ddot{f}_{\rm rot}$ should not be interpreted as giving the long term braking index (see A. F. Vargas & A. Melatos 2023).

3. GW Data

The O4 run of the advanced laser-interferometric GW detectors began on 2023 May 27 and, after a commissioning break with several interventions to further improve sensitivity, its second part O4b ran from 2024 April 10 to 2025 January 28. In O4b, the two LIGO detectors (J. Aasi et al. 2015) in Hanford (Washington, US) and Livingston (Louisiana, US) and the Virgo detector (F. Acernese et al. 2015) in Cascina (Italy) participated. KAGRA (T. Akutsu et al. 2021) in Japan rejoined O4 later. The upgrades to LIGO for O4 allowed it to reach unprecedented GW strain sensitivity (D. Ganapathy et al. 2023; W. Jia et al. 2024; E. Capote et al. 2025).

At the time of the Vela glitch on 2024 April 29, the LIGO Hanford (H1), LIGO Livingston (L1), and Virgo (V1) detectors were all operating in a stable state; see Figure 2. The burst-type searches in Section 4 use data within two days of the glitch time. The coincident data taking of the two LIGO detectors with similar sensitivity across most of the frequency band was essential because a single-detector search of this type loses an order of magnitude in sensitivity (e.g., M. Ball & R. Frey 2025) due to missing suppression capability toward instrumental glitches (not to be confused with pulsar glitches).

The longer-duration searches in Section 5 cover a maximum extent starting one day before the glitch epoch and ending on 2024 August 28. For part of this time stretch, only L1 data are available because H1 had to be taken offline to diagnose and repair a problem in the output optics chain from 13 July to 24 August and V1 went into a downtime for limiting noise factors from 22 July to 2 August. The analyzable LIGO data segments (E. Goetz & K. Riles 2024) over this extended timescale are also shown in Figure 2.

Due to the large difference in sensitivity, in terms of the detectors' Amplitude Spectral Densities (ASDs), Virgo data is not used in this paper. From LIGO, we use data from the `GDS-CALIB_STRAIN_CLEAN` frame channel, corresponding to the standard online calibration (A. Viets et al. 2018; L. Sun et al. 2020, 2021; M. Wade et al. 2025) with some noise subtraction applied (G. Vajente et al. 2020; A. Viets & M. Wade 2021; A. G. Abac et al. 2026c). For several searches in Section 5, additional time-domain removal of large noise excursions was performed (P. Astone et al. 2005; D. Davis et al. 2025) before creating Fourier-domain data products as described later for each analysis method. Data quality has been investigated with methods similar to those described for O4a in S. Soni et al. (2025).

4. Searches for GW Bursts

In the context of this paper, we refer to any signals that last from milliseconds up to, at most, a few minutes as "GW bursts." The main physical emission channel considered are NS f-modes excited by the glitch and damping away again on the signal timescale (N. Andersson & K. D. Kokkotas 1998). However, all three search methods that we use here are unmodeled or very weakly modeled, i.e., they do not rely on matched filtering. Thus, they are also sensitive to other emission mechanisms in the same time and frequency ranges. The allowed signal durations and the on-source windows (time range in which the signal might start) for the three methods are summarized in Figure 3. Here, the glitch time is the GPS time at the detector.

These, or similar, methods have been routinely used for all-sky GW burst searches in LVK data (e.g., R. Abbott et al. 2021a, 2021b; A. G. Abac et al. 2026, 2025c), which would have also been sensitive to signals from pulsar glitches with sufficiently high amplitudes (D. Lopez et al. 2022), and also for analyzing bursting magnetars (e.g., A. G. Abac et al. 2024; R. Abbott et al. 2024). However, the last targeted search for GW bursts from a pulsar glitch dates back to the era of the initial LIGO detectors, when the 2006 Vela glitch was analyzed (J. Abadie et al. 2011) using the two Hanford detectors available at the time. With the two Advanced LIGO detectors and improved analysis methods, we now obtain results that are orders of magnitude better than that study.

In this section, after briefly discussing the f-mode scenario, we introduce the three pipelines used and summarize their results. They cover different time and frequency ranges to increase robustness to different emission scenarios. For each search, after finding no significant candidates, we conduct injections of simulated signals into the GW data to estimate search sensitivity and provide upper limits; this is discussed in Section 4.5. A detailed interpretation is given in Section 6.

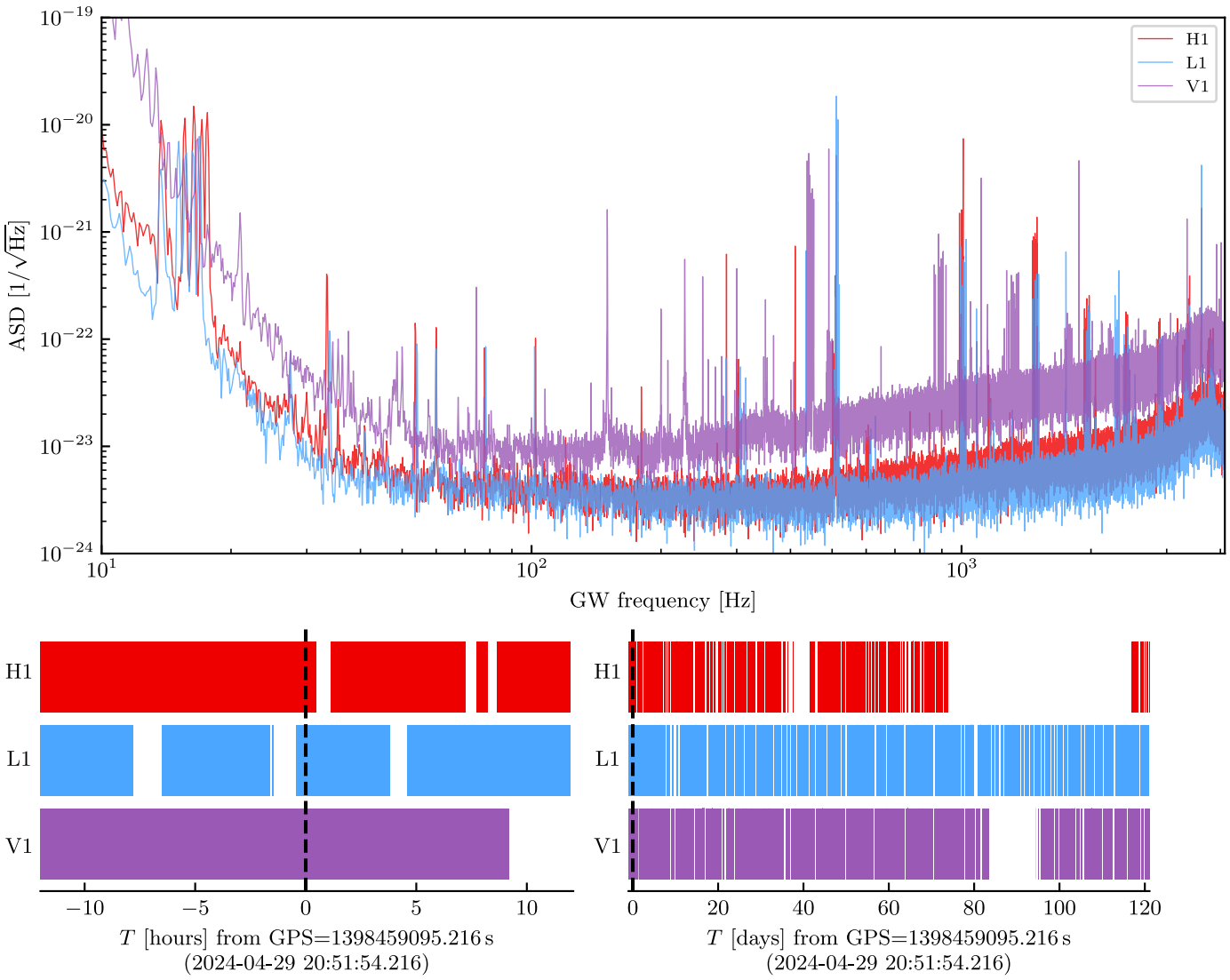

Figure 2. Top panel: GW detector sensitivities within $T_{gl} \pm 20$ s around the Vela glitch on 2024 April 29 in terms of their ASDs (computed with the Welch method in `gwpy`, D. M. Macleod et al. 2021). Bottom left panel: GW data availability over 24 hr around the glitch, as used for the burst searches in Section 4. Bottom right panel: LIGO data availability for the four following months, as used in the long-duration searches in Section 5. Virgo data is not used in either type of search. The glitch time is highlighted in the two bottom panels with a vertical dashed line.

4.1. Emission Models

Glitching pulsars can emit short-duration GW signals via mechanisms such as an avalanche of unpinning superfluid vortices (see, e.g., L. Warszawski & A. Melatos 2012; F. De Lillo et al. 2023, and references therein) or oscillation modes of the NS (N. Andersson & K. D. Kokkotas 1998; L. Keer & D. I. Jones 2015; G. Yim & D. I. Jones 2023; O. H. Wilson & W. C. G. Ho 2024).

The situation is complicated because NSs can support a variety of oscillations modes, classified according to the dominant restoring force, e.g., pressure, buoyancy, or rotation (K. D. Kokkotas & B. G. Schmidt 1999). We mostly focus on the fundamental (f-)modes, which are good candidates for our searches for several reasons: they are well understood, with frequencies depending only on the gross features of the NS equation of state, typically in the kHz range accessible by LVK detectors; they are also extremely efficient GW emitters, in the sense that almost all energy deposited in the mode by the glitch is emitted in quadrupolar GWs, with very little energy loss to viscosity (F. Echeverria 1989; L. S. Finn 1992; W. C. G. Ho et al. 2020).

Regardless of the precise emission mechanism, we can define a characteristic energy scale as the apparent change in kinetic energy of the NS caused by the glitch,

$$\Delta E_{\rm c} \equiv 4\pi^2 I f_{\rm rot}\, \Delta f_{\rm rot}\,, \tag{3}$$

where I is the NS moment of inertia. Following the derivation in R. Prix et al. (2011), the $\Delta f_{\rm rot}$ here would be the total glitch step size (permanent+temporary parts). But since $\Delta f_{\rm rot}^{d,i} \ll \Delta f_{\rm rot}$ for this glitch, we can directly insert values for $f_{\rm rot}$ and $\Delta f_{\rm rot}$ from Table 1 and a fiducial $I = 10^{45}$ g cm^2, obtaining $\Delta E_{\rm c} \approx 1.15 \times 10^{43}$ erg.

The actual energy budget of a realistic glitching multi-component NS and the relation of this energy scale to actual radiated GW energies is highly model-dependent; see G. Yim et al. (2024) for a summary of the literature. In particular, the energy transferred to the f-mode could be much smaller than $\Delta E_{\rm c}$ if the timescale associated with the glitch trigger

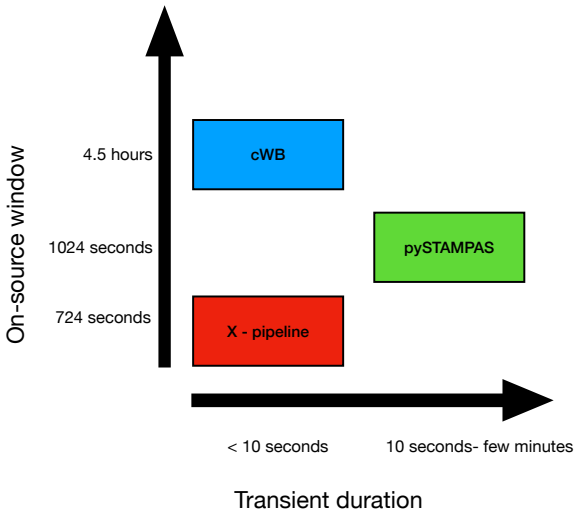

Figure 3. This schematic summarizes the burst-like transient searches performed for this paper as a function of the duration of anticipated signals and the on-source windows used by each. The on-source window time for `X-pipeline` is 1σ uncertainty around the estimated glitch arrival time using the timing model. The on-source window for `cWB` is the broadest window in radio observation within which the glitch occurred. The choice for `PySTAMPAS` is based on analysis requirements and longer duration of the signal.

(possibly crust cracking, or vortex unpinning) is much longer than the $\mathcal{O} \sim 1$ ms timescale characteristic of an f-mode oscillation, as discussed in the context of magnetar flares in Y. Levin & M. van Hoven (2011). It is also possible that other modes, with oscillation periods closer to the glitch trigger timescale, might be more efficiently excited, e.g., the torsional crustal oscillations considered in the context of Vela glitches in A. Bransgrove et al. (2020); such oscillations are relatively weak GW emitters.

With these caveats in mind, we will nevertheless choose f-modes as the reference model for evaluating the performance of our (unmodeled) searches and use ΔE_c as a useful energy scale to compare our results against. For a signal starting at t_0, the f-mode signal can be written as (J. Abadie et al. 2011)

$$h_+(t) = A_+ \cos\left(2\pi f_{\rm gw}(t - t_0) + \phi_0\right) e^{-(t-t_0)/\tau}, \quad (4a)$$

$$h_\times(t) = A_\times \sin\left(2\pi f_{\rm gw}(t - t_0) + \phi_0\right) e^{-(t-t_0)/\tau}. \quad (4b)$$

The amplitudes A_+ and $A_\times$ depend on the NS inclination angle ι as $1 + \cos^2(\iota)$ and $2\cos(\iota)$. τ is the damping time and ϕ_0 is the initial phase. The frequency and damping time depend on the equation of state of NS matter, with ranges of $\sim$[1, 4] kHz and $\lesssim$1 s for most realistic models (see, e.g., N. Andersson & K. D. Kokkotas 1998; O. H. Wilson & W. C. G. Ho 2024). These ranges are covered by the searches described below.

The actual emission from a glitching NS can be more complex than the simplistic assumptions made here. To mitigate this, we have employed three pipelines that do not depend explicitly on the morphology of the incoming GW signal. The damped sinusoid model of Equation (4) is then used for sensitivity measures and computing upper limits.

4.2. Coherent WaveBurst (`cWB`)

Coherent WaveBurst (cWB) (S. Klimenko et al. 2016; M. Drago et al. 2021; A. Martini et al. 2026) is a GW search and reconstruction algorithm based on maximum-likelihood statistics that uses the excess signal power in the detector network and does not rely on a precise signal model of the incoming GWs. The time series strain data are transformed into a multiresolution time-frequency map using the Wilson–Daubechies–Meyer (WDM) wavelet transform (V. Necula et al. 2012), then excess power clusters of pixels are identified for each detector in the network and a likelihood is computed for these selected pixels as a function of sky direction. `cWB` is used routinely for the search and reconstruction of GW transients in LVK data (R. Abbott et al. 2021a, 2023; A. G. Abac et al. 2026b, 2025c, 2025d). The version of the pipeline used here is the same as in the O4a all-sky short-duration search (A. G. Abac et al. 2025c). `cWB` is sensitive to signals expected from NS glitches, such as f-modes (D. Lopez et al. 2022).

The `cWB` analysis searches for short-duration transient signals (less than 10 s) in the frequency range of 512–4000 Hz. It covers a time window of 4.5 hr around the estimated glitch time (at Earth, rounded to the nearest integer, corresponding to 1398458994 GPS seconds), addressing the broadest possible uncertainty from radio observations. The analysis is restricted to sky directions within 1 square degree centered around the Vela pulsar. For the 4.5 hr of on-source time window, we perform time slides to estimate the background (M. Was et al. 2010). The total background generated is 6.6 yr, allowing false-alarm probability estimates at the level of 7.5×10^{-5}. The search does not find any triggers in the on-source time window above the thresholds applied within the pipeline.

4.3. `PySTAMPAS`

`PySTAMPAS`(A. Macquet et al. 2021) is an unmodeled coherent search pipeline based on the cross correlation of multiresolution time-frequency maps and targeting long-duration GW transient signals. The analysis uses the same version of the pipeline as in the O4a all-sky long-duration bursts search (A. G. Abac et al. 2026). The pipeline splits data into 512 s segments and generates S/N spectrograms for each detector using short-time Fourier transforms (STFTs) over short windows (0.5, 1, 2, and 4 s, each Hann-windowed with 50% overlap) to form multiresolution spectrograms covering 512–4020 Hz, with the power spectral density (PSD) in each frequency bin estimated as the median of the squared STFT magnitudes. A seed-based clustering algorithm then identifies candidate triggers, which are cross-correlated with the corresponding spectrogram from the second detector to compute a coherent detection statistic. The search is performed considering the Vela sky position given in Table 1. The on-source window is $\pm$512 s long centered at the glitch time 1398458994, to ensure covering the full signal power also for longer-duration signals of 50–100 s. We consider two days of data around the glitch time excluding the on-source window to estimate the background distribution of noise triggers by 25 time-shifts of the time-frequency maps by more than 1000 s to effectively simulate 31 days of background data. This procedure establishes a 3σ detection threshold corresponding to a false-alarm rate (FAR) of 3.3×10^{-6} Hz. The search does not find any event in the on-source time window below this FAR, the loudest event has FAR more than an order of magnitude higher corresponding to a p-value of around 0.6, which is compatible with Gaussian noise fluctuations.

Table 2
Parameters of the Damped Sinusoid Injection Sets Used by Each Pipeline

Pipeline	f_{gw} (Hz)	τ (s)
cWB	650, 1100, 2100, 3900	0.01, 0.1, 0.5
X-pipeline	290, 650, 1100, 2100, 3900	0.01, 0.1, 0.5
PySTAMPAS	800, 1050, 1300, 1600, 2000, 2200, 2500, 2750, 3000, 3250	10

4.4. X-pipeline

The X-pipeline is an unmodeled coherent search pipeline where the data from each detector is coherently combined in the multiresolution time-frequency domain. The brightest 1% of pixels are selected along with nearby pixels that form a cluster and then assigned likelihood-based ranking statistics (P. J. Sutton et al. 2010; M. Was et al. 2012). Spurious noise triggers are rejected by applying vetoes to the coherent and incoherent power across the detector network.

The search performed for this paper was done on an on-source time window of ±362 s centered at GPS time 1398458994, representing 1σ uncertainty in the glitch time estimate. The frequency band of the analysis is 200–4000 Hz. The off-source time window used for background computation is ±1.5 hr around the glitch time. The loudest event found in the analysis has a p-value of 0.8 which is compatible with Gaussian noise fluctuations.

4.5. Search Sensitivity

While the burst searches are independent of a specific GW waveform, to assess their sensitivity we inject simulated damped sinusoid waveforms, as a simple stand-in model for emission from f-modes, into the detector data around the time of the glitch. These injections are fixed to the sky direction and inclination of the Vela pulsar. Since the NS equation of state and the precise glitch mechanism are not known, we also use a range of central frequencies and damping times for the damped sinusoids. We list the injection sets used for each pipeline in Table 2. These cover different timescales due to the different search ranges, as previously summarized in Figure 3 and, for practical reasons, somewhat different but overlapping frequency ranges.

We then vary the amplitude of each damped sinusoid to obtain an efficiency curve for each pipeline, ranging from 0% to 100%. We fix a detection threshold of 3σ for each pipeline, which corresponds to inverse FARs of 0.2 yr, 0.008 yr, and 0.009 yr for cWB, X-pipeline and PySTAMPAS, respectively, due to differences in the on-source time window. The upper limits apply only to signals during coincident data availability from the LIGO detectors, similar to choices made in previous works (e.g., the search for GWs from SN 2023ixf, A. G. Abac et al. 2025a).

We present the results in terms of the quantity

$$h_{\rm rss} = \sqrt{\int_{-\infty}^{\infty} \left(h_+^2(t) + h_\times^2(t)\right) dt}\,, \tag{5}$$

where $h_+(t)$ and $h_\times(t)$ are the amplitudes for the two GW polarizations. The Vela pulsar's inclination angle dictates the relative content of h_+ and $h_\times$ of the waveform. We perform a set of injections over a range of amplitudes of $[10^{-23}, 10^{-21}]$ and recover them with each of the search pipelines. We then measure the $h_{\rm rss}$ needed to achieve the detection efficiency 90%. We show this $h_{\rm rss}^{90\%}$, at a 3σ detection threshold and as a function of GW frequency, for all pipelines and various damping times in Figure 4.

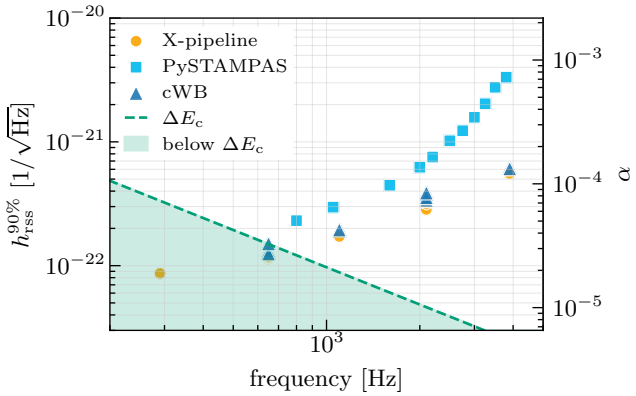

Figure 4. $h_{\rm rss}^{90\%}$ at a detection threshold of 3σ (p-value 10^{-3}) for the three GW burst searches (circle, square, and triangle markers), shown against the frequency of damped sinusoids signals. For cWB and X-pipeline, multiple markers at fixed frequencies denote different damping times (see Table 2), which do not affect the sensitivity drastically. Strains corresponding to the characteristic energy ΔE_c of the glitch from Equation (3) are shown as the dashed green line and GW emission would be consistent with it in the shaded region below. The right-hand vertical axis shows the f-mode amplitude α that would correspond to a given $h_{\rm rss}$ level. See Section 6.1 for interpretation of these results in terms of ΔE_c and α.

The results are different due to both methodological aspects and the different parameter spaces, as summarized in Figure 3. PySTAMPAS probes longer-duration signals, which are more difficult to detect with unmodeled methods. The difference between X-pipeline and cWB can be in part explained by X-pipeline's tighter on-source window. Even with the same FAR threshold between the pipelines, there would still be variations due to the antennae pattern functions and noise properties changing over the different time windows, hence a fair comparison cannot be made and is also out-of-scope of this work.

In the same figure, we have also shown the $h_{\rm rss}$ corresponding to GWs with the full characteristic glitch energy from Equation (3); see Section 6.1 for its derivation and interpretation. The X-pipeline and cWB results compare more favorably with the available energy budget below 1 kHz than at higher frequencies, while for PySTAMPAS only injections at higher frequencies were done.

In the O4a all-sky burst search (A. G. Abac et al. 2025c), the minimum relative glitch size for Vela-like pulsars to be detected was around $\Delta f_{\rm rot}/f_{\rm rot} \approx 2 \times 10^{-5}$, which is an order of magnitude larger than the $\Delta f_{\rm gl}$ of this glitch. But the search sensitivity in that paper was computed with injections above 2000 Hz, which along with all-sky and all-time averaging makes those results not directly comparable to the ones in this paper.

5. Searches for Quasi-monochromatic Long-transient GWs

Quasi-monochromatic long-duration GW signals at frequencies coupled to the pulsar's rotation may be triggered by glitches (R. Prix et al. 2011) and can be searched for with

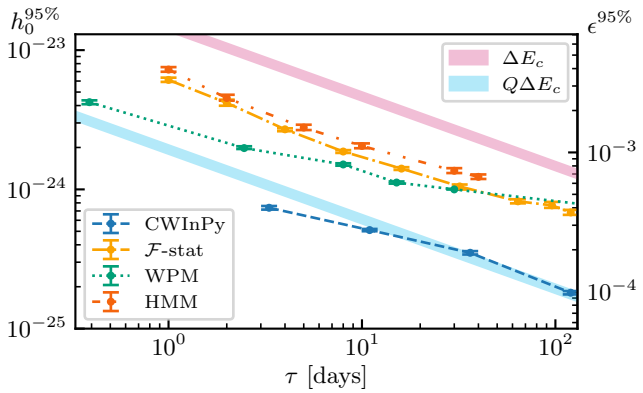

Figure 5. Selected upper limits at 95% confidence from the four CW-like postglitch searches, in terms of initial strain amplitude (left-hand axis) and NS ellipticity ϵ (right-hand axis), both defined at the start of signals with exponentially decay parameters τ. The results were chosen to illustrate how upper limits scale with the strictness of prior assumptions built into each search configuration. The `CWInPy` results have the strictest constraints (fixed frequency evolution and constrained orientation angles), while the three other results are for narrow-band searches, with $\mathcal{F}$-statistic results marginalized over all durations, WPM results for search configurations optimized at each τ point, and HMM results for $T_{\rm coh} = 9$ hr. For comparison, GW emission at the characteristic energy scale ΔE_c from Equation (3) is shown as the magenta shaded band near the top, while the sky-blue shaded band further down shows the emission if the GW energy output is suppressed by a factor $Q \approx 0.017$, as in G. Yim & D. I. Jones's (2020) transient mountain model.

methods derived from those for CWs; see K. Riles (2023) for a review. The first such searches were done on O2 data (D. Keitel et al. 2019), including the 2016 Vela glitch (J. Palfreyman et al. 2018) and a glitch of the Crab pulsar, and on O3 data (L. M. Modafferi et al. 2021; R. Abbott et al. 2022a), covering six glitching pulsars but with no Vela glitch during that run. Detection prospects for this type of GW signal were studied in J. Moragues et al. (2023), indicating that Vela glitches from O4 on would allow for physical constraints below the indirect energy estimate previously introduced by R. Prix et al. (2011), equivalent to our Equation (3). G. Yim et al. (2024) also identified Vela as a priority search target.

In this section, we first discuss emission models for this type of signal. We then present several analyses that differ in the strictness of their model assumptions: two fully coherent and two semicoherent search methods, each with different allowances for the degree of mismatch between the GW and EM phase evolution and varying flexibility in signal start times and durations. The motivation is to probe as deep as possible into the noise floor for the strictest model assumptions, while also maintaining chances to detect sufficiently strong signals with different parameters or time evolution.

Since there are no significant detection candidates from either search, we report upper limits on GW strain from all of them, which are compared in Section 5.6 and Figure 5. More detailed results from each method are contained in the appendices. A detailed interpretation is given in Section 6.

5.1. Emission Models

Models for transient CW-like emission following a pulsar glitch, as summarized by B. Haskell & D. I. Jones (2024) and G. Yim et al. (2024), can be divided into two classes: GW emission caused by motions of the fluid core, or by quadrupolar deformations supported by the solid outer crust.

For fluid motion in the core, the leading model involves Ekman pumping, where the sudden spin-up of the crust induces a meridional flow in the interior fluid (C. A. van Eysden & A. Melatos 2008), which may be nonaxisymmetric. Calculations by M. F. Bennett et al. (2010) and A. Singh (2017) found emission via both the mass and current quadrupoles and at both the $f_{\rm rot}$ and $2f_{\rm rot}$ harmonics. The GW amplitude depends on the NS equation of state via the matter compressibility.

For asymmetries in the crust, the key idea is that, for any combination of elastic fracture and superfluid unpinning causing the glitch, the process happens in a nonaxisymmetric way, so that a large-scale (quadrupolar) deformation is produced in the solid outer crust, which then relaxes away on some (poorly constrained) viscous timescale of the crust. This relaxation may leave an imprint in the postglitch spin evolution, as exploited in G. Yim & D. I. Jones's (2020) model, which attributes the exponentially decaying excess spin-down seen after most glitches to the formation of a transient mountain, causing GW emission that provides the increased spin-down torque.

We can again use the characteristic glitch energy scale of Equation (3) to describe such transient-CW emission but inserting a dimensionless parameter Q describing how much of this energy is radiated in GWs,

$$\Delta E_{\rm c,tCW} = 4\pi^2 I f_{\rm rot}\, \Delta f_{\rm rot}\, Q. \tag{6}$$

In G. Yim & D. I. Jones's (2020) transient mountain model only the part of $\Delta f_{\rm rot}$ that decays away in the postglitch relaxation contributes to GW emission, at $2f_{\rm rot}$. In this case, the fraction of energy corresponds to the healing parameter

$$Q = \frac{\Delta f^d_{\rm rot}}{\Delta f_{\rm rot}} \tag{7}$$

as usually defined in pulsar timing (D. Antonopoulou et al. 2022). For the 2024 Vela glitch, $\Delta f^d_{\rm rot}$ can be taken as the sum of the three decay components identified in radio pulsar timing (Section 2). Using the parameters in Table 1, we find $Q \approx 0.017$, i.e., only about 1.7% of the characteristic glitch energy would be radiated in GWs in this scenario.

More energetic emission mechanisms with $Q \sim 1$ have been speculated upon (see section II.C. of R. Prix et al. 2011 and Table 1 of G. Yim et al. 2024). However, these scenarios lack the detailed emission mechanisms of the Ekman pumping or Yim & Jones's decaying mountain models, reflecting our uncertainty in the nature of transient GW emission.

Furthermore, if the NS is excited into free precession following the glitch, a CW-like signal would be emitted, decaying on a timescale determined by the strength of dissipative processes within the star (M. Zimmermann & E. Szedenits 1979; D. I. Jones & N. Andersson 2002). The signal would contain harmonics at (or close) to both $f_{\rm rot}$ and $2f_{\rm rot}$, with the lower harmonic dominating in the case of a small angular misalignment between the NS symmetry axis and its (fixed) angular momentum vector. Such precessional motion would also leave an imprint on the radio pulsar signal, modulating the frequency and pulse profile (D. I. Jones & N. Andersson 2001). No such modulations have been reported, although they may occur with too small an amplitude and/or on too long a timescale to be apparent.

Given the wide range of long-transient GW emission mechanisms and strengths found in the literature, we carried out a number of relatively agnostic searches, as described below. All allow for a wide range of signal durations, and

some also for emission at both the $f_{\rm rot}$ and $2f_{\rm rot}$ harmonics. Additionally, we consider GW amplitude evolution profiles that are either constant, i.e., set by a rectangular-window function

$$h(t;\,\lambda,\,\mathcal{A},\,\mathcal{T}) = \begin{cases} h(t;\,\lambda,\,\mathcal{A}) & \text{if} \quad t_0 \leqslant t < t_0 + \tau; \\ 0 & \text{otherwise}, \end{cases} \tag{8}$$

a single exponentially decaying window function,

$$h(t;\,\lambda,\,\mathcal{A},\,\mathcal{T}) = \begin{cases} e^{-(t-t_0)/\tau} h(t;\,\lambda,\,\mathcal{A}) & \text{if} \quad t \geqslant t_0; \\ 0 & \text{otherwise}, \end{cases} \tag{9}$$

or a combination of three exponentials, following Equation (2). Here, $h(t;\,\lambda,\,\mathcal{A})$ would be a standard persistent CW signal (P. Jaranowski et al. 1998; K. Riles 2023) with two polarization components, described by amplitude parameters $\mathcal{A}$ (including a constant characteristic strain amplitude h_0, inclination ι, polarization angle ψ, and an initial phase) and phase-evolution parameters λ (frequency, frequency derivatives, and sky position); and $\mathcal{T} = \{t_0, \tau\}$ are the transient window parameters: t_0 is the start of the signal window and τ is the rectangular-window length or exponential decay constant. In the following, we also define for convenience $h_0(t) \equiv e^{-(t-t_0)/\tau} h_0$ in the exponentially decaying case, with $h_0(t = t_0) = h_0$.

All the searches and upper limits presented here are set up to correctly take into account the gaps in GW data (as seen in Figure 2), as is standard for CW search methods.

5.2. Time-domain Bayesian Search (`CWInPy`)

The time-domain Bayesian method (R. J. Dupuis & G. Woan 2005; M. Pitkin et al. 2017) has been widely used for targeted CW searches (e.g., R. Abbott et al. 2022a, 2022b; A. G. Abac et al. 2025b), where the signal amplitude is assumed as constant over the entire observation period. The implementation in the `CWInPy` package (M. Pitkin 2022) also allows for transient time-dependent profiles as per Equations (8) or (9), though all signals considered will have fixed start time (chosen here as $t_0 = T_{\rm gl}$) and only vary in τ (from 1 hr to 120 days).

To make the inference computationally tractable, the data are massively compressed (R. J. Dupuis & G. Woan 2005). First, they are heterodyned to account for the motion of the detectors with respect to the source as well as any intrinsic phase evolution, fixing to the best-fit parameters from Table 1. These heterodyned data are then lowpass-filtered and down-sampled. `CWInPy` then uses the `bilby` (G. Ashton et al. 2019) and `dynesty` (J. S. Speagle 2020) packages for nested sampling inference to produce a Bayesian evidence value and posterior probability distribution for the unknown source parameters, given the compressed data.

Eight `CWInPy` analyses were performed, toggling three different options: (i) a rectangular or exponential amplitude profile; (ii) unconstrained ι and ψ or observationally motivated constraints on these angles from modeling of the pulsar wind nebula (C. Y. Ng & R. W. Romani 2008); and (iii) emission only from the $l = m = 2$ mass quadrupole modes near $2f_{\rm rot}$, or allowing for both the $l = 2$, $m = 1$, 2 modes, with emission at both the $f_{\rm rot}$ and $2f_{\rm rot}$ (D. I. Jones 2010; B. P. Abbott et al. 2019) harmonics. See Appendix A for a full description of these options, other prior choices, and results.

No evidence for coherent signals across H1 and L1 was found. The posterior probability distributions on signal amplitudes have been used to define 95% credible upper limits as a function of the binned signal duration.

5.3. Transient $\mathcal{F}$-statistic Search

This method (R. Prix et al. 2011) builds on the standard matched-filter CW maximum-likelihood $\mathcal{F}$-statistic (P. Jaranowski et al. 1998) in its `LALSuite` (LVK 2025) frequency-domain implementation. It has already been used in O2 and O3 postglitch GW searches (D. Keitel et al. 2019; L. M. Modafferi et al. 2021, 2023; R. Abbott et al. 2022a).

We use 1800 s short Fourier transforms (SFTs; B. Allen et al. 2024) produced from time-domain gated data (D. Davis et al. 2025), combined coherently across both LIGO detectors (C. Cutler & B. F. Schutz 2005) and the full observing time. The detection statistic is a Bayes factor $\mathcal{B}_{tS/G}$ marginalized over start times and durations (R. Prix et al. 2011), under the two amplitude profiles from Equations (8) and (9), and evaluated over a template bank in $f_{\rm rot}$, $\dot{f}_{\rm rot}$, $\ddot{f}_{\rm rot}$, and $\dddot{f}_{\rm rot}$. Unlike `CWInPy`, this search does not use inclination and polarization constraints. (They can be incorporated into an $\mathcal{F}$-statistic framework as per P. Jaranowski & A. Królak 2010 but this has not yet been implemented for transients.)

We allow for signal start times t_0 within ± 1 day of $T_{\rm gl}$ and duration parameters τ up to 120 days, covering data from 2024 April 28 to August 28. The search ranges are given in Table 3 of Appendix B. Rectangular-window (constant amplitude) signals can be searched for efficiently on CPUs with code in `LALSuite` (LVK 2025), while exponentially decaying signals require the GPU implementation in `PyFstat` (D. Keitel & G. Ashton 2018; D. Keitel et al. 2021). Both are called via the `tCWip` (transient-CW-investigation pipeline) package (D. Keitel et al. 2025).

We find no statistically significant candidates above a threshold set to the expected loudest outlier from an empirical background estimation (R. Tenorio et al. 2022a). We obtain upper limits on the initial strain amplitude h_0 via simulated signal injection and recovery. See Appendix B for details of the method, upper limits procedure and full results.

5.4. Weighted Peakmap Search

As a complementary approach to the two coherent searches, we also run a semicoherent search based on weighted peakmaps (WPM). This uses time-domain band-sampled data (BSD) files (O. J. Piccinni et al. 2019), including a glitch cleaning step (P. Astone et al. 2005). The search starts 2000 s before the glitch time and covers $T_{\rm tot} = 101.7$ days. Given the significant ASD difference of the L1 and H1 detectors, only L1 data are used. Data over a 0.2 Hz frequency band around the putative signal frequency are extracted from the BSDs and heterodyned (R. Abbott et al. 2022b) to remove the Doppler modulation induced by the Earth's motion and the Vela pulsar's secular spin-down, using values measured immediately after the glitch, see Table 4. The corrected data are divided in segments of duration $T_{\rm seg}$ (see Appendix C) and from each an equalized spectrum is computed. Local maxima above a given threshold are selected, creating a so-called peakmap (P. Astone et al. 2014).

We then search for peaks in the projection of the peakmap on the frequency axis, as expected for sufficiently strong signals. Peaks are weighted by their amplitude before projection, increasing the contribution of peaks from the early part of the signal, which is expected to be stronger. The detection statistic is the critical ratio $\mathrm{CR} = (\mathcal{P} - \mu_{\mathcal{P}})/\sigma_{\mathcal{P}}$, where $\mathcal{P}$ is the sum of the weighted peaks and $\mu_{\mathcal{P}}$, $\sigma_{\mathcal{P}}$ are the corresponding projection mean value and standard deviation.

This procedure is independent of the assumed signal model. But by assuming a specific signal model we can make an "optimal" choice of the observation window $T_{\mathrm{obs}} \leqslant T_{\mathrm{tot}}$ and segment duration T_{seg}—see Appendix C and the resulting choices in Table 5 for the seven considered search setups.

For each of these setups, we select the 10 most significant outliers as those with the highest CR from each of 10 sub-bands of 0.02 Hz. Those with false-alarm probability (taking into account the trials factor) larger than 0.01 are discarded. Three outliers remain: one corresponding to $\tau = 8$ days with frequency 22.455 Hz ($\mathrm{CR} = 6.65$), one to $\tau = 30$ days with frequency 22.5011 Hz ($\mathrm{CR} = 7.55$), and one to $\tau = 1000$ days with the same frequency ($\mathrm{CR} = 5.15$). They are subjected to a follow-up procedure based on different methods, see Appendix C.2. While the last two are associated with an instrumental spectral line, the first one is more difficult to interpret, see Appendix C.2. Since it is statistically marginal, we do not consider it a promising detection candidate and also proceed for this method to compute upper limits.

The upper limits are placed in terms of the initial signal strain amplitude via simulated signal injections. For the polarization parameters ψ and ι, we use both the restricted prior described for `CWInPy` in Appendix A and an unrestricted uniform distribution. See Appendix C for details, with Figure 12 and Table 5 including the full results.

5.5. Hidden Markov Model Search

The fourth search for transient quasi-monochromatic GWs combines the semicoherent $\mathcal{F}$-statistic (P. Jaranowski et al. 1998; LVK 2025) with hidden Markov model (HMM) tracking (S. Suvorova et al. 2016; L. Sun et al. 2018) at both once and twice the Vela spin frequency (L. Sun et al. 2019). It uses the same 1800 s SFTs as the transient $\mathcal{F}$-statistic method.

Instead of a fully coherent analysis, the HMM pipeline divides the data into segments of duration T_{coh} and evaluates the standard $\mathcal{F}$-statistic over a template grid coherently in each segment (without explicitly applying time-windowed search templates), which are then recombined incoherently.

The HMM signal model allows for a drift in frequency between each segment, i.e., for stochastic spin-wandering or other deviations from the standard Taylor phase model of Equation (1). We employ the Viterbi algorithm (A. Viterbi 1967) to determine the optimal frequency path for both the single-harmonic ($2f_{\mathrm{rot}}$) and dual-harmonic (f_{rot} and $2f_{\mathrm{rot}}$) scenarios. The detection statistic is the log-likelihood of the optimal path normalized by the number of segments, $\bar{\mathcal{L}} \equiv \mathcal{L}/N_T$.

The configuration of the HMM search is described in Table 7 in Appendix D. It covers a 0.05 Hz band centered on $f_{\mathrm{gw}} = f_{\mathrm{rot}}$ and 0.1 Hz band centered on $f_{\mathrm{gw}} = 2f_{\mathrm{rot}}$, with frequency resolutions of $1/(4T_{\mathrm{coh}})$ and $1/(2T_{\mathrm{coh}})$, respectively. The observation window covers $T_{\mathrm{obs}} = 90$ days. For added flexibility, we repeat the HMM analysis with three values of T_{coh}, each corresponding to one of the three glitch recovery timescales. Shorter T_{coh} reduces sensitivity but can track a more rapidly fluctuating signal.

Empirical detection thresholds are set using two methods (see Appendix D), based on either repeating the search on numerous realizations of Gaussian noise data or repeating the search at randomly chosen off-target sky positions.

The full results of the HMM search are compiled in Table 8, where we list the max-$\bar{\mathcal{L}}$ statistics obtained with single- or dual-harmonic tracking for each value of T_{coh}. Our analysis does not recover any outliers with false-alarm probability below 1%. We therefore find no statistically significant outliers for the HMM search.

We set upper limits by injecting simulated transient signals with varying durations τ into the detector data and then recovering the injection using the same HMM search configurations with single- or dual-harmonic tracking. Upper limit results for the single-harmonic emission ($2f_{\mathrm{rot}}$ only) scenario with $T_{\mathrm{coh}} = 9$ hr are included in Figure 5, with the full set of upper limits shown in Appendix D and Figure 14.

5.6. Comparison of Upper Limits Results

In Figure 5, we compare a selection of upper limits from each of the four methods, focusing on signals at twice the pulsar's rotation frequency and with exponential amplitude decay. The results were chosen to span the range of assumptions of varying strictness covered by the set of pipelines: the strictest upper limits for such signals are obtained by the fully coherent targeted `CWInPy` search with constrained orientation angles, while the semicoherent HMM search with the least prior assumptions provides the least strict constraints. The two other methods and other configuration choices provide intermediate strictness of both assumptions and resulting constraints. The figure also contains comparisons with theoretical expectations on possible postglitch GW strains, which will be discussed in the following section.

These limits concern arbitrary exponentially decaying CW-like transients within the search ranges, and at least for the $\mathcal{F}$-statistic method it is known that the exact amplitude evolution only has a small effect on its sensitivity (R. Prix et al. 2011; D. Keitel et al. 2019). In addition, from the WPM method, we also report a dedicated upper limit for GW amplitudes following the three-component frequency decay observed in the radio, for which we find $h_0^{95\%} = 4.5 \times 10^{-24}$ assuming uniform priors on the polarization parameters and 4.7×10^{-24} for restricted priors. (See also Table 5 in Appendix C.1.)

How deep a search has probed below the detector noise floor can be stated as a sensitivity depth (B. Behnke et al. 2015; C. Dreissigacker et al. 2018; K. Wette 2023) $\mathcal{D} = \sqrt{S_n(f)}/h_0$, where $\sqrt{S_n}$ is the ASD suitably averaged over the observation time. These searches have probed below the average 4 month H1+L1 ASD by $\mathcal{D}$ factors from $4\,\mathrm{Hz}^{-1/2}$ for the most flexible HMM search (at $\tau = 1$ day) to $170\,\mathrm{Hz}^{-1/2}$ for the most restrictive `CWInPy` analysis (at $\tau = 120$ days).

6. Interpreting the Observational Constraints

We now provide some interpretation of our results. In Section 6.1 we discuss what conclusions can be drawn given the lack of detection of a burst-like signal. In Section 6.2, we discuss the same for the nondetection of long-duration transient quasi-monochromatic signals. In Section 6.3, we

discuss the combined constraints from both on GW emission models and NS properties.

Before looking at the separate burst and long-transient cases, it is useful to assemble some formulae relevant to both. Despite searching for signals over very different frequencies and durations, both types of search cover signals of fixed source frequency and of finite duration. Hence, we can also describe the burst analyses from Section 4 (for the case of f-mode or similar signals) with the same notation as for CW-like signals from Section 5, using the explicit $h_0(t)$ and converting to the average $h_{\rm rss}$ where needed. The total GW energy in such a signal is then given by (see e.g., Equation (3) of R. Prix et al. 2011)

$$E_{\rm gw} = \frac{2\pi^2}{5}\frac{c^3}{G} f_{\rm gw}^2 d^2 \int_{t_0}^{t_0+T_{\rm obs}} h_0^2(t)\,dt, \tag{10}$$

where $T_{\rm obs}$ is the observation time. This applies regardless of the time variation of the signal amplitude $h_0(t)$. The corresponding optimal S/N is

$$\rho_0^2 = \int_{t_0}^{t_0+T_{\rm obs}} \frac{B(t;\hat{n},\iota,\psi)\,h_0^2(t)}{S_h(t,f_{\rm gw})}dt, \tag{11}$$

where $S_h(t, f_{\rm gw})$ is the PSD of the detector noise and $B(t;\hat{n},\iota,\psi)$ summarizes location- and orientation-dependent factors (for details see P. Jaranowski et al. 1998; R. Prix et al. 2011; R. Prix 2015).

For a simple exponential decay on timescale τ, the amplitudes $h_{\rm rss}$ and h_0 are related by

$$h_{\rm rss} = h_0\sqrt{\frac{\tau}{2}}, \tag{12}$$

as can easily verified by assuming an exponential time dependence for the integrand in Equation (5).

We will now use these formulae to interpret the results from Sections 4 and 5, and compare with the characteristic energy scale of Equation (3) and additional model-specific constraints.

6.1. Interpretation: Burst Results

The results of our burst searches are presented in Figure 4. For the decaying exponentials assumed in the injections to set these limits, Equation (11) reduces to $\rho_0^2 \propto h_{\rm rss}^2/S_h(f_{\rm gw})$, defining $S_h(f_{\rm gw})$ as a time average over $S_h(t, f_{\rm gw})$. Hence, at fixed S/N, the minimum detectable $h_{\rm rss}$ scales as $\propto\sqrt{S_h(f_{\rm gw})}$. This accounts for the limits weakening with increasing frequency, reflecting the slope of the detector noise curve as seen in Figure 2.

To interpret the astrophysical significance of the results, we can similarly rewrite Equation (10) to give

$$E_{\rm gw} = \frac{2\pi^2}{5}\frac{c^3}{G} f_{\rm gw}^2 d^2 h_{\rm rss}^2. \tag{13}$$

Setting $E_{\rm gw}$ equal to the characteristic energy of Equation (3) then gives the corresponding $h_{\rm rss}$ as a function of $f_{\rm gw}$, with scaling $h_{\rm rss} \propto 1/f_{\rm gw}$. Inserting values for the 2024 April 29 Vela glitch, we obtain $h_{\rm rss}(f_{\rm gw}) \approx 9.7 \times 10^{-20}\,{\rm Hz}^{-1/2}/(f_{\rm gw}/{\rm Hz})$, which is plotted as the dashed green line in Figure 4.

The search upper limits constrain the actual GW energy to be less than this at sufficiently low frequencies. For instance, for the `X-pipeline`, this characteristic energy scale is surpassed for frequencies below about 800 Hz and at the lowest injection frequency of 290 Hz, $h_{\rm rss}$ is constrained to a factor of ≈3 below the characteristic scale. Given the scaling $E_{\rm gw} \sim h_{\rm rss}^2$ of Equation (13), this corresponds to a factor of ≈9 in radiated energy. However, emission at such low frequencies would not correspond to the f-modes considered most plausible to be excited by pulsar glitches. For example, see O. H. Wilson & W. C. G. Ho (2024) where f-mode emission was studied for a catalog of 15 equations of state (eight for standard NSs and seven for quark stars).

Our upper limits on $h_{\rm rss}$ can be converted into upper limits on a (dimensionless) amplitude α of the f-mode excitation, such that a point on the surface of the NS oscillates about its equilibrium position by a distance $\sim\alpha R$, with R the stellar radius. This conversion depends on the NS mass M and equation of state. To provide a quantitative example of this, we will make use of the analytic results given in G. Yim & D. I. Jones (2023) for uniform density stars. Combining Equations (5) and (10) of G. Yim & D. I. Jones (2023), and making use of our Equation (12), one obtains

$$\alpha = \left(\frac{2\pi}{15}\right)^{1/2}\left(\frac{c^3}{G}\right)^{1/2}\frac{h_{\rm rss}\,d}{M^{1/2}R}. \tag{14}$$

Inserting $M = 1.4\,M_\odot$ and $R = 10^6$ cm, and the distance for Vela, we find

$$\alpha \approx 7 \times 10^{-5}\left(\frac{h_{\rm rss}}{3\times10^{-22}\,{\rm Hz}^{-1/2}}\right), \tag{15}$$

where we have chosen the scaling in $h_{\rm rss}$ based on the upper limits on $h_{\rm rss}$ of Figure 4, at a frequency of about 1.5 kHz, typical for an f-mode. Roughly speaking, we have constrained the oscillation amplitude αR of a particle on Vela's surface to be no larger than about 70 cm for a typical f-mode frequency. However, at these frequencies our upper limits on $h_{\rm rss}$ fall short of the values corresponding to the characteristic energy by about a factor of ∼4.

6.2. Interpretation: Long-transient Results

As discussed in Section 5.1, there are two main mechanisms for producing CW-like transients following a glitch. The first we discussed was Ekman pumping. Using Equation (55) of M. F. Bennett et al. (2010) and the parameters for the 2024 April 29 Vela glitch, we obtain an estimate of the signal strength of $h_0 \approx 7 \times 10^{-26}$. While this estimate is conservative, mainly due to uncertainties on the lag between the components in the NS's interior (which may be larger than the observed glitch size, B. Haskell & A. Melatos 2015), and unknown nuclear physics parameters that enter the model, the predicted strain is significantly lower than the upper limits on h_0 from our analyses (Figure 5), which are hence not yet sensitive enough to set constraints on this mechanism.

The second emission mechanism we discussed was the formation of a transient mountain that then relaxes away (G. Yim & D. I. Jones 2020). To help interpret results from Figure 5 under this mechanism, we can insert the assumption of exponential decay on a timescale τ, Equation (9), as would be expected for dissipative mountain decay, into Equation (10) for $E_{\rm gw}$. If we assume $\tau \ll T_{\rm obs}$, we obtain

$$E_{\rm gw} = \frac{\pi^2}{5}\frac{c^3}{G} f_{\rm gw}^2 d^2 h_0^2(0)\tau. \tag{16}$$

For a fixed $E_{\rm gw}$, this shows that $h_0 \sim \tau^{-1/2}$, explaining the slope of the upper limits in the figure.

To understand the astrophysical significance of these results, we can use Equation (6) where only a fraction Q of the characteristic glitch energy of Equation (3) goes into GW emission. This yields for the initial GW strain amplitude

$$h_0^{Q\Delta E_{\rm c}} \approx \frac{1}{d}\sqrt{\frac{5G}{2c^3}\frac{I}{\tau}Q\frac{\Delta f_{\rm rot}}{f}}. \tag{17}$$

For $Q = 1$, this corresponds to what was discussed as "indirect energy limits" in R. Prix et al. (2011), D. Keitel et al. (2019), and R. Abbott et al. (2022a), and is shown (as a function of τ) as the magenta band in Figure 5. The width of the band includes uncertainties on the Vela pulsar distance and its timing parameters, but not on the NS's moment of inertia, which could vary by up to another factor of 3 for conventional models or 5 for extreme matter compositions (N. K. Johnson-McDaniel & B. J. Owen 2013; J. M. Lattimer 2021). The observational GW upper limits from all analyses are stricter than this by factors of ∼3 to ∼10. Notwithstanding the phenomenological nature of this indirect benchmark, this is a significant milestone for postglitch transient GW analyses.

To interpret the results in terms of a more specific model, we consider the G. Yim & D. I. Jones (2020) prediction of the energy fraction Q corresponding to the healing parameter defined in Equation (7). The 2024 April 29 Vela glitch had three observed recovery components (see Equation (2)), but to be consistent with the other quantities in Figure 5 the sky-blue band shows a simplified result, approximating the logic of the model: the result of Equation (17) with $Q \approx 0.017$ and as a function of a single τ.

Most upper limits are still above this prediction, while the result from the most constrained `CWInPy` search just reaches this level of emission. So, under optimal assumptions, a detection would have been just about possible under this model, depending on the assumed GW signal duration τ and the actual moment of inertia I of the Vela NS. The quantitative implications of nondetection under this model are considered in Section 6.3.

We can also recast our results in terms of the additional ellipticity ϵ imparted to the Vela pulsar right after the glitch, which is related to the GW amplitude by the equation (see e.g., K. Riles 2023)

$$h_0 = \frac{4\pi^2 G\epsilon I f_{\rm gw}^2}{c^4 d}. \tag{18}$$

When applied to Vela this gives

$$\epsilon \approx 5.4 \times 10^{-4}\left(\frac{h_0}{10^{-24}}\right), \tag{19}$$

interpreted as the initial transient ellipticity increase that then decays away again.

From Figure 5, we see that our limits on h_0 span the range $[2 \times 10^{-25}, 8 \times 10^{-24}]$, depending on the search and on τ, corresponding to an ellipticity range of $[10^{-4}, 3 \times 10^{-3}]$. In an astrophysical context, these are very large values—about three orders of magnitude larger than the largest mountains that an NS crust is estimated to be able to support (see e.g., N. K. Johnson-McDaniel & B. J. Owen 2013; K. Glampedakis & L. Gualtieri 2018). However, such estimates assume a persistent (i.e., infinitely long-lived) mountain. A realistic crust may respond plastically to the stresses that support such a mountain (D. A. Baiko & A. I. Chugunov 2018), so that the exponential postglitch relaxation may represent the plastic decay of a larger asymmetry. For this reason, the upper limits we have obtained are of astrophysical interest, despite being larger than the theoretical ones for permanent mountains. For further comparison, the `CWInPy` upper limit on a persistent ellipticity of the Vela pulsar from 8 months of O4a data was $\epsilon \leqslant 4.7 \times 10^{-5}$, also at 95% confidence (A. G. Abac et al. 2025b).

As discussed in Section 5.1, if the glitch caused the Vela pulsar to go into transient free precession, there would be additional emission at $f_{\rm gw} \approx f_{\rm rot}$. Due to the steep detector noise curve at low frequencies, strain upper limits are less constraining by an order of magnitude in this regime. Quantitative details are given in Appendices A and D.

6.3. Interpretation: Joint Analysis and NS Properties

We now show how our nondetections can be used to make statements about the NS parameter ranges under which specific GW emission models can be valid. Since this is the first time that both short- and long-duration GW searches have been performed for the same pulsar glitch, we aim to illustrate the benefit of considering results from the two types of searches jointly. So, we assume that both a burst signal and a longer-duration quasi-monochromatic transient were produced at the glitch. The fact that these signals were not detected either (i) rules out emission models that predict GW energy fractions in one of the signal channels that our searches would have detected or (ii) places nontrivial constraints on the NS mass and radius in the sense that Vela could still have emitted GW energy as predicted by the models, but at parameters leading to reduced detectability.

Following the method presented by M. Ball & R. Frey (2025), we assume specific models for both short- and long-duration waveforms. For bursts, we assume a rapidly damping sinusoid, consistent with an f-mode, in the form used by W. C. G. Ho et al. (2020) and parameterized by $h_{\rm rss}$, as discussed in Section 4.1. Meanwhile, the long-transient model corresponds to the decay of a transient mountain (G. Yim & D. I. Jones 2020), as discussed in Section 5.1, with an initial strength h_0.

We parameterize $E_{\rm gw}$ in each channel as some fraction f of the energy $\Delta E_{\rm c}$ from Equation (3). This gives $E_{\rm gw} = E_{\rm CW} + E_{\rm fmode} f_{\rm CW}\,\Delta E_{\rm c} + f_{\rm fmode}\Delta E_{\rm c}$. We employ an equation-of-state independent universal relation from K. Yagi & N. Yunes (2017) to connect the pulsar's moment of inertia I to the nonrotating mass and radius. We use another set of equation-of-state independent universal relations from B. K. Pradhan et al. (2022) to connect the f-mode frequency and damping time to the nonrotating mass and radius.

We perform Monte Carlo simulations of the parameter space, drawing samples from a set of prior distributions. For each prior sample, the initial CW-like signal amplitude h_0 and the f-mode integrated strain $h_{\rm rss}$ are calculated. These values are compared to detection efficiency curves of a search pipeline for simulated waveforms, i.e., the probability of the search recovering a signal with some morphology at different amplitudes. The priors are described in Appendix E, along with how the likelihood function is constructed from the

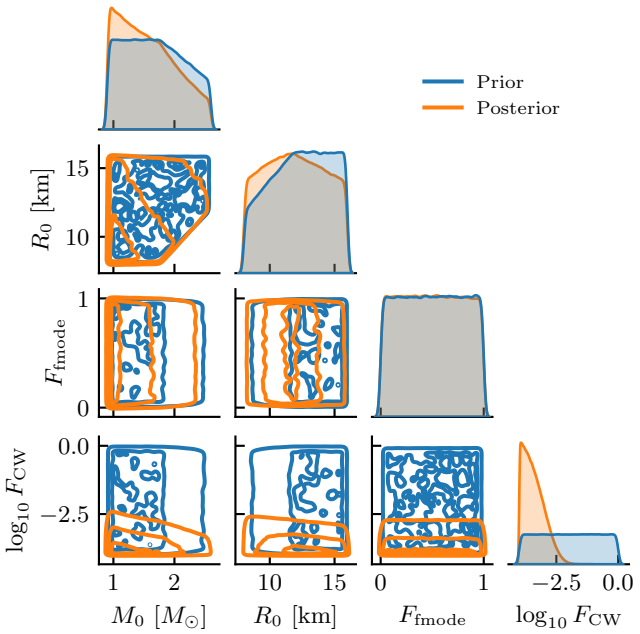

Figure 6. Prior and posterior distributions of NS mass, radius, and energy fractions $f_{\rm fmode}$ and $\log_{10}(f_{\rm CW})$ under the assumption that GWs from both a short-duration f-mode and a long-duration transient mountain scenario were emitted but not detected. After including the search results, there is little effect on the allowed f-mode energy in the physically motivated region $f_{\rm fmode} < 1$ but a measurable effect on the allowed CW energy ($f_{\rm CW}$). Contours show 10%, 50%, and 90% credible intervals.

`X-pipeline` analysis and the most constrained `CWInPy` configuration as representatives of the two search types.

We first let $f_{\rm fmode}$ and $f_{\rm CW}$ independently vary up to a maximum of 1. The posterior distribution for mass, radius, $f_{\rm fmode}$, and $f_{\rm CW}$ is shown in Figure 6. Consistent with the discussion above of the relative strictness of the upper limits from both types of searches in comparison to the $\Delta E_{\rm c}$ energy scale, burst search limits have little to no effect on the posterior distribution, while CW search limits strongly constrain $f_{\rm CW}$. From this posterior, we constrain $f_{\rm CW}$ to below 5.65×10^{-3} with 95% confidence.

Given the minimal effect of $f_{\rm fmode}$, we then fix it to an arbitrary value of 0.8 and explore the allowed mass and radius values if we assume that G. Yim & D. I. Jones's (2020) model correctly predicts $f_{\rm CW}$, yet no detection was made. Figure 7 shows how setting $f_{\rm CW}$ equal to the healing parameter $Q \approx 0.017$ defined in Equation (7) requires a smaller mass and radius for the Vela pulsar if GW emission as, per this model, would have been present after this glitch. This effect is driven by the moment of inertia relation from B. K. Pradhan et al. (2022).

In addition to being dependent on the specific emission model considered and the tightest prior assumptions among the set considered in our analyses, these results are still less informative compared to other NS mass–radius limits from the binary NS merger GW170817 (B. Abbott et al. 2017, 2018), observations of NSs in binary systems (e.g., J. H. Taylor & J. M. Weisberg 1982; E. D. Barr et al. 2024), or NICER pulse profile modeling (e.g., G. Raaijmakers et al. 2021; T. E. Riley et al. 2021).

Under a continued lack of detections from future glitches with improved GW detector sensitivity, this method could place stronger constraints on models such as G. Yim & D. I. Jones (2020), which would allow us to probe different emission scenarios and to gain stronger benefits from a joint burst–CW analysis.

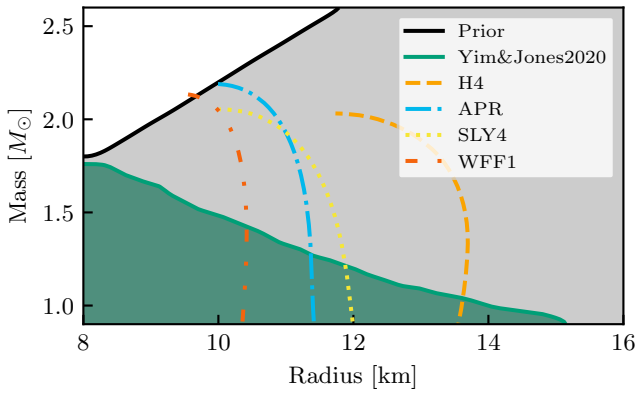

Figure 7. NS mass and radius regions for which the Vela pulsar could have emitted GWs according to G. Yim & D. I. Jones's (2020) model after its 2024 glitch, but without our searches detecting them (within the green shaded region at the lower left, at 90% confidence). This is compared to the assumed prior ranges (larger black contour) and to mass–radius curves for some example equations of state (R. B. Wiringa et al. 1988; A. Akmal et al. 1998; F. Douchin & P. Haensel 2001; B. D. Lackey et al. 2006), for which allowed NS configurations would lie along each curve. Here, we fixed $f_{\rm CW} = 0.017$ to match the healing parameter Q defined in Equation (7) and arbitrarily chose $f_{\rm fmode} = 0.8$ (which has little effect). We see that the Yim & Jones model is only compatible with our nondetection for smaller mass and radius ranges.

7. Conclusions

Pulsar glitches are unique probes of the structure and dynamics of NSs. The improved sensitivity of the LIGO detectors during the O4 run and the detailed timing information from the IAR and MPRO radio telescopes have now allowed us, for the first time, to place physically meaningful upper limits on the GW emission from a glitching pulsar, constraining it to below the indirectly inferred energy scale for at least part of the relevant parameter space.

Informed by an ephemeris fit to the combined IAR–MPRO data, we have analyzed LIGO data around and after the 2024 April 29 glitch of the Vela pulsar, one of the closest and most prolific glitching pulsars known. None of the GW searches found promising detection candidates.

Our search with three unmodeled methods for GW bursts covering different signal durations from milliseconds to minutes has set constraints on the GW strain that up to 700 Hz are, for the first time, stricter than the values corresponding to the full glitch excess energy. The tightest constraint is $h_{\rm rss} \approx 8.6 \times 10^{-23}$ at 290 Hz, a factor of $\sim$3 below the characteristic energy scale.

We also searched for quasi-monochromatic long-duration transients of up to 4 months near twice the Vela pulsar's rotation frequency. With four methods of varying strictness in their assumptions, we have excluded GW strain as low as a factor of 10 below the characteristic scale if all energy liberated at the glitch were converted into exponentially decaying quasi-monochromatic GWs and under the strictest assumptions, and still put constrains below that energy scale even under relaxed assumptions and phase-evolution models. We also searched for similar signals from free precession at the rotation frequency, but the results are less constraining due to the steep rise of the LIGO noise curve toward lower frequencies.

Previous searches for GW bursts from the Vela pulsar (J. Abadie et al. 2011), all-sky GW burst searches (A. G. Abac et al. 2026b, 2025c), and quasi-monochromatic GW transient searches for Vela and other glitching pulsars (D. Keitel et al. 2019; L. M. Modafferi et al. 2021, 2023; R. Abbott et al. 2022a) all yielded results above the characteristic glitch energy scale. In contrast, our new results for the first time allow meaningful comparisons with specific emission models.

Under the burst scenario, we can constrain emission only at lower frequencies but not yet at a kHz or above, which most NS equations of state predict (see, e.g., N. Andersson & K. D. Kokkotas 1998; O. H. Wilson & W. C. G. Ho 2024) but where detector sensitivity is worse, primarily being limited by laser shot noise (E. Capote et al. 2025).

Under G. Yim & D. I. Jones's (2020) "transient mountain" scenario, the scale of long-duration emission is set by the transient part of the glitch's spin-down change, which in the case of this Vela glitch is unfortunately a small fraction, and hence we only reach the sensitivity to probe this model's predictions under the most constraining prior assumptions in one of our searches.

Combining the most constraining burst and long-duration search results, respectively, we have also illustrated how a joint analysis can constrain the NS mass and radius ranges consistent with specific emission models under a nondetection of postglitch GWs. However, further improvement, particularly in the *f*-mode upper limits, will be required to ensure the full benefits of this method.

With the sensitivity of the LVK detector network further improving toward its fifth observing run (B. P. Abbott et al. 2020) and the Vela pulsar producing large glitches every two to three years, we can expect further improvements to this type of analysis in the coming years. Other glitching pulsars may also be promising targets, though the Vela pulsar stands out due to its low distance and strong glitches (D. Lopez et al. 2022; J. Moragues et al. 2023; G. Yim et al. 2024). Going beyond the nondetection constraints we introduced here, a positive detection of GWs from a glitching pulsar would be another important milestone in NS astrophysics.

Data products associated with this paper are released at DOI: 10.5281/zenodo.17735648.

Acknowledgments

This material is based upon work supported by NSF's LIGO Laboratory, which is a major facility fully funded by the National Science Foundation. The authors also gratefully acknowledge the support of the Science and Technology Facilities Council (STFC) of the United Kingdom, the Max-Planck-Society (MPS), and the State of Niedersachsen/Germany for support of the construction of Advanced LIGO and construction and operation of the GEO 600 detector. Additional support for Advanced LIGO was provided by the Australian Research Council. The authors gratefully acknowledge the Italian Istituto Nazionale di Fisica Nucleare (INFN), the French Centre National de la Recherche Scientifique (CNRS), and the Netherlands Organization for Scientific Research (NWO) for the construction and operation of the Virgo detector and the creation and support of the EGO consortium. The authors also gratefully acknowledge research support from these agencies as well as by the Council of Scientific and Industrial Research of India, the Department of Science and Technology, India, the Science & Engineering Research Board (SERB), India, the Ministry of Human Resource Development, India, the Spanish Agencia Estatal de Investigación (AEI), the Spanish Ministerio de Ciencia, Innovación y Universidades, the European Union NextGenerationEU/PRTR (PRTR-C17.I1), the ICSC—CentroNazionale di Ricerca in High Performance Computing, Big Data and Quantum Computing, funded by the European Union NextGenerationEU, the Comunitat Autonòma de les Illes Balears through the Conselleria d'Educació i Universitats, the Conselleria d'Innovació, Universitats, Ciència i Societat Digital de la Generalitat Valenciana and the CERCA Programme Generalitat de Catalunya, Spain, the Polish National Agency for Academic Exchange, the National Science Centre of Poland and the European Union - European Regional Development Fund; the Foundation for Polish Science (FNP), the Polish Ministry of Science and Higher Education, the Swiss National Science Foundation (SNSF), the Russian Science Foundation, the European Commission, the European Social Funds (ESF), the European Regional Development Funds (ERDF), the Royal Society, the Scottish Funding Council, the Scottish Universities Physics Alliance, the Hungarian Scientific Research Fund (OTKA), the French Lyon Institute of Origins (LIO), the Belgian Fonds de la Recherche Scientifique (FRS-FNRS), Actions de Recherche Concertées (ARC) and Fonds Wetenschappelijk Onderzoek - Vlaanderen (FWO), Belgium, the Paris Iˆle-de-France Region, the National Research, Development and Innovation Office of Hungary (NKFIH), the National Research Foundation of Korea, the Natural Sciences and Engineering Research Council of Canada (NSERC), the Canadian Foundation for Innovation (CFI), the Brazilian Ministry of Science, Technology, and Innovations, the International Center for Theoretical Physics South American Institute for Fundamental Research (ICTP-SAIFR), the Research Grants Council of Hong Kong, the National Natural Science Foundation of China (NSFC), the Israel Science Foundation (ISF), the US-Israel Binational Science Fund (BSF), the Leverhulme Trust, the Research Corporation, the National Science and Technology Council (NSTC), Taiwan, the United States Department of Energy, and the Kavli Foundation. The authors gratefully acknowledge the support of the NSF, STFC, INFN, and CNRS for the provision of computational resources. This work was supported by MEXT, the JSPS Leading-edge Research Infrastructure Program, JSPS Grant-in-Aid for Specially Promoted Research 26000005, JSPS Grant-in-Aid for Scientific Research on Innovative Areas 2402: 24103006, 24103005, and 2905: JP17H06358, JP17H06361, and JP17H06364, JSPS Core-to-Core Program A. Advanced Research Networks, JSPS Grants-in-Aid for Scientific Research (S) 17H06133 and 20H05639, JSPS Grant-in-Aid for Transformative Research Areas (A) 20A203: JP20H05854, the joint research program of the Institute for Cosmic Ray Research, University of Tokyo, the National Research Foundation (NRF), the Computing Infrastructure Project of the Global Science experimental Data hub Center (GSDC) at KISTI, the Korea Astronomy and Space Science Institute (KASI), the Ministry of Science and ICT (MSIT) in Korea, Academia Sinica (AS), the AS Grid Center (ASGC), and the National Science and Technology Council (NSTC) in Taiwan under grants including the Science Vanguard Research Program, the Advanced Technology Center (ATC) of NAOJ, and the Mechanical Engineering Center of KEK and Vietnam National Foundation for Science

and Technology Development > (NAFOSTED) 103.01-2025.147. The activities at the Instituto Argentino de Radioastronomía (IAR) are supported by the national agency CONICET, the Province of Buenos Aires agency (CIC), and the National University of La Plata (UNLP).

Additional acknowledgments for support of individual authors may be found in the following document: https://dcc.ligo.org/LIGO-M2300033/public. For the purpose of open access, the authors have applied a Creative Commons Attribution (CC BY) license to any Author Accepted Manuscript version arising. We request that citations to this article use "A. G. Abac et al. (LIGO–Virgo–KAGRA Collaboration), ..." or similar phrasing, depending on journal convention.

This article has been assigned document No. LIGOP2500086.

Facilities: LIGO, MtPO:26m, IAR.

Software: `astropy` (T. P. Robitaille et al. 2013; A. M. Price-Whelan et al. 2018), `cWB` (S. Klimenko et al. 2016; M. Drago et al. 2021; A. Martini et al. 2026), `CWInPy` (M. Pitkin 2022), `distromax` (R. Tenorio et al. 2022a, 2022b), `DSPSR` (W. van Straten & M. Bailes 2011), `gwpy` (D. M. Macleod et al. 2021), `LALSuite` (LVK 2025), `PyFstat` (D. Keitel et al. 2021; G. Ashton et al. 2025), `matplotlib` (J. D. Hunter 2007), `numpy` (C. R. Harris et al. 2020), `PRESTO` (S. Ransom 2011), `PSRCHIVE` (A. W. Hotan et al. 2004), `PySTAMPAS` (A. Macquet et al. 2021), `ROOT` (R. Brun & F. Rademakers 1997), `scipy` (P. Virtanen et al. 2020), `scikit-image` (S. van der Walt et al. 2014), `SWIGLAL` (K. Wette 2020), `tCWip` (D. Keitel et al. 2025), `TEMPO2` (G. B. Hobbs et al. 2006; R. T. Edwards et al. 2006), `X-pipeline` (P. J. Sutton et al. 2010; M. Was et al. 2012).

Appendix

This appendix includes additional details of the setups and results of the four CW-like long-duration postglitch searches covered in Section 5 of the main text, as well as of the joint analysis of burst and CW results covered in Section 6.3.

Appendix A
Details of the `CWInPy` Analysis

As mentioned in Section 5.2, eight search configurations were used for fully coherent targeted time-domain Bayesian analyses with the `CWInPy` package, corresponding to all combinations of toggling three options. These options are described here in more detail, followed by the full results.

The first option allows the GW strain amplitude to have either a rectangular or exponential decay profile. The rectangular analysis uses a uniform prior on its duration τ ranging from $\tau_{\rm min} = 1\,{\rm hr}$ to $\tau_{\rm max} = 120\,{\rm days}$, i.e., $p(\tau) = (\tau_{\rm max} - \tau_{\rm min})^{-1}$. The prior on the exponential profile's decay factor τ has the same range. In both cases, t_0 is fixed at the glitch epoch.

The second option either allows the orientation angle ι and polarization angle ψ of the source to be unconstrained over their physically allowable ranges or to use observationally motivated constraints on their prior ranges derived from modeling of the pulsar wind nebula (C. Y. Ng & R. W. Romani 2008). The angle ι corresponds to the inclination of the rotation axis with respect to the line of sight, and ψ measures the orientation of the rotation axis in the plane perpendicular to the line of sight. For the unconstrained case, the prior distributions for both are uniform over the surface of a sphere, such that $p(\iota) = \sin\iota$ over the range $[0, \pi)$ and $p(\psi) = 2\pi^{-1}$ over the range $[0, \pi/2)$. When constrained, the prior distribution for ι is a double-peaked Gaussian distribution with peaks at 1.1048 and 2.0368 radians and $\sigma = 10.5\,{\rm mrad}$, and the prior distribution for ψ is a Gaussian distribution centered at 2.2799 radians and $\sigma = 1.5$ mrad (see Appendix B of B. P. Abbott et al. 2017).

The third option covers the cases of a search assuming emission only from the $l = m = 2$ mass quadrupole mode at only twice the rotation frequency, or a search with potential emission from both the $l = 2$, $m = 1, 2$ modes, with dual-harmonic emission at both once and twice the rotation frequency (D. I. Jones 2010; B. P. Abbott et al. 2019). In the latter case, there is a characteristic amplitude for each mode, C_{21} and C_{22}, both of which will have the same decay profile applied to them. This also requires the input data to be processed via heterodyning at both frequencies.

In all cases, we use a broad unphysical uniform prior on the amplitude h_0, or on both C_{21} and C_{22} for the dual-harmonic mode (see Equations (1) and (2) of R. Abbott et al. 2022b), bounded in the range $[0, 10^{-21})$. The upper range is chosen to be large enough that the likelihood will be negligible at this point, while otherwise allowing the likelihood to dominate the posterior. This allows us to provide upper limits that are based on the data only.

Furthermore, in each search configuration, data from the H1 and L1 detectors were analyzed both coherently and incoherently (i.e., with the H1 and L1 datasets combined or analyzed separately), providing Bayesian evidence values for a coherent signal between detectors and independent signals in each detector. This evidence, along with that from assuming purely Gaussian noise in both detectors, has been combined to give an odds ratio comparing a coherent multidetector signal to incoherent signals in each detector or noise (see, e.g., B. P. Abbott et al. 2017).

None of the results indicate more evidence for a coherent signal than for either an incoherent signal or none at all, with the highest $\log_{10}$ Bayesian odds only reaching -3.45 from the configuration with exponential decay, unconstrained (ι, ψ), $l = m = 2$ mode only. Full results from all configurations are included in the data release for this paper.

Due to the absence of evidence for coherent signals, we place upper limits from the posteriors on GW signal amplitudes as a function of τ for each search configuration. Figures 8 and 9 show upper limits $h_0^{95\%}$ for the case where $l = m = 2$, and $C_{21}^{95\%}$ and $C_{22}^{95\%}$ in the case for $l = 2$, $m = 1, 2$, respectively. In each figure, results are included from analyses assuming the rectangular time dependence from Equation (8) or the exponential dependence from Equation (9), and for unconstrained and constrained orientation angles, ι and ψ. All of these upper limits were calculated using samples from the posterior distributions constrained within the τ bins indicated by the horizontal bars in each figure. The `CWInPy` line in Figure 5 corresponds to the exponential window and constrained orientation results, i.e., the dashed orange line in the first panel of Figure 8.

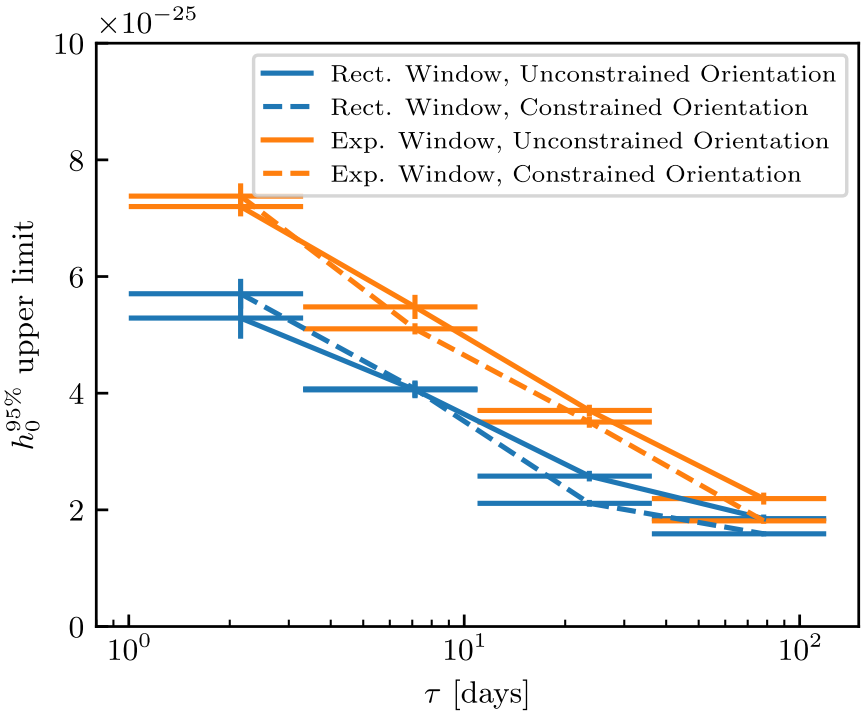

Figure 8. Upper limits from the fully coherent targeted time-domain Bayesian search (`CWInPy`) in terms of $h_0^{95\%}$ as a function of signal duration τ. This search assumes emission only from the $l = m = 2$ mass quadrupole mode. "Rect. Window" lines correspond to the time dependence given in Equation (8), and "Exp. Window" lines to that in Equation (9). The solid and dashed lines indicate searches with unconstrained and constrained orientation angles, ι and ψ, respectively.

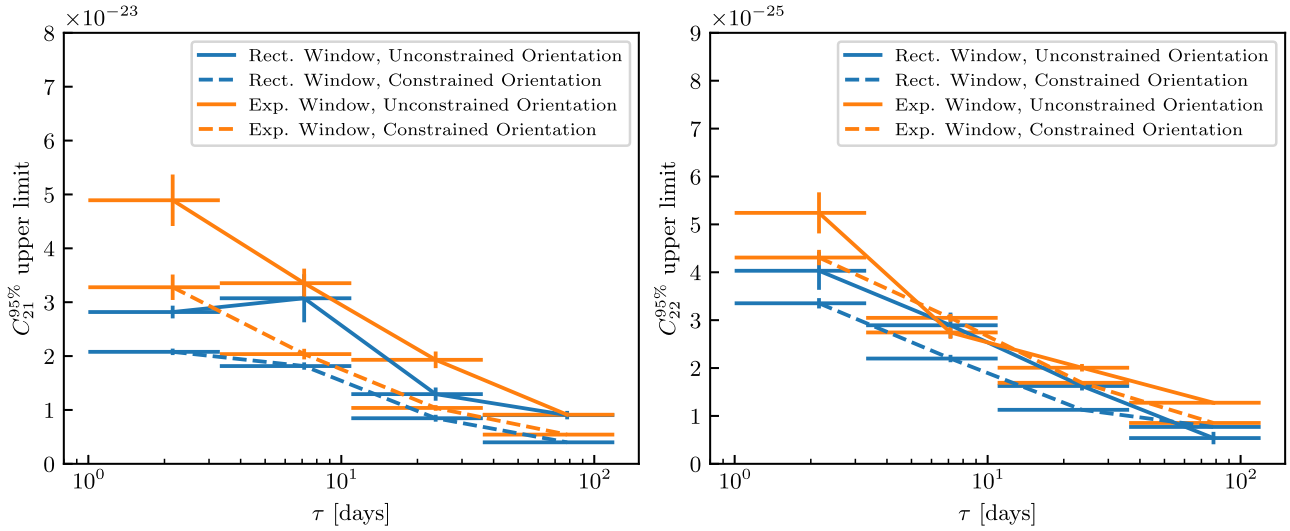

Figure 9. Upper limits from the time-domain Bayesian search (`CWInPy`) in terms of $C_{21}^{95\%}$ and $C_{22}^{95\%}$ as a function of signal duration, τ. This search assumes emission from the $l = 2$, $m = 1$, 2 mass quadrupole modes, where the first panel contains searches for $C_{21}^{95\%}$ and the second panel for $C_{22}^{95\%}$. "Rect. Window" lines correspond to the time dependence given in Equation (8) and "Exp. Window" lines to that in Equation (9). The solid and dashed lines indicate searches with unconstrained and constrained orientation angles, ι and ψ, respectively.

Appendix B
Details of the Transient $\mathcal{F}$-statistic Analysis

Here, we provide additional details of the setup and results of the transient $\mathcal{F}$-statistic search, as summarized in Section 5.3 of the main text. For O4, the search setup, distributed job management and postprocessing from the previous O2 and O3 searches (D. Keitel et al. 2019; L. M. Modafferi et al. 2021, 2023; R. Abbott et al. 2022a) have been refactored as the `tCWip` ("transient continuous-wave investigation pipeline") package (D. Keitel et al. 2025). This wraps CPU code in `LALSuite` (LVK 2025) for rectangular-window (constant amplitude) signals and a `PyCUDA` GPU implementation for exponentially decaying signals in `PyFstat` (D. Keitel & G. Ashton 2018; D. Keitel et al. 2021).

The same grid of templates is used to cover the frequency and frequency derivatives (up to $\ddot{f}_{\rm gw}$) ranges for both amplitude evolution options. The grid spacings are calculated to yield a maximum metric mismatch (R. Prix 2007; K. Wette et al. 2008) of 0.02 over the full $T_{\rm obs}$. The search ranges in all relevant parameters are summarized in Table 3.

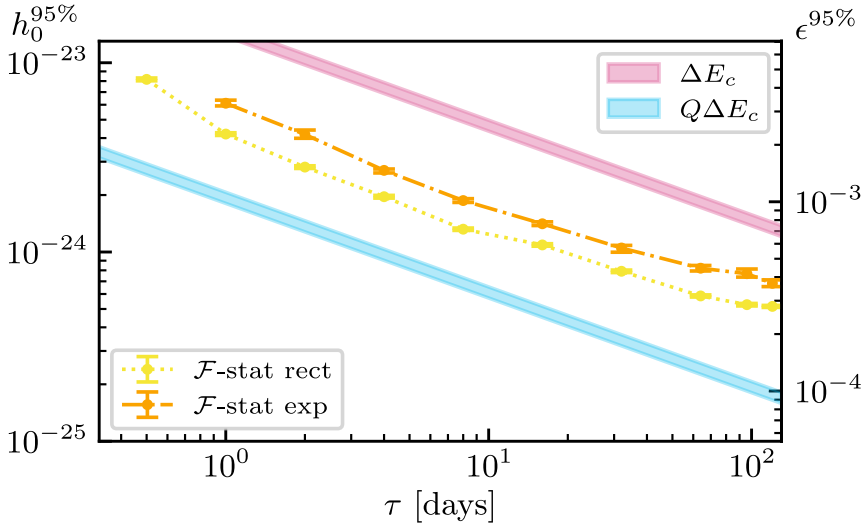

Figure 10. Upper limits from the transient $\mathcal{F}$-statistic search in terms of strain amplitude $h_0^{95\%}$ (left-hand axis) and NS ellipticity $\epsilon^{95\%}$ (right-hand axis) as functions of the signal duration parameter τ. Results are included for both signals with constant amplitude ("rect"), as per Equation (8), and for exponentially decaying signals ("exp"), as per Equation (9). The same indirect energy limits are shown for comparison as in Figure 5, corresponding to Equation (17) with $Q = 1$ (magenta) and $Q \approx 0.017$ (sky blue).

To determine whether there are significant candidates from one of the two analyses, we use the empirical background estimation procedure (R. Tenorio et al. 2022a) implemented in the `distromax` package (R. Tenorio et al. 2022b)—we divide the search results into batches of 5000 templates, fit the distribution of the per-batch maximum detection statistics, and extrapolate this to obtain an estimate of the expected loudest outlier from the full template bank. The automated notching that is also described in R. Tenorio et al. (2022a) is used to reduce the impact of moderate-strength noise disturbances, with one iteration step for the rectangular-window search results and two steps for the exponential-window search results. For rectangular signals, the threshold is set at $\log_{10}\mathcal{B}^{\mathrm{thr}}_{tS/G} \approx 10.02$ while the loudest candidate has $\max \log_{10}\mathcal{B}_{tS/G} \approx 9.65$. For the exponential-window search, the threshold is set to $\log_{10}\mathcal{B}^{\mathrm{thr}}_{tS/G} \approx 9.30$ and the loudest candidate has $\max \log_{10}\mathcal{B}_{tS/G} \approx 9.20$.

We then obtain Frequentist 95% upper limits on the initial strain amplitude h_0 by simulating signals with rectangular windows or single exponential decay windows, following Equations (8) or (9). That is, these upper limits are not making statements about a specific model following the three-component decay observed in the radio but about arbitrary CW-like transients within the search range as long as they fall within the range spanned by frequency and amplitude evolution templates. In fact, the effects of different amplitude evolutions on the sensitivity are relatively minor, see (R. Prix et al. 2011; D. Keitel et al. 2019) but still notable enough to motivate the use of two separate search configurations for rectangular and exponential window functions.

For each window, the simulated signals cover a set of discrete τ values to sample the h_0 upper limits curves, as shown in Figure 10. At each τ value, a discrete set of h_0 values is covered to provide a detection efficiency curve, with 50 injections at each h_0 step. For the injections, the start time t_0 is randomly drawn from the ± 1 day search range, the frequency-evolution parameters are drawn uniformly from the same ranges as covered by the search, and orientation angles are also uniformly sampled. For each h_0, we then count those injections that exceed the threshold from the search with the corresponding window as detectable.

A sigmoid is fitted to the efficiency curve with `scipy` (P. Virtanen et al. 2020) and the $h_0^{95\%}$ value is inferred along with its error bar. Since the detection statistic is a Bayes factor $\mathcal{B}_{tS/G}$ marginalized over start times and durations (R. Prix et al. 2011), the upper limits at each injected τ value automatically include the full trials factor over

Table 3
Setup for the Transient $\mathcal{F}$-statistic Search

Parameter	Value
T_{ref} [s]	1398372935
$t_{0,\mathrm{min}}$ [s]	1398372935
Δt_0 [days]	2
τ_{min} [s]	3600
$\Delta\tau$ [days]	120
f_{gw} [Hz]	22.35453888321711
Δf_{gw} [Hz]	0.022365721744089156
$\dot{f}_{\mathrm{gw}}$ [Hz s^{-1}]	$-3.12874187125924 \times 10^{-11}$
$\Delta\dot{f}_{\mathrm{gw}}$ [Hz s^{-1}]	$2.061675716980504 \times 10^{-13}$
$\ddot{f}_{\mathrm{gw}}$ [Hz s^{-2}]	$1.213100115859692 \times 10^{-21}$
$\Delta\ddot{f}_{\mathrm{gw}}$ [Hz s^{-2}]	$2.639553012031674 \times 10^{-23}$
$\dddot{f}_{\mathrm{gw}}$ [Hz s^{-3}]	$2.5365827014929 \times 10^{-28}$
$\Delta\dddot{f}_{\mathrm{gw}}$ [Hz s^{-3}]	$5.940719999999962 \times 10^{-30}$
N_λ	757016

Note. The reference time T_{ref} for the GW frequency and spin-down parameters f_{gw}, $\dot{f}_{\mathrm{gw}}$, etc., is the first signal start time considered $t_{0,\mathrm{min}}$, which in turn is set to the earliest SFT data timestamp in $T_{\mathrm{gl}} \pm \min(\Delta T_{\mathrm{gl}}, 1\ \mathrm{d})$. The minimum signal duration τ_{min} is, for implementation reasons (R. Prix 2015), set to two SFT lengths. Δt_0 and $\Delta\tau$ are the ranges of start times and durations considered. The minimum frequency f_{gw} and frequency bandwidth Δf_{gw}, and similarly for the three frequency derivatives, are set from the pulsar ephemeris (Table 1), using at each derivative order the maximum of (i) 0.001 times the central value of the parameter, (ii) 3σ uncertainties on it, and (iii) for f_{gw} and $\dot{f}_{\mathrm{gw}}$, the glitch step size. See L. M. Modafferi et al. (2021) for details on this setup procedure. N_λ is the total number of frequency-evolution templates.

the full allowed τ range of the search (i.e., the search is not optimized differently depending on τ).

Appendix C
Details of the WPM Analysis

For the WPM search summarized in Section 5.4, we provide here additional details of the setup and results, as well as a summary of investigations into the three outlier candidates produced by the search.

C.1. Details of the WPM Setup and Results

The WPM search uses the time and frequency parameters reported in Table 4. The segment duration is chosen so that the residual, uncorrected, spin-down due to an NS deformation induced by the glitch would produce a frequency variation confined within a single frequency bin. Moreover, the Doppler modulation correction is robust with respect to a frequency mismatch (i.e., a difference between the frequency used in the heterodyne step, $f_{\rm gw}$ in Table 4, and the actual signal frequency) as large as $\simeq$0.2 Hz, larger than half the analyzed band.

A relevant issue in the search setup concerns the choice of the optimal observation window and segment duration. As a general rule, it is not convenient to consider an observation window which extends to times at which the signal amplitude is significantly decreased because this would correspond to diluting the signal peaks in the noise.

We have studied the optimal window duration (considering a range from 0.5 days to $T_{\rm tot}$, which is the total amount of data at our disposal) and segment duration (among four possible values of $T_{\rm seg}$ equal to 48000, 68000, 96000, and 172332 s) assuming both a signal with a single exponential decay, with various decay times, and a generalization of the model described by G. Yim & D. I. Jones (2023), describing the amplitude evolution by a combination of three decaying exponentials, with decay times derived from the frequency evolution observed in the radio. Given one of these signal models, for each value of the observing window and of the segment duration, we have injected simulated signals of different amplitudes into O4b data and run the analyses, computing for each case the maximum CR. For each signal model, the values $T_{\rm obs}^{\rm best}$ and $T_{\rm seg}^{\rm best}$ that maximize the CR are our optimal choice.

As an example, in Figure 11 we show the CR as a function of the observing window for the multi-τ signal model, and for which the optimal segment duration is $T_{\rm seg}^{\rm best} = 96000$ s, for different signal amplitudes ($[2.1,\ 4.2,\ 6.3,\ 8.4] \times 10^{-24}$) injected into L1 O4b data. The maximum of the CR is at $T_{\rm obs}^{\rm best} \simeq 5.5$ days.

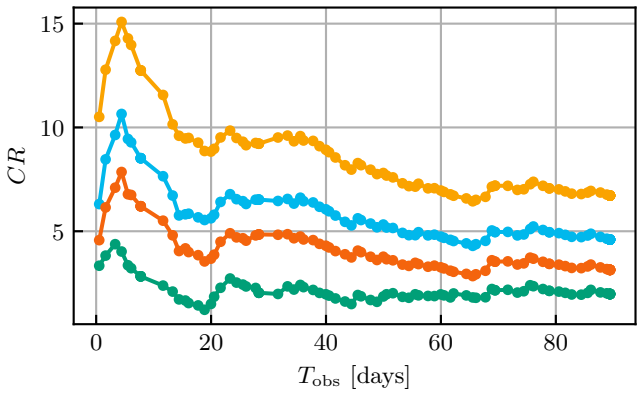

Figure 11. CR as a function of the observing window for the multi-τ signal model and using the optimal segment duration $T_{\rm seg}^{\rm best} = 96000$ s. The plot has been obtained by injecting simulated signals into L1 data with four different signal amplitudes (going from the bottom to the top curve: $[2.1,\ 4.2,\ 6.3,\ 8.4] \times 10^{-24}$). The "optimal" observing window corresponds to the maximum of the CR, which is nearly independent of the signal amplitude, taking place at $T_{\rm obs}^{\rm best} \simeq 5.5$ days.

Table 4
Main Parameters of the WPM Search

Parameter	Value
$T_{\rm start}$ [MJD]	60429.8466
$T_{\rm tot}$ [days]	101.7
$T_{\rm ref}$ [MJD]	60429.86975
$[f_{\rm start},\ f_{\rm stop}]$ [Hz]	[22.306, 22.506] Hz
$f_{\rm gw}$ [Hz]	22.365772235265929
$\dot{f}_{\rm gw}$ [Hz s^{-1}]	$-3.128837145670767 \times 10^{-11}$
$\ddot{f}_{\rm gw}$ [Hz s^{-2}]	$1.248409284183266 \times 10^{-21}$
$\dddot{f}_{\rm gw}$ [Hz s^{-3}]	$2.566286301492900 \times 10^{-28}$

Note. $T_{\rm start}$ is the time of the first sample of the analyzed dataset, 2000 s before the glitch. $T_{\rm ref}$ is the reference time for Vela's position and rotational parameters, and corresponds to the glitch time. $[f_{\rm start},\ f_{\rm stop}]$ defines the frequency interval over which the search is run. The values of the frequency $f_{\rm gw}$ and the first order spin-down, as used for heterodyning, include the variation due to the glitch, $2\Delta f_{\rm rot}$, $2\Delta \dot{f}_{\rm rot}$ respectively, see Table 1.

The full results of this optimization process are shown in columns (2) and (3) of Table 5, together with the numerical values of the final upper limits derived from the search. The full set of upper limits is also plotted in Figure 12.

Upper limits are computed by simulated signal injections into the data, taking the amplitude such that 95% of the injected signals have a CR larger than the highest CR found in the analysis with the same setup, taking into account the specific 0.02 Hz sub-band in which each injection has been done.

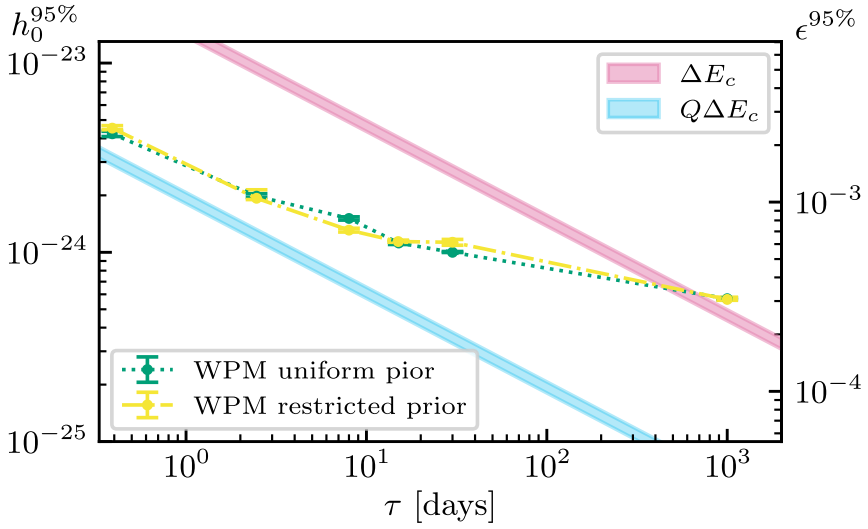

Figure 12. Upper limits (95% C.L.) from the WPM search in terms of strain amplitude and NS ellipticity immediately after the glitch, as a function of the signal decay time τ. The two lines correspond to the upper limits for, respectively, uniform and constrained priors on polarization parameters. See Section 5.2 for a discussion of the constrained parameters. For each τ, the search is run on a time window $T_{\rm obs}^{\rm best}$ and using segments of duration $T_{\rm seg}^{\rm best}$ as shown in Table 5.

Table 5
Summary of the Setup Choices for the WPM Search and 95% C.L. Upper Limits Obtained for Each Search Configuration

τ (days)	$T_{\rm obs}^{\rm best}$ (days)	$T_{\rm seg}^{\rm best}$ (s)	$h_0^{95\%,\rm restr}$	$h_0^{95\%,\rm unif}$
15.11, 2.46, 0.39	5.5	96,000	4.7×10^{-24}	4.5×10^{-24}
0.39	1.1	68,000	4.5×10^{-24}	4.2×10^{-24}
2.46	5.0	96,000	1.9×10^{-24}	2.0×10^{-24}
8	6.0	96,000	1.3×10^{-24}	1.5×10^{-24}
15.11	5.5	96,000	1.1×10^{-24}	1.1×10^{-24}
30	25	172,332	1.1×10^{-24}	1.0×10^{-24}
1000	101.7	172,332	5.6×10^{-25}	5.7×10^{-25}

Note. The first row corresponds to a search for a signal with amplitude varying in time according to a combination of three exponentials, with decay times inferred from the frequency evolution seen in radio observations. The other rows assume a signal amplitude described by a single exponential decay. The last row describes a signal with a nearly constant amplitude. $T_{\rm obs}^{\rm best}$ and $T_{\rm seg}^{\rm best}$ are, respectively, the optimal observation window and segment duration for the assumed signal model. These values depend not only on the signal model but also on the presence and position of gaps in the data. The penultimate column gives the upper limit for restricted priors on polarization parameters and the last column for unrestricted uniform priors.

C.2. Follow-up of Outliers

In this section, we discuss the follow-up of the three outliers found in the WPM search.

The second and third outliers are likely due to an instrumental noise line. Indeed, by rerunning the analysis without Doppler correction, their frequency shifts to 22.5 Hz and the corresponding CR increases significantly (by almost a factor of two), as expected for a detector disturbance.

The first outlier, which is more difficult to discard, has frequency 22.45538 Hz, spin-down $-3.108294 \times 10^{-11}$ Hz s^{-1} (at reference GPS time 1396742418), CR = 6.65, and has been found in the search configuration with $\tau = 8$ days, $T_{\rm obs} = 6$ days and $T_{\rm seg} = 96000$ s. Most of the follow-up tests that we have done have not shown a clear incompatibility with an astrophysical signal.

As a first veto, we have again rerun the analysis switching off the Doppler modulation correction. This results in a decrease in CR from 6.65 to −0.96, which is compatible with what we expect for a real signal.

A second test consisted of running a semicoherent search, using the semicoherent 5-vector method (S. D'Antonio et al. 2023), with segment duration of 2, 3, and 6 days. Actually, these analyses produce three nearby candidates, with very similar CR, compatible with the original one, which are all considered in the next steps. The candidates remain significant when a segment duration of 2 days is used. For an astrophysical signal, we expect the CR to increase with longer segment duration. This does not happen when passing from 2 to 3 days (the CR remains nearly unchanged), while it happens when 6 days are used (going from ∼7.5 at 2 days to ∼10.7 at 6 days).

We then repeated the analysis with a single data segment of 6 days shifting the starting time both backward and forward (−3.0, −1.5, −0.5, +0.5, +1.5, +3 days with respect to the signal reference starting time). The resulting CRs have been compared with what we would expect for a real signal which starts around the glitch time, both assuming an exponential decay with $\tau = 8$ days over a time window of 6 days and a constant amplitude signal of duration 5 or 7 days. We find that the CR steadily decreases both when the observing window is shifted backward and forward, becoming fully compatible with noise for a shift of ±3 days. Overall, this test seems to indicate that there is a feature in the data which switches on around the glitch time and switches off after 5–7 days.

Finally, we have used the fully coherent 5-vector method (P. Astone et al. 2010) to estimate the parameters of the potential signal associated to the candidates from the semicoherent 5-vector step, using the frequency and spin-down values found in the $T_{\rm seg} = 6$ days analysis. The estimated parameters for the three candidates that we have analyzed are shown in Table 6. The last column, in particular, is an estimation of the so-called 5-vector "coherence," which is a measure (between 0 and 1) of how much the data resembles the best matching template. The highest value we get, $\mathcal{C} = 0.91$, for the second candidate corresponds to a false-alarm probability (in Gaussian noise) of about 0.012, after taking the trial factor into account.

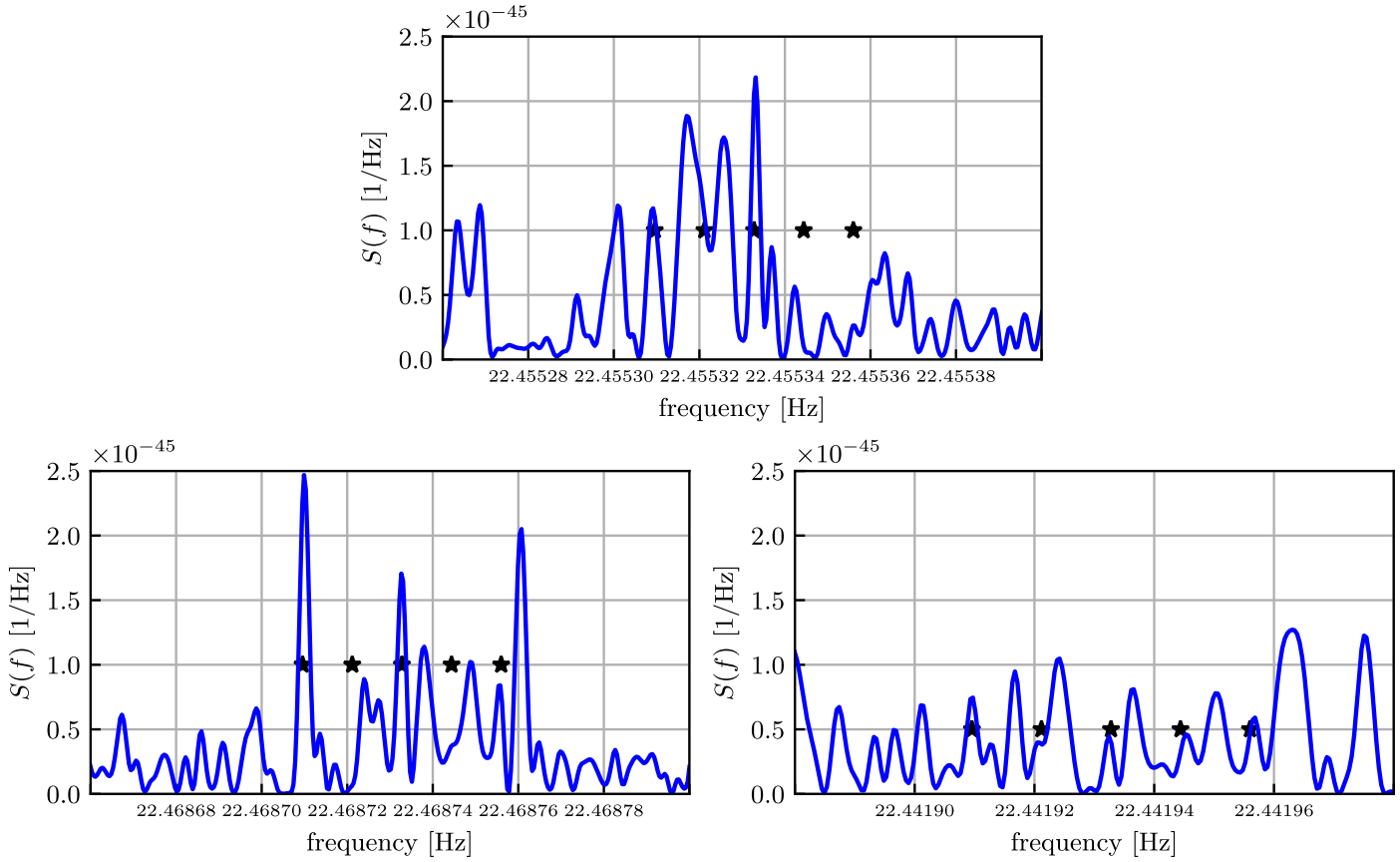

Figure 13. Top plot: Power spectrum $S(f)$ of the LIGO data, after correction of the Doppler effect and spin-down of the second candidate in Table 6. The two other plots show the corrected power spectrum after the injection of a simulated signal with the same parameters as the second candidate in Table 6 but with frequency shifted by +13.4 mHz (bottom left) and −13.4 mHz (bottom right). The asterisks denote the position of the five expected peaks produced by the sidereal modulation.

Table 6
Main Parameters of the WPM Outliers After Coherent 5-vector Follow-up

Outlier	Frequency (Hz)	Spin-down (Hz s^{-1})	h_0	η	ψ (deg)	CR	$\mathcal{C}$
1	22.455332	-3.316×10^{-11}	5.62×10^{-25}	−0.455	9.79	10.6	0.81
2	22.455333	-3.129×10^{-11}	7.72×10^{-25}	0.037	6.78	10.7	0.91
3	22.455334	-3.129×10^{-11}	4.64×10^{-25}	−0.20	9.80	10.7	0.54

Note. Parameter estimation, with the fully coherent 5-vector method, for the three candidates associated with the first outlier from the main search. Rotational parameters are referred to MJD time 60429.8466 (GPS 1398457164.24).

We have then inspected the power spectrum of the data after Doppler and spin-down correction: in the presence of a sufficiently strong astrophysical signal, we expect to see the typical 5-vector signature, due to the signal's sidereal modulation. The spectrum after correcting the data for the parameters of the second candidate in Table 6 (i.e., that with the highest coherence) is shown in the top plot of Figure 13. The five asterisks denote the expected frequency of the five peaks (not the amplitude). We can see that at least two, out of five, peaks have a rather clear counterpart in the data. As a cross-check, we have computed the spectrum after injecting a simulated signal with the same parameters as those estimated for the second candidate, except for the frequency that has been shifted by some random amount. As an example, in Figure 13 we show the spectra for shifts of ±13.4 mHz. At the higher frequency, the spectrum looks slightly better when compared to the expected peak position, with two peaks clearly corresponding to features in the data (the first and the third peak, as for the real analysis candidate) and, possibly, also the fourth. At the lower frequency, on the other hand, the situation is much less clear, with only one convincing correspondence among the expected peak frequencies and the features in the data.

Overall, our tests for this outlier have been inconclusive. Our conclusion is that even if a GW signal was really present in the data, it is very marginal and a detection cannot be claimed with sufficient confidence.

Appendix D
Details of the HMM Analysis

Here, we provide additional details concerning the HMM search. The template parameters, search band, and coherence times are summarized in Table 7.

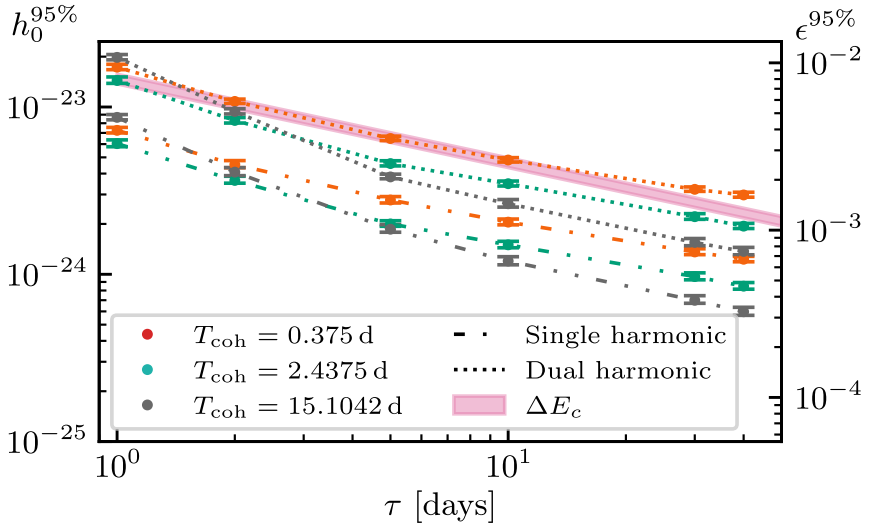

Figure 14. Upper limits on long-transient GWs from Vela inferred by the single (dashed–dotted lines) and dual-harmonic (dotted lines) HMM analyses as a function of the exponential signal decay time parameter τ. Upper limits are expressed in terms of strain amplitude $h_0^{95\%}$ (left axis) and NS ellipticity $\epsilon^{95\%}$ (right axis). The magenta shaded comparison band labeled ΔE_c corresponds to Equation (17) with $Q = 1$.

Table 7
Search Setup for the HMM Search

Parameter	Value
$T_{\rm start}$ [GPS]	1398458994
$T_{\rm ref}$ [GPS]	1398459095.043
$T_{\rm obs}$ [days]	90
$T_{\rm coh}$ [days]	0.375, 2.4374, 15.1042
$f_{\rm rot}$ [Hz]	11.1828595
$\dot{f}_{\rm rot}$ [Hz s^{-1}]	$-1.5540586 \times 10^{-11}$
$\ddot{f}_{\rm rot}$ [Hz s^{-2}]	6.242×10^{-22}
$\dddot{f}_{\rm rot}$ [Hz s^{-3}]	1.28×10^{-28}
$\Delta f_{\rm rot}$ [Hz]	0.05
N_T	240, 36, 5

Note. The GPS start time is rounded to the last SFT timestamp before the glitch arrival time at the detectors. The coherence times are similarly rounded down to the nearest multiple of 1800 s. The reference time is the glitch arrival time at the solar system barycenter and the spin frequencies are extrapolated to this time. The frequency, bandwidth, and frequency derivative correspond to the Vela spin frequency; the values at twice the spin frequency are found by multiplying these quantities by two.

Table 8
Detection Statistic Thresholds for the HMM Search

Statistic	$T_{\rm coh} = 0.375$ days	2.4374 days	15.1042 days
$\bar{\mathcal{L}}^{\rm 2F}_{\rm th,G}$	7.05	9.33	17.14
$\bar{\mathcal{L}}^{\rm 2F}_{\rm th,OT}$	6.99	9.32	17.06
$\bar{\mathcal{L}}^{\rm 2F}_{\rm max}$	6.85	8.43	14.44
$\bar{\mathcal{L}}^{\rm 1F+2F}_{\rm th,G}$	11.86	14.77	24.43
$\bar{\mathcal{L}}^{\rm 1F+2F}_{\rm th,OT}$	11.5	14.38	24.09
$\bar{\mathcal{L}}^{\rm 1F+2F}_{\rm max}$	11.46	13.56	19.59

Note. All log-likelihood thresholds are quoted at the level of 1% false-alarm probability, including trials factors.

As discussed in Section 5.5, empirical detection thresholds are set using one of two methods. In the first method, we perform the search on 10^4 realizations of synthetic Gaussian noise data to accumulate log-likelihood samples $\bar{\mathcal{L}}_i$, keeping the same search parameters given in Table 7. We set thresholds based on the Viterbi log-likelihood $\bar{\mathcal{L}}_{\rm th}$ at which a desired fraction α of the samples derived from Gaussian noise simulations is above the threshold, $\bar{\mathcal{L}}_i > \bar{\mathcal{L}}_{\rm th}$. In the second method, we set thresholds in exactly the same way, but instead the log-likelihood samples are derived from searching real detector data at 10^4 off-target sky positions. We sample off-target sky positions by shifting the search from the true Vela position by a random angle between $\pm(5^\circ$ and $15^\circ)$ in R.A. and $\pm 5^\circ$ in Decl. In both methods, we set the false-alarm probability at $\alpha = 0.01/3$ for each choice of $T_{\rm coh}$, such that the overall rate of false alarms, accounting for the trials factor from three different coherence times, is 1%. The resulting thresholds for each choice of $T_{\rm coh}$ and sampling method are shown in Table 8, where we also list the maximum statistics obtained from the single- and dual-harmonic HMM searches.

In simulating the injections used to set upper limits, the relative amplitudes of each harmonic depend on the angle, θ, between the NS's axis of rotation and the principal moment of inertia, where $\theta = \pi/2$ corresponds to a GW emission at $f_{\rm gw} = 2f_{\rm rot}$ only (e.g., P. Jaranowski et al. 1998). We therefore fix $\theta = \pi/2$ for the single-harmonic injections and $\theta = \pi/4$ for the dual-harmonic injections, where the latter corresponds to roughly equal strain amplitudes at $f_{\rm rot}$ and $2f_{\rm rot}$. Figure 14 shows upper limits on the strain amplitude and ellipticity, respectively, inferred by the HMM analysis. Different curves correspond to different choices of the coherence time and whether the signal model is assumed to have one component at twice the Vela spin frequency or at both once and twice the spin frequency. Unfortunately, because of the large disparity in the detector noise floors between 11 and 22 Hz, the band at $f_{\rm gw} = f_{\rm rot}$ mostly contributes noise for any reasonable range of h_0. Hence, our upper limits that assume dual-harmonic emission are consistently worse by a factor of $\sim$2.3.

Appendix E
Details of the Joint NS Properties Inference

To sample the parameter space for joint inference under the assumption of the Vela pulsar emitting GWs both from an f-mode and a transient mountain, we use the following priors. The NS mass prior is uniform in $[0.9\,M_\odot, 2.6\,M_\odot]$. The NS radius prior is uniform in [8 km, 16 km]. Constraints are enforced such that the mass and radius obey causality and the NS does not collapse to a black hole (see black contour in Figure 6). The prior for the glitch-induced spin change $\Delta f_{\rm rot}/f_{\rm rot}$ is a Gaussian distribution centered at 2.377×10^{-6} with $\sigma = 4.47 \times 10^{-11}$. We choose the inclination angle ι prior to be a double-peaked Gaussian distribution with peaks at 1.1048 and 2.0368 radians and $\sigma = 10.5$ mrad in order to match the astrophysical prior used in Section 5.2 and based on C. Y. Ng & R. W. Romani (2008). The distance d prior is a Gaussian centered on 287 pc with $\sigma = 9.5$ pc, matching R. Dodson et al. (2003). The mountain decay time $\tau_{\rm CW}$ prior is uniform from 1 hr to 120 days, matching the search durations covered in Section 5. The prior for the mountain energy scaling factor $f_{\rm CW}$ is log-uniform from 10^{-4} to 1.0 (none of the searches would be sensitive below the cutoff) and the prior for the f-mode energy scaling factor $f_{\rm fmode}$ is uniform between 0 and 1 (Figure 6) or fixed to 0.8 (Figure 7). For the model-specific results reported in Figure 7, we also set the prior on the duration parameter $\tau_{\rm CW}$ of CW-like signals to a Gaussian distribution peaked at twice the first decay time $\tau_d^1 = 15.1$ days of the radio-frequency evolution, with $\sigma = 0.2$ days, to match G. Yim & D. I. Jones's (2020) model and Table 1.

We then combine the nondetection results from one representative pipeline each for the burst-type search for f-modes and the CW-like search for long transients from postglitch mountain formation. For the f-mode, we use the ringdown injection curves generated by `X-pipeline` for different frequencies and damping times. These curves are linearly interpolated and subtracted from unity to give the probability that a waveform generated by a particular set of parameters would be detected by `X-pipeline`. For the mountain model, we use the posterior distribution on amplitude h_0 and CW damping time $\tau_{\rm CW}$ produced by `CWInPy` for an exponential decay profile and constrained orientation, as described in Appendix A. This likelihood distribution is interpreted as the probability that a given parameter would generate a waveform consistent with background noise.

For each sample, we compute the probability of nondetection using the `X-pipeline`-informed likelihood function and the probability of consistency with background using the `CWInPy`-informed likelihood function. We then reweigh the prior samples with the product of these likelihoods according to Bayes's theorem to give a posterior distribution on the sampled parameters consistent with search results. This reweighting is done via rejection sampling, where the product of the two likelihoods is used as the probability that a given sample will not be rejected. Samples with higher likelihood are thus more likely to be preserved, and samples with lower likelihoods are more likely to be rejected.

Further details of the implementation are described in M. Ball & R. Frey (2025).

ORCID iDs

A. G. Abac https://orcid.org/0000-0003-4786-2698
K. Ackley https://orcid.org/0000-0002-8648-0767
C. Adamcewicz https://orcid.org/0000-0001-5525-6255
S. Adhicary https://orcid.org/0009-0004-2101-5428
N. Adhikari https://orcid.org/0000-0002-4559-8427
R. X. Adhikari https://orcid.org/0000-0002-5731-5076
S. Afroz https://orcid.org/0009-0004-4459-2981
D. Agarwal https://orcid.org/0000-0002-8735-5554
M. Agathos https://orcid.org/0000-0002-9072-1121
O. D. Aguiar https://orcid.org/0000-0002-2139-4390
L. Aiello https://orcid.org/0000-0003-2771-8816
A. Ain https://orcid.org/0000-0003-4534-4619
P. Ajith https://orcid.org/0000-0001-7519-2439
T. Akutsu https://orcid.org/0000-0003-0733-7530
S. Albanesi https://orcid.org/0000-0001-7345-4415
A. Allocca https://orcid.org/0000-0002-5288-1351
P. A. Altin https://orcid.org/0000-0001-8193-5825
S. Alvarez-Lopez https://orcid.org/0009-0003-8040-4936
A. Amato https://orcid.org/0000-0001-9557-651X
F. Amicucci https://orcid.org/0009-0005-2139-4197
S. B. Anderson https://orcid.org/0000-0003-2219-9383
W. G. Anderson https://orcid.org/0000-0003-0482-5942
M. Andia https://orcid.org/0000-0003-3675-9126
M. Andrés-Carcasona https://orcid.org/0000-0002-8738-1672
T. Andrić https://orcid.org/0000-0002-9277-9773
S. Ansoldi https://orcid.org/0000-0002-5613-7693
J. M. Antelis https://orcid.org/0000-0003-3377-0813
S. Antier https://orcid.org/0000-0002-7686-3334
S. K. Apple https://orcid.org/0009-0007-4490-5804
K. Arai https://orcid.org/0000-0001-8916-8915
A. Araya https://orcid.org/0000-0002-6884-2875
M. C. Araya https://orcid.org/0000-0002-6018-6447
M. Arca Sedda https://orcid.org/0000-0002-3987-0519
J. S. Areeda https://orcid.org/0000-0003-0266-7936
F. Armato https://orcid.org/0000-0002-8856-8877
S. Armstrong https://orcid.org/0009-0009-4285-2360
N. Arnaud https://orcid.org/0000-0001-6589-8673
M. Arogeti https://orcid.org/0000-0001-5124-3350
S. M. Aronson https://orcid.org/0000-0001-7080-8177
G. Ashton https://orcid.org/0000-0001-7288-2231
Y. Aso https://orcid.org/0000-0002-1902-6695
P. Astone https://orcid.org/0000-0003-4981-4120
F. Attadio https://orcid.org/0009-0008-8916-1658
F. Aubin https://orcid.org/0000-0003-1613-3142
K. AultONeal https://orcid.org/0000-0002-6645-4473
G. Avallone https://orcid.org/0000-0001-5482-0299
E. A. Avila https://orcid.org/0009-0008-9329-4525
S. Babak https://orcid.org/0000-0001-7469-4250
S. Bae https://orcid.org/0000-0003-2429-3357
S. Bagnasco https://orcid.org/0000-0001-6062-6505
L. Baiotti https://orcid.org/0000-0003-0458-4288
R. Bajpai https://orcid.org/0000-0003-0495-5720
T. Baker https://orcid.org/0000-0001-5470-7616
G. Baldi https://orcid.org/0000-0001-8963-3362
N. Baldicchi https://orcid.org/0009-0009-8888-291X
S. Banagiri https://orcid.org/0000-0001-7852-7484
B. Banerjee https://orcid.org/0000-0002-8008-2485
D. Bankar https://orcid.org/0000-0002-6068-2993
P. Baral https://orcid.org/0000-0001-6308-211X
M. Baratti https://orcid.org/0009-0003-5744-8025

P. Barneo https://orcid.org/0000-0002-8883-7280
F. Barone https://orcid.org/0000-0002-8069-8490
B. Barr https://orcid.org/0000-0002-5232-2736
L. Barsotti https://orcid.org/0000-0001-9819-2562
M. Barsuglia https://orcid.org/0000-0002-1180-4050
D. Barta https://orcid.org/0000-0001-6841-550X
M. A. Barton https://orcid.org/0000-0002-9948-306X
A. Basalaev https://orcid.org/0000-0001-5623-2853
R. Bassiri https://orcid.org/0000-0001-8171-6833
A. Basti https://orcid.org/0000-0003-2895-9638
M. Bawaj https://orcid.org/0000-0003-3611-3042
J. C. Bayley https://orcid.org/0000-0003-2306-4106
A. C. Baylor https://orcid.org/0000-0003-0918-0864
F. Beirnaert https://orcid.org/0000-0002-4003-7233
M. Bejger https://orcid.org/0000-0002-4991-8213
D. Belardinelli https://orcid.org/0000-0001-9332-5733
A. S. Bell https://orcid.org/0000-0003-1523-0821
L. Bellizzi https://orcid.org/0000-0002-2071-0400
W. Benoit https://orcid.org/0000-0003-4750-9413
I. Bentara https://orcid.org/0009-0000-5074-839X
J. D. Bentley https://orcid.org/0000-0002-4736-7403
S. Bera https://orcid.org/0000-0003-0907-6098
F. Bergamin https://orcid.org/0000-0002-1113-9644
B. K. Berger https://orcid.org/0000-0002-4845-8737
S. Bernuzzi https://orcid.org/0000-0002-2334-0935
M. Beroiz https://orcid.org/0000-0001-6486-9897
D. Bersanetti https://orcid.org/0000-0002-7377-415X
J. Betzwieser https://orcid.org/0000-0003-1533-9229
D. Beveridge https://orcid.org/0000-0002-1481-1993
G. Bevilacqua https://orcid.org/0000-0002-7298-6185
N. Bevins https://orcid.org/0000-0002-4312-4287
D. Bhattacharjee https://orcid.org/0000-0001-6623-9506
S. Bhaumik https://orcid.org/0000-0001-8492-2202
V. Biancalana https://orcid.org/0000-0002-1642-5391
G. Billingsley https://orcid.org/0000-0002-4141-2744
A. Binetti https://orcid.org/0000-0001-6449-5493
S. Bini https://orcid.org/0000-0002-0267-3562
O. Birnholtz https://orcid.org/0000-0002-7562-9263
S. Biscoveanu https://orcid.org/0000-0001-7616-7366
M. Bitossi https://orcid.org/0000-0002-9862-4668
M.-A. Bizouard https://orcid.org/0000-0002-4618-1674
J. K. Blackburn https://orcid.org/0000-0002-3838-2986
N. Bode https://orcid.org/0000-0002-7101-9396
G. Boileau https://orcid.org/0000-0002-3576-6968
M. Boldrini https://orcid.org/0000-0001-9861-821X
G. N. Bolingbroke https://orcid.org/0000-0002-7350-5291
L. D. Bonavena https://orcid.org/0000-0002-2630-6724
R. Bondarescu https://orcid.org/0000-0003-0330-2736
F. Bondu https://orcid.org/0000-0001-6487-5197
E. Bonilla https://orcid.org/0000-0002-6284-9769
M. S. Bonilla https://orcid.org/0000-0003-4502-528X
R. Bonnand https://orcid.org/0000-0001-5013-5913
V. Boschi https://orcid.org/0000-0001-8665-2293
Y. Bothra https://orcid.org/0000-0002-9380-6390
P. R. Brady https://orcid.org/0000-0002-4611-9387
M. Branchesi https://orcid.org/0000-0003-1643-0526
T. Briant https://orcid.org/0000-0002-6013-1729
E. Brockmueller https://orcid.org/0000-0002-1489-942X
A. F. Brooks https://orcid.org/0000-0003-4295-792X
M. L. Brozzetti https://orcid.org/0000-0002-5260-4979
R. Bruntz https://orcid.org/0000-0002-0840-8567
F. Bucci https://orcid.org/0000-0003-1726-3838
O. Bulashenko https://orcid.org/0000-0003-1720-4061
A. Buonanno https://orcid.org/0000-0002-5433-1409
R. Buscicchio https://orcid.org/0000-0002-7387-6754
C. Buy https://orcid.org/0000-0003-2872-8186
G. S. Cabourn Davies https://orcid.org/0000-0002-4289-3439
R. Cabrita https://orcid.org/0000-0003-0133-1306
V. Cáceres-Barbosa https://orcid.org/0000-0001-9834-4781
L. Cadonati https://orcid.org/0000-0002-9846-166X
G. Cagnoli https://orcid.org/0000-0002-7086-6550
C. Cahillane https://orcid.org/0000-0002-3888-314X
S. R. Callos https://orcid.org/0000-0003-0639-9342
G. Caneva Santoro https://orcid.org/0000-0002-2935-1600
K. C. Cannon https://orcid.org/0000-0003-4068-6572
E. Capocasa https://orcid.org/0000-0003-3762-6958
E. Capote https://orcid.org/0009-0007-0246-713X
G. Capurri https://orcid.org/0000-0003-0889-1015
J. B. Carlin https://orcid.org/0000-0001-5694-0809
M. Carpinelli https://orcid.org/0000-0002-8205-930X
J. J. Carter https://orcid.org/0000-0001-8845-0900
G. Carullo https://orcid.org/0000-0001-9090-1862
J. Casanueva Diaz https://orcid.org/0000-0002-2948-5238
C. Casentini https://orcid.org/0000-0001-8100-0579
M. Cavaglià https://orcid.org/0000-0002-3835-6729
R. Cavalieri https://orcid.org/0000-0001-6064-0569
G. Cella https://orcid.org/0000-0002-0752-0338
P. Cerdá-Durán https://orcid.org/0000-0003-4293-340X
E. Cesarini https://orcid.org/0000-0001-9127-3167
A. Chakraborty https://orcid.org/0009-0004-4937-4633
P. Chakraborty https://orcid.org/0000-0002-0994-7394
S. Chalathadka Subrahmanya https://orcid.org/0000-0002-9207-4669
J. C. L. Chan https://orcid.org/0000-0002-3377-4737
S. Chao https://orcid.org/0000-0003-3853-3593
P. Charlton https://orcid.org/0000-0002-4263-2706
E. Chassande-Mottin https://orcid.org/0000-0003-3768-9908
C. Chatterjee https://orcid.org/0000-0001-8700-3455
Debarati Chatterjee https://orcid.org/0000-0002-0995-2329
Deep Chatterjee https://orcid.org/0000-0003-0038-5468
S. Chaty https://orcid.org/0000-0002-5769-8601
A. Chen https://orcid.org/0000-0001-9174-7780
D. Chen https://orcid.org/0000-0003-1433-0716
H. Y. Chen https://orcid.org/0000-0001-5403-3762
Yitian Chen https://orcid.org/0000-0002-8664-9702
P. Chessa https://orcid.org/0000-0001-9092-3965
H. T. Cheung https://orcid.org/0000-0003-3905-0665
F. Chiadini https://orcid.org/0000-0002-9339-8622
A. Chincarini https://orcid.org/0000-0003-4094-9942
M. L. Chiofalo https://orcid.org/0000-0002-6992-5963
A. Chiummo https://orcid.org/0000-0003-2165-2967
S. Choudhary https://orcid.org/0000-0003-0949-7298
N. Christensen https://orcid.org/0000-0002-6870-4202
S. S. Y. Chua https://orcid.org/0000-0001-8026-7597
G. Ciani https://orcid.org/0000-0003-4258-9338
P. Ciecielag https://orcid.org/0000-0002-5871-4730
M. Cieślar https://orcid.org/0000-0001-8912-5587
M. Cifaldi https://orcid.org/0009-0007-1566-7093
J. A. Clark https://orcid.org/0000-0003-3243-1393
T. A. Clarke https://orcid.org/0000-0002-6714-5429
E. Codazzo https://orcid.org/0000-0001-7170-8733

P.-F. Cohadon https://orcid.org/0000-0003-3452-9415
S. Colace https://orcid.org/0009-0007-9429-1847
M. Colleoni https://orcid.org/0000-0002-7214-9088
S. Colloms https://orcid.org/0009-0009-9828-3646
A. Colombo https://orcid.org/0000-0002-7439-4773
L. Conti https://orcid.org/0000-0003-2731-2656
T. R. Corbitt https://orcid.org/0000-0002-5520-8541
I. Cordero-Carrión https://orcid.org/0000-0002-1985-1361
S. Corezzi https://orcid.org/0000-0002-3437-5949
N. J. Cornish https://orcid.org/0000-0002-7435-0869
A. Corsi https://orcid.org/0000-0001-8104-3536
M. W. Coughlin https://orcid.org/0000-0002-8262-2924
P. Couvares https://orcid.org/0000-0002-2823-3127
R. Coyne https://orcid.org/0000-0002-5243-5917
J. D. E. Creighton https://orcid.org/0000-0003-3600-2406
P. Cremonese https://orcid.org/0000-0001-6472-8509
J. R. Cudell https://orcid.org/0000-0002-2003-4238
T. J. Cullen https://orcid.org/0000-0001-8075-4088
A. Cumming https://orcid.org/0000-0003-4096-7542
E. Cuoco https://orcid.org/0000-0002-6528-3449
M. Cusinato https://orcid.org/0000-0003-4075-4539
L. V. Da Conceição https://orcid.org/0000-0002-5042-443X
T. Dal Canton https://orcid.org/0000-0001-5078-9044
S. Dal Pra https://orcid.org/0000-0002-1057-2307
G. Dálya https://orcid.org/0000-0003-3258-5763
B. D'Angelo https://orcid.org/0000-0001-9143-8427
S. Danilishin https://orcid.org/0000-0001-7758-7493
S. D'Antonio https://orcid.org/0000-0003-0898-6030
L. P. Dartez https://orcid.org/0000-0002-2216-0465
V. Dattilo https://orcid.org/0000-0002-8816-8566
D. Davis https://orcid.org/0000-0001-5620-6751
M. C. Davis https://orcid.org/0000-0001-7663-0808
P. Davis https://orcid.org/0009-0004-5008-5660
E. J. Daw https://orcid.org/0000-0002-3780-5430
M. Dax https://orcid.org/0000-0001-8798-0627
J. De Bolle https://orcid.org/0000-0002-5179-1725
J. Degallaix https://orcid.org/0000-0002-1019-6911
M. De Laurentis https://orcid.org/0000-0002-3815-4078
F. De Lillo https://orcid.org/0000-0003-4977-0789
S. Della Torre https://orcid.org/0000-0002-7669-0859
W. Del Pozzo https://orcid.org/0000-0003-3978-2030
F. De Marco https://orcid.org/0000-0002-5411-9424
F. De Matteis https://orcid.org/0000-0001-7860-9754
T. Dent https://orcid.org/0000-0003-1354-7809
A. Depasse https://orcid.org/0000-0003-1014-8394
R. De Pietri https://orcid.org/0000-0003-1556-8304
R. De Rosa https://orcid.org/0000-0002-4004-947X
C. De Rossi https://orcid.org/0000-0002-5825-472X
M. Desai https://orcid.org/0009-0003-4448-3681
R. DeSalvo https://orcid.org/0000-0002-4818-0296
A. Dhani https://orcid.org/0000-0001-9930-9101
M. C. Díaz https://orcid.org/0000-0002-7555-8856
M. Di Cesare https://orcid.org/0009-0003-0411-6043
T. Dietrich https://orcid.org/0000-0003-2374-307X
C. Di Fronzo https://orcid.org/0000-0002-2693-6769
M. Di Giovanni https://orcid.org/0000-0003-4049-8336
T. Di Girolamo https://orcid.org/0000-0003-2339-4471
J. Ding https://orcid.org/0000-0003-1693-3828
S. Di Pace https://orcid.org/0000-0001-6759-5676
I. Di Palma https://orcid.org/0000-0003-1544-8943
F. Di Renzo https://orcid.org/0000-0002-5447-3810
Divyajyoti https://orcid.org/0000-0002-2787-1012
A. Dmitriev https://orcid.org/0000-0002-0314-956X
Z. Doctor https://orcid.org/0000-0002-2077-4914
N. Doerksen https://orcid.org/0009-0002-3776-5026
L. D'Onofrio https://orcid.org/0000-0001-9546-5959
K. L. Dooley https://orcid.org/0000-0002-1636-0233
S. Doravari https://orcid.org/0000-0001-8750-8330
M. Drago https://orcid.org/0000-0002-3738-2431
J. C. Driggers https://orcid.org/0000-0002-6134-7628
L. Dunn https://orcid.org/0000-0002-1769-6097
P.-A. Duverne https://orcid.org/0000-0002-3906-0997
D. D'Urso https://orcid.org/0000-0002-8215-4542
P. Dutta Roy https://orcid.org/0000-0001-8874-4888
H. Duval https://orcid.org/0000-0002-2475-1728
M. Ebersold https://orcid.org/0000-0003-4631-1771
T. Eckhardt https://orcid.org/0000-0002-1224-4681
G. Eddolls https://orcid.org/0000-0002-5895-4523
A. Effler https://orcid.org/0000-0001-8242-3944
J. Eichholz https://orcid.org/0000-0002-2643-163X
M. Emma https://orcid.org/0000-0001-7943-0262
R. Enficiaud https://orcid.org/0000-0003-3908-1912
L. Errico https://orcid.org/0000-0003-2112-0653
M. Esposito https://orcid.org/0009-0009-8482-9417
R. C. Essick https://orcid.org/0000-0001-8196-9267
H. Estellés https://orcid.org/0000-0001-6143-5532
M. Evans https://orcid.org/0000-0001-8459-4499
J. M. Ezquiaga https://orcid.org/0000-0002-7213-3211
F. Fabrizi https://orcid.org/0000-0002-3809-065X
V. Fafone https://orcid.org/0000-0003-1314-1622
S. Fairhurst https://orcid.org/0000-0001-8480-1961
A. M. Farah https://orcid.org/0000-0002-6121-0285
B. Farr https://orcid.org/0000-0002-2916-9200
W. M. Farr https://orcid.org/0000-0003-1540-8562
G. Favaro https://orcid.org/0000-0002-0351-6833
M. Favata https://orcid.org/0000-0001-8270-9512
M. Fays https://orcid.org/0000-0002-4390-9746
M. Fazio https://orcid.org/0000-0002-9057-9663
R. Felicetti https://orcid.org/0009-0005-6263-5604
E. Fenyvesi https://orcid.org/0000-0003-2777-3719
T. Fernandes https://orcid.org/0009-0006-6820-2065
S. Ferraiuolo https://orcid.org/0009-0005-5582-2989
M. Ferrer https://orcid.org/0009-0008-9801-9506
F. Fidecaro https://orcid.org/0000-0002-6189-3311
P. Figura https://orcid.org/0000-0002-8925-0393
A. Fiori https://orcid.org/0000-0003-3174-0688
I. Fiori https://orcid.org/0000-0002-0210-516X
M. Fishbach https://orcid.org/0000-0002-1980-5293
R. Fittipaldi https://orcid.org/0000-0003-2096-7983
V. Fiumara https://orcid.org/0000-0003-3644-217X
S. M. Fleischer https://orcid.org/0000-0001-7884-9993
J. A. Font https://orcid.org/0000-0001-6650-2634
B. Fornal https://orcid.org/0000-0003-3271-2080
F. Frasconi https://orcid.org/0000-0003-4204-6587
Z. Frei https://orcid.org/0000-0002-0181-8491
A. Freise https://orcid.org/0000-0001-6586-9901
O. Freitas https://orcid.org/0000-0002-2898-1256
R. Frey https://orcid.org/0000-0003-0341-2636
G. G. Fronzé https://orcid.org/0000-0003-0966-4279
M. Fuentes-Garcia https://orcid.org/0000-0003-3390-8712
B. Gadre https://orcid.org/0000-0002-1534-9761
J. R. Gair https://orcid.org/0000-0002-1671-3668
S. Galaudage https://orcid.org/0000-0002-1819-0215

A. Gamboa https://orcid.org/0000-0001-8391-5596
D. Ganapathy https://orcid.org/0000-0003-3028-4174
A. Ganguly https://orcid.org/0000-0001-7394-0755
B. Garaventa https://orcid.org/0000-0003-2490-404X
J. García-Bellido https://orcid.org/0000-0002-9370-8360
C. García-Quirós https://orcid.org/0000-0002-8059-2477
J. W. Gardner https://orcid.org/0000-0002-8592-1452
J. Gargiulo https://orcid.org/0000-0002-3507-6924
X. Garrido https://orcid.org/0000-0002-7088-5831
A. Garron https://orcid.org/0000-0002-1601-797X
F. Garufi https://orcid.org/0000-0003-1391-6168
C. Gasbarra https://orcid.org/0000-0001-8335-9614
F. Gautier https://orcid.org/0000-0001-8006-9590
V. Gayathri https://orcid.org/0000-0002-7167-9888
G. Gemme https://orcid.org/0000-0002-1127-7406
A. Gennai https://orcid.org/0000-0003-0149-2089
V. Gennari https://orcid.org/0000-0002-0190-9262
R. George https://orcid.org/0000-0002-7797-7683
O. Gerberding https://orcid.org/0000-0001-7740-2698
L. Gergely https://orcid.org/0000-0003-3146-6201
Archisman Ghosh https://orcid.org/0000-0003-0423-3533
Shaon Ghosh https://orcid.org/0000-0001-9901-6253
Suprovo Ghosh https://orcid.org/0000-0002-1656-9870
Tathagata Ghosh https://orcid.org/0000-0001-9848-9905
J. A. Giaime https://orcid.org/0000-0002-3531-817X
C. Gier https://orcid.org/0000-0003-0897-7943
S. Gkaitatzis https://orcid.org/0000-0001-9420-7499
J. Glanzer https://orcid.org/0009-0000-0808-0795
F. Glotin https://orcid.org/0000-0003-2637-1187
P. Godwin https://orcid.org/0000-0002-7489-4751
A. S. Goettel https://orcid.org/0000-0002-6215-4641
E. Goetz https://orcid.org/0000-0003-2666-721X
S. Gomez Lopez https://orcid.org/0000-0002-9557-4706
B. Goncharov https://orcid.org/0000-0003-3189-5807
G. González https://orcid.org/0000-0003-0199-3158
P. Goodarzi https://orcid.org/0009-0008-1093-6706
A. W. Goodwin-Jones https://orcid.org/0000-0002-0395-0680
R. Gouaty https://orcid.org/0000-0001-5372-7084
A. Grado https://orcid.org/0000-0002-0501-8256
V. Graham https://orcid.org/0000-0003-3633-0135
A. E. Granados https://orcid.org/0000-0003-2099-9096
M. Granata https://orcid.org/0000-0003-3275-1186
V. Granata https://orcid.org/0000-0003-2246-6963
R. Gray https://orcid.org/0000-0002-5556-9873
A. C. Green https://orcid.org/0000-0002-6287-8746
S. R. Green https://orcid.org/0000-0002-6987-6313
H. L. Griggs https://orcid.org/0000-0001-5018-7908
C. Grimaud https://orcid.org/0000-0001-7736-7730
H. Grote https://orcid.org/0000-0002-0797-3943
S. Grunewald https://orcid.org/0000-0003-4641-2791
D. Guerra https://orcid.org/0000-0003-0029-5390
D. Guetta https://orcid.org/0000-0002-7349-1109
G. M. Guidi https://orcid.org/0000-0002-3061-9870
F. Gulminelli https://orcid.org/0000-0003-4354-2849
H. Guo https://orcid.org/0000-0002-3777-3117
W. Guo https://orcid.org/0000-0002-4320-4420
Y. Guo https://orcid.org/0000-0002-6959-9870
Anuradha Gupta https://orcid.org/0000-0002-5441-9013
I. Gupta https://orcid.org/0000-0001-6932-8715
V. Gupta https://orcid.org/0000-0002-7672-0480
F. Guzman https://orcid.org/0000-0001-9136-929X
M. Haberland https://orcid.org/0000-0001-9816-5660
E. D. Hall https://orcid.org/0000-0001-9018-666X
E. Z. Hamilton https://orcid.org/0000-0003-0098-9114
G. Hammond https://orcid.org/0000-0002-1414-3622
C. Hanna https://orcid.org/0000-0002-0965-7493
O. A. Hannuksela https://orcid.org/0000-0002-3887-7137
A. G. Hanselman https://orcid.org/0000-0002-8304-0109
S. Harikumar https://orcid.org/0000-0002-2653-7282
T. Harmark https://orcid.org/0000-0002-2795-7035
J. Harms https://orcid.org/0000-0002-7332-9806
G. M. Harry https://orcid.org/0000-0002-8905-7622
I. W. Harry https://orcid.org/0000-0002-5304-9372
C.-J. Haster https://orcid.org/0000-0001-8040-9807
K. Haughian https://orcid.org/0000-0002-1223-7342
J. Heinze https://orcid.org/0000-0001-8692-2724
H. Heitmann https://orcid.org/0000-0003-0625-5461
F. Hellman https://orcid.org/0000-0002-9135-6330
A. F. Helmling-Cornell https://orcid.org/0000-0002-7709-8638
G. Hemming https://orcid.org/0000-0001-5268-4465
O. Henderson-Sapir https://orcid.org/0000-0002-1613-9985
M. Hendry https://orcid.org/0000-0001-8322-5405
M. H. Hennig https://orcid.org/0000-0003-1531-8460
C. Henshaw https://orcid.org/0000-0002-4206-3128
M. Heurs https://orcid.org/0000-0002-5577-2273
A. L. Hewitt https://orcid.org/0000-0002-1255-3492
Y. Himemoto https://orcid.org/0000-0002-6856-3809
W. C. G. Ho https://orcid.org/0000-0002-6089-6836
I. J. Hollows https://orcid.org/0000-0002-3404-6459
D. E. Holz https://orcid.org/0000-0002-0175-5064
J. Hough https://orcid.org/0000-0003-3242-3123
S. Hourihane https://orcid.org/0000-0002-9152-0719
E. J. Howell https://orcid.org/0000-0001-7891-2817
C. G. Hoy https://orcid.org/0000-0002-8843-6719
H.-F. Hsieh https://orcid.org/0000-0002-8947-723X
W.-F. Hsu https://orcid.org/0000-0001-5234-3804
Q. Hu https://orcid.org/0000-0002-3033-6491
H. Y. Huang https://orcid.org/0000-0002-1665-2383
Y. Huang https://orcid.org/0000-0002-2952-8429
V. Hui https://orcid.org/0000-0002-0233-2346
S. Husa https://orcid.org/0000-0002-0445-1971
L. Iampieri https://orcid.org/0009-0004-1161-2990
G. A. Iandolo https://orcid.org/0000-0003-1155-4327
G. Iannone https://orcid.org/0000-0001-8347-7549
G. Iorio https://orcid.org/0000-0003-0293-503X
P. Iosif https://orcid.org/0000-0003-1621-7709
J. Irwin https://orcid.org/0000-0002-2364-2191
M. Isi https://orcid.org/0000-0001-8830-8672
K. S. Isleif https://orcid.org/0000-0001-7032-9440
Y. Itoh https://orcid.org/0000-0003-2694-8935
B. R. Iyer https://orcid.org/0000-0002-4141-5179
P.-E. Jacquet https://orcid.org/0000-0001-9552-0057
S. P. Jadhav https://orcid.org/0000-0003-0554-0084
A. L. James https://orcid.org/0000-0001-9165-0807
K. Jani https://orcid.org/0000-0003-1007-8912
J. Janquart https://orcid.org/0000-0003-2888-7152
S. Jaraba https://orcid.org/0000-0002-4759-143X
P. Jaranowski https://orcid.org/0000-0001-8085-3414
R. Jaume https://orcid.org/0000-0001-8691-3166
J. Jiang https://orcid.org/0000-0002-0154-3854
H.-B. Jin https://orcid.org/0000-0002-6217-2428

M. C. Johnston https://orcid.org/0000-0002-0663-9193
D. H. Jones https://orcid.org/0000-0003-3987-068X
P. Joshi https://orcid.org/0000-0002-4148-4932
L. Ju https://orcid.org/0000-0002-7951-4295
K. Jung https://orcid.org/0000-0003-4789-8893
J. Junker https://orcid.org/0000-0002-3051-4374
H. B. Kabagoz https://orcid.org/0000-0002-0900-8557
T. Kajita https://orcid.org/0000-0003-1207-6638
V. Kalogera https://orcid.org/0000-0001-9236-5469
M. Kalomenopoulos https://orcid.org/0000-0001-6677-949X
M. Kamiizumi https://orcid.org/0000-0001-7216-1784
N. Kanda https://orcid.org/0000-0001-6291-0227
S. Kandhasamy https://orcid.org/0000-0002-4825-6764
G. Kang https://orcid.org/0000-0002-6072-8189
S. J. Kapadia https://orcid.org/0000-0001-5318-1253
D. P. Kapasi https://orcid.org/0000-0001-8189-4920
M. Kasprzack https://orcid.org/0000-0003-4618-5939
R. Kaushik https://orcid.org/0000-0003-4888-5154
D. Keitel https://orcid.org/0000-0002-2824-626X
L. J. Kemperman https://orcid.org/0009-0009-5254-8397
J. Kennington https://orcid.org/0000-0002-6899-3833
R. Kesharwani https://orcid.org/0009-0002-2528-5738
J. S. Key https://orcid.org/0000-0003-0123-7600
F. Y. Khalili https://orcid.org/0000-0001-7068-2332
F. Khan https://orcid.org/0000-0001-6176-853X
N. M. Khusid https://orcid.org/0000-0001-9304-7075
W. Kiendrebeogo https://orcid.org/0000-0002-9108-5059
N. Kijbunchoo https://orcid.org/0000-0002-2874-1228
K. Kim https://orcid.org/0000-0003-1653-3795
M. H. Kim https://orcid.org/0009-0009-9894-3640
S. Kim https://orcid.org/0000-0003-1437-4647
Y.-M. Kim https://orcid.org/0000-0001-8720-6113
C. Kimball https://orcid.org/0000-0001-9879-6884
J. S. Kissel https://orcid.org/0000-0002-1702-9577
A. M. Knee https://orcid.org/0000-0003-0703-947X
N. Knust https://orcid.org/0000-0002-5984-5353
S. M. Koehlenbeck https://orcid.org/0000-0002-3842-9051
K. Kohri https://orcid.org/0000-0003-3764-8612
K. Kokeyama https://orcid.org/0000-0002-2896-1992
S. Koley https://orcid.org/0000-0002-5793-6665
P. Kolitsidou https://orcid.org/0000-0002-6719-8686
A. E. Koloniari https://orcid.org/0000-0002-0546-5638
K. Komori https://orcid.org/0000-0002-4092-9602
A. K. H. Kong https://orcid.org/0000-0002-5105-344X
A. Kontos https://orcid.org/0000-0002-1347-0680
M. Korobko https://orcid.org/0000-0002-3839-3909
A. Koushik https://orcid.org/0000-0002-7638-4544
N. Kouvatsos https://orcid.org/0000-0002-5497-3401
N. V. Krishnendu https://orcid.org/0000-0002-3483-7517
A. Królak https://orcid.org/0000-0003-4514-7690
J. Kubisz https://orcid.org/0000-0001-7258-8673
S. Kulkarni https://orcid.org/0000-0001-8057-0203
A. Kulur Ramamohan https://orcid.org/0000-0003-3681-1887
Praveen Kumar https://orcid.org/0000-0002-2288-4252
Prayush Kumar https://orcid.org/0000-0001-5523-4603
J. Kume https://orcid.org/0000-0003-3126-5100
K. Kuns https://orcid.org/0000-0003-0630-3902
S. Kuroyanagi https://orcid.org/0000-0001-6538-1447
S. Kuwahara https://orcid.org/0009-0009-2249-8798
K. Kwak https://orcid.org/0000-0002-2304-7798
S. Kwon https://orcid.org/0009-0006-3770-7044
D. Laghi https://orcid.org/0000-0001-7462-3794
M. Lalleman https://orcid.org/0000-0002-2254-010X
R. N. Lang https://orcid.org/0000-0002-4804-5537
R. Langgin https://orcid.org/0000-0002-5116-6217
B. Lantz https://orcid.org/0000-0002-7404-4845
I. L. Rosa https://orcid.org/0000-0003-0107-1540
A. Lartaux-Vollard https://orcid.org/0000-0003-1714-365X
P. D. Lasky https://orcid.org/0000-0003-3763-1386
J. Lawrence https://orcid.org/0000-0003-1222-0433
M. Laxen https://orcid.org/0000-0001-7515-9639
C. Lazarte https://orcid.org/0000-0002-6964-9321
A. Lazzarini https://orcid.org/0000-0002-5993-8808
P. Leaci https://orcid.org/0000-0002-3997-5046
Y. K. Lecoeuche https://orcid.org/0000-0002-9186-7034
H. M. Lee https://orcid.org/0000-0003-4412-7161
H. W. Lee https://orcid.org/0000-0002-1998-3209
K. Lee https://orcid.org/0000-0003-0470-3718
R.-K. Lee https://orcid.org/0000-0002-7171-7274
Sungho Lee https://orcid.org/0000-0001-6034-2238
M. Le Jean https://orcid.org/0009-0003-8047-3958
A. Lemaiˆtre https://orcid.org/0000-0002-6865-9245
M. Lenti https://orcid.org/0000-0002-2765-3955
M. Leonardi https://orcid.org/0000-0002-7641-0060
N. Leroy https://orcid.org/0000-0002-2321-1017
M. Lethuillier https://orcid.org/0000-0001-6185-2045
K. L. Li https://orcid.org/0000-0001-8229-2024
X. Li https://orcid.org/0000-0002-3780-7735
E. T. Lin https://orcid.org/0000-0002-0030-8051
L. C.-C. Lin https://orcid.org/0000-0003-4083-9567
Y.-C. Lin https://orcid.org/0000-0003-4939-1404
A. Liu https://orcid.org/0000-0003-1081-8722
G. C. Liu https://orcid.org/0000-0001-5663-3016
Jian Liu https://orcid.org/0000-0001-6726-3268
J. Llobera-Querol https://orcid.org/0000-0003-3322-6850
R. K. L. Lo https://orcid.org/0000-0003-1561-6716
A. Longo https://orcid.org/0000-0003-4254-8579
D. Lopez https://orcid.org/0000-0003-3342-9906
M. Lorenzini https://orcid.org/0000-0002-2765-7905
A. Lorenzo-Medina https://orcid.org/0009-0006-0860-5700
G. Losurdo https://orcid.org/0000-0003-0452-746X
T. P. Lott IV https://orcid.org/0009-0002-2864-162X
J. D. Lough https://orcid.org/0000-0002-5160-0239
C. O. Lousto https://orcid.org/0000-0002-6400-9640
N. Lu https://orcid.org/0000-0002-8861-9902
L. Lucchesi https://orcid.org/0000-0002-5916-8014
D. Lumaca https://orcid.org/0000-0002-3628-1591
A. P. Lundgren https://orcid.org/0000-0002-0363-4469
A. W. Lussier https://orcid.org/0000-0002-4507-1123
R. Macas https://orcid.org/0000-0002-6096-8297
D. M. Macleod https://orcid.org/0000-0002-1395-8694
I. A. O. MacMillan https://orcid.org/0000-0002-6927-1031
A. Macquet https://orcid.org/0000-0001-5955-6415
S. Maenaut https://orcid.org/0000-0003-1464-2605
R. M. Magee https://orcid.org/0000-0001-9769-531X
E. Maggio https://orcid.org/0000-0002-1960-8185
M. Magnozzi https://orcid.org/0000-0003-4512-8430
D. Malakar https://orcid.org/0000-0003-4234-4023
U. Mali https://orcid.org/0009-0003-1285-2788
L. Mallick https://orcid.org/0000-0001-8624-9162

A.-K. Malz https://orcid.org/0009-0004-7196-4170
M. Mancarella https://orcid.org/0000-0002-0675-508X
V. Mandic https://orcid.org/0000-0001-6333-8621
V. Mangano https://orcid.org/0000-0001-7902-8505
G. L. Mansell https://orcid.org/0000-0003-4736-6678
M. Manske https://orcid.org/0000-0002-7778-1189
M. Mantovani https://orcid.org/0000-0002-4424-5726
M. Mapelli https://orcid.org/0000-0001-8799-2548
C. Marinelli https://orcid.org/0000-0002-3596-4307
F. Marion https://orcid.org/0000-0002-8184-1017
S. Marsat https://orcid.org/0000-0001-9449-1071
F. Martelli https://orcid.org/0000-0003-3761-8616
I. W. Martin https://orcid.org/0000-0001-7300-9151
R. M. Martin https://orcid.org/0000-0001-9664-2216
V. Martinez https://orcid.org/0000-0001-5852-2301
J. C. Martins https://orcid.org/0000-0002-6099-4831
M. Masso-Reid https://orcid.org/0000-0001-6177-8105
S. Mastrogiovanni https://orcid.org/0000-0003-1606-4183
T. Matcovich https://orcid.org/0009-0004-1209-008X
M. Matiushechkina https://orcid.org/0000-0002-9957-8720
N. Mavalvala https://orcid.org/0000-0003-0219-9706
D. E. McClelland https://orcid.org/0000-0001-6210-5842
L. McCuller https://orcid.org/0000-0003-0851-0593
G. I. McGhee https://orcid.org/0000-0001-5038-2658
J. McIver https://orcid.org/0000-0003-0316-1355
A. McLeod https://orcid.org/0000-0001-5424-8368
I. McMahon https://orcid.org/0000-0002-4529-1505
R. McTeague https://orcid.org/0009-0004-3329-6079
D. Meacher https://orcid.org/0000-0001-5882-0368
C. S. Menoni https://orcid.org/0000-0001-9185-2572
R. A. Mercer https://orcid.org/0000-0001-8372-3914
J. R. Mérou https://orcid.org/0000-0002-5776-6643
C. Messick https://orcid.org/0000-0002-8230-3309
Z. Metzler https://orcid.org/0000-0002-1236-8510
M. Meyer-Conde https://orcid.org/0000-0003-2230-6310
F. Meylahn https://orcid.org/0000-0002-9556-142X
A. Miani https://orcid.org/0000-0001-7737-3129
C. Michel https://orcid.org/0000-0003-0606-725X
Y. Michimura https://orcid.org/0000-0002-2218-4002
H. Middleton https://orcid.org/0000-0001-5532-3622
D. P. Mihaylov https://orcid.org/0000-0002-8820-407X
S. J. Miller https://orcid.org/0000-0001-5670-7046
M. Millhouse https://orcid.org/0000-0002-8659-5898
E. Milotti https://orcid.org/0000-0001-7348-9765
V. Milotti https://orcid.org/0000-0003-4732-1226
Ll. M. Mir https://orcid.org/0000-0002-4276-715X
L. Mirasola https://orcid.org/0009-0004-0174-1377
M. Miravet-Tenés https://orcid.org/0000-0002-8766-1156
C.-A. Miritescu https://orcid.org/0000-0002-7716-0569
C. Mishra https://orcid.org/0000-0002-8115-8728
T. Mishra https://orcid.org/0000-0002-7881-1677
S. Mitra https://orcid.org/0000-0002-0800-4626
V. P. Mitrofanov https://orcid.org/0000-0002-6983-4981
O. Miyakawa https://orcid.org/0000-0002-9085-7600
S. Miyoki https://orcid.org/0000-0002-1213-8416
G. Mo https://orcid.org/0000-0001-6331-112X
L. Mobilia https://orcid.org/0009-0000-3022-2358
S. R. Mohite https://orcid.org/0000-0003-1356-7156
M. Molina- Ruiz https://orcid.org/0000-0003-4892-3042
A. More https://orcid.org/0000-0001-7714-7076
S. More https://orcid.org/0000-0002-2986-2371
C. Moreno https://orcid.org/0000-0002-0496-032X
E. A. Moreno https://orcid.org/0000-0001-5666-3637
S. Morisaki https://orcid.org/0000-0002-8445-6747
Y. Moriwaki https://orcid.org/0000-0002-4497-6908
G. Morras https://orcid.org/0000-0002-9977-8546
A. Moscatello https://orcid.org/0000-0001-5480-7406
M. Mould https://orcid.org/0000-0001-5460-2910
B. Mours https://orcid.org/0000-0002-6444-6402
C. M. Mow-Lowry https://orcid.org/0000-0002-0351-4555
L. Muccillo https://orcid.org/0009-0000-6237-0590
F. Muciaccia https://orcid.org/0000-0003-0850-2649
D. Mukherjee https://orcid.org/0000-0001-7335-9418
Suvodip Mukherjee https://orcid.org/0000-0002-3373-5236
N. Mukund https://orcid.org/0000-0002-8666-9156
P. G. Murray https://orcid.org/0000-0002-8218-2404
D. Nabari https://orcid.org/0009-0006-8500-7624
N. Nagarajan https://orcid.org/0000-0003-3695-0078
K. Nakamura https://orcid.org/0000-0001-6148-4289
H. Nakano https://orcid.org/0000-0001-7665-0796
D. Nanadoumgar-Lacroze https://orcid.org/0009-0009-7255-8111
P. Narayan https://orcid.org/0009-0009-0599-532X
I. Nardecchia https://orcid.org/0000-0001-5558-2595
L. Naticchioni https://orcid.org/0000-0003-2918-0730
R. K. Nayak https://orcid.org/0000-0002-6814-7792
A. Nelson https://orcid.org/0000-0002-5909-4692
A. Neunzert https://orcid.org/0000-0003-0323-0111
L. Nguyen Quynh https://orcid.org/0000-0002-1828-3702
A. B. Nielsen https://orcid.org/0000-0001-8694-4026
A. Nishizawa https://orcid.org/0000-0003-3562-0990
W. Niu https://orcid.org/0000-0003-1470-532X
J. Novak https://orcid.org/0000-0002-6029-4712
R. Nowicki https://orcid.org/0009-0008-6626-0725
J. F. Nuño Siles https://orcid.org/0000-0001-8304-8066
L. K. Nuttall https://orcid.org/0000-0002-8599-8791
J. Oberling https://orcid.org/0009-0001-4174-3973
E. Oelker https://orcid.org/0000-0002-3916-1595
M. Oertel https://orcid.org/0000-0002-1884-8654
M. Ohashi https://orcid.org/0000-0001-8072-0304
F. Ohme https://orcid.org/0000-0003-0493-5607
R. Oliveri https://orcid.org/0000-0002-7497-871X
K. Oohara https://orcid.org/0000-0002-7518-6677
B. O'Reilly https://orcid.org/0000-0002-3874-8335
M. Orselli https://orcid.org/0000-0003-3563-8576
R. O'Shaughnessy https://orcid.org/0000-0001-5832-8517
S. Oshino https://orcid.org/0000-0002-2794-6029
I. Ota https://orcid.org/0000-0001-5045-2484
D. J. Ottaway https://orcid.org/0000-0001-6794-1591
B. J. Owen https://orcid.org/0000-0003-3919-0780
A. E. Pace https://orcid.org/0009-0003-4044-0334
R. Pagano https://orcid.org/0000-0001-8362-0130
M. A. Page https://orcid.org/0000-0002-5298-7914
A. Pai https://orcid.org/0000-0003-3476-4589
S. Pal https://orcid.org/0000-0003-2172-8589
M. A. Palaia https://orcid.org/0009-0007-3296-8648
C. Palomba https://orcid.org/0000-0002-4450-9883
P. Palud https://orcid.org/0000-0002-5850-6325
K. C. Pan https://orcid.org/0000-0002-1473-9880
F. Pannarale https://orcid.org/0000-0002-7537-3210
F. Paoletti https://orcid.org/0000-0001-8898-1963
A. Paolone https://orcid.org/0000-0002-4839-7815
A. Papadopoulos https://orcid.org/0009-0006-1882-996X

L. Papalini https://orcid.org/0000-0002-5219-0454
G. Papigkiotis https://orcid.org/0009-0008-2205-7426
A. Parisi https://orcid.org/0000-0003-0251-8914
J. Park https://orcid.org/0000-0002-7510-0079
W. Parker https://orcid.org/0000-0002-7711-4423
D. Pascucci https://orcid.org/0000-0003-1907-0175
A. Pasqualetti https://orcid.org/0000-0003-0620-5990
R. Passaquieti https://orcid.org/0000-0003-4753-9428
O. Patane https://orcid.org/0000-0002-4850-2355
A. V. Patel https://orcid.org/0000-0001-6872-9197
B. Patricelli https://orcid.org/0000-0001-6709-0969
K. Paul https://orcid.org/0000-0002-8406-6503
S. Paul https://orcid.org/0000-0002-4449-1732
E. Payne https://orcid.org/0000-0003-4507-8373
A. Pele https://orcid.org/0000-0002-1873-3769
F. E. Peña Arellano https://orcid.org/0000-0002-8516-5159
S. Penn https://orcid.org/0000-0003-4956-0853
A. Perego https://orcid.org/0000-0002-0936-8237
C. Périgois https://orcid.org/0000-0002-9779-2838
G. Perna https://orcid.org/0000-0002-7364-1904
A. Perreca https://orcid.org/0000-0002-6269-2490
J. Perret https://orcid.org/0009-0006-4975-1536
S. Perriès https://orcid.org/0000-0003-2213-3579
H. P. Pfeiffer https://orcid.org/0000-0001-9288-519X
K. A. Pham https://orcid.org/0000-0002-7650-1034
K. S. Phukon https://orcid.org/0000-0003-1561-0760
L. Piccari https://orcid.org/0009-0000-0247-4339
O. J. Piccinni https://orcid.org/0000-0001-5478-3950
M. Pichot https://orcid.org/0000-0002-4439-8968
M. Piendibene https://orcid.org/0000-0003-2434-488X
F. Piergiovanni https://orcid.org/0000-0001-8063-828X
L. Pierini https://orcid.org/0000-0003-0945-2196
G. Pierra https://orcid.org/0000-0003-3970-7970
V. Pierro https://orcid.org/0000-0002-6020-5521
M. Pillas https://orcid.org/0000-0003-3224-2146
F. Pilo https://orcid.org/0000-0003-4967-7090
L. Pinard https://orcid.org/0000-0002-8842-1867
I. M. Pinto https://orcid.org/0000-0002-2679-4457
M. Pinto https://orcid.org/0009-0003-4339-9971
B. J. Piotrzkowski https://orcid.org/0000-0001-8919-0899
M. D. Pitkin https://orcid.org/0000-0003-4548-526X
A. Placidi https://orcid.org/0000-0001-8032-4416
E. Placidi https://orcid.org/0000-0002-3820-8451
M. L. Planas https://orcid.org/0000-0001-8278-7406
W. Plastino https://orcid.org/0000-0002-5737-6346
C. Plunkett https://orcid.org/0000-0002-1144-6708
R. Poggiani https://orcid.org/0000-0002-9968-2464
L. Pompili https://orcid.org/0000-0002-0710-6778
C. Posnansky https://orcid.org/0009-0009-7137-9795
R. Poulton https://orcid.org/0000-0003-2049-520X
J. Powell https://orcid.org/0000-0002-1357-4164
M. Pracchia https://orcid.org/0009-0001-8343-719X
B. K. Pradhan https://orcid.org/0000-0002-2526-1421
T. Pradier https://orcid.org/0000-0001-5501-0060
K. Prasai https://orcid.org/0000-0001-6552-097X
G. Pratten https://orcid.org/0000-0003-4984-0775
G. Principe https://orcid.org/0000-0003-0406-7387
G. A. Prodi https://orcid.org/0000-0001-5256-915X
A. Puecher https://orcid.org/0000-0003-1357-4348
J. Pullin https://orcid.org/0000-0001-8248-603X
M. Pürrer https://orcid.org/0000-0002-3329-9788
H. Qi https://orcid.org/0000-0001-6339-1537
J. Qin https://orcid.org/0000-0002-7120-9026
G. Quéméner https://orcid.org/0000-0001-6703-6655
B. Rajbhandari https://orcid.org/0000-0001-7568-1611
K. E. Ramirez https://orcid.org/0000-0003-2194-7669
F. A. Ramis Vidal https://orcid.org/0000-0001-6143-2104
M. Ramos Arevalo https://orcid.org/0009-0003-1528-8326
A. Ramos-Buades https://orcid.org/0000-0002-6874-7421
S. Ranjan https://orcid.org/0000-0001-7480-9329
P. Rapagnani https://orcid.org/0000-0002-1865-6126
A. Ray https://orcid.org/0000-0002-7322-4748
V. Raymond https://orcid.org/0000-0003-0066-0095
M. Razzano https://orcid.org/0000-0003-4825-1629
D. H. Reitze https://orcid.org/0000-0002-5756-1111
A. I. Renzini https://orcid.org/0000-0002-4589-3987
B. Revenu https://orcid.org/0000-0002-7629-4805
L. Ricca https://orcid.org/0009-0002-1638-0610
F. Ricci https://orcid.org/0000-0001-5475-4447
M. Ricci https://orcid.org/0009-0008-7421-4331
A. Ricciardone https://orcid.org/0000-0002-5688-455X
J. W. Richardson https://orcid.org/0000-0002-1472-4806
K. Riles https://orcid.org/0000-0002-6418-5812
S. Rinaldi https://orcid.org/0000-0001-5799-4155
A. Rocchi https://orcid.org/0000-0002-1382-9016
L. Rolland https://orcid.org/0000-0003-0589-9687
J. G. Rollins https://orcid.org/0000-0002-9388-2799
A. E. Romano https://orcid.org/0000-0002-0314-8698
R. Romano https://orcid.org/0000-0002-0485-6936
A. Romero https://orcid.org/0000-0003-2275-4164
S. Ronchini https://orcid.org/0000-0003-0020-687X
T. J. Roocke https://orcid.org/0000-0003-2640-9683
D. Rosińska https://orcid.org/0000-0002-3681-9304
M. P. Ross https://orcid.org/0000-0002-8955-5269
M. Rossello-Sastre https://orcid.org/0000-0002-3341-3480
S. Rowan https://orcid.org/0000-0002-0666-9907
S. K. Roy https://orcid.org/0000-0001-9295-5119
S. Roy https://orcid.org/0000-0003-2147-5411
D. Rozza https://orcid.org/0000-0002-7378-6353
E. Ruiz Morales https://orcid.org/0000-0002-0995-595X
S. Sachdev https://orcid.org/0000-0002-0525-2317
P. Saffarieh https://orcid.org/0009-0000-7504-3660
S. Safi-Harb https://orcid.org/0000-0001-6189-7665
M. R. Sah https://orcid.org/0009-0005-9881-1788
S. Saha https://orcid.org/0000-0002-3333-8070
T. Sainrat https://orcid.org/0009-0003-0169-266X
S. Sajith Menon https://orcid.org/0009-0008-4985-1320
Y. Sakai https://orcid.org/0000-0001-8810-4813
M. Sakellariadou https://orcid.org/0000-0002-2715-1517
S. Sakon https://orcid.org/0000-0002-5861-3024
O. S. Salafia https://orcid.org/0000-0003-4924-7322
F. Salces-Carcoba https://orcid.org/0000-0001-7049-4438
M. Saleem https://orcid.org/0000-0002-3836-7751
F. Salemi https://orcid.org/0000-0002-9511-3846
M. Sallé https://orcid.org/0000-0002-6620-6672
S. Salvador https://orcid.org/0000-0003-3444-7807
A. Samajdar https://orcid.org/0000-0002-0857-6018
N. Sanchis-Gual https://orcid.org/0000-0001-5375-7494
E. M. Sänger https://orcid.org/0009-0003-6642-8974
F. Santoliquido https://orcid.org/0000-0003-3752-1400
A. Sasli https://orcid.org/0000-0001-7357-0889
P. Sassi https://orcid.org/0000-0002-4920-2784
B. Sassolas https://orcid.org/0000-0002-3077-8951
O. Sauter https://orcid.org/0000-0003-2293-1554

R. L. Savage https://orcid.org/0000-0003-3317-1036
T. Sawada https://orcid.org/0000-0001-5726-7150
M. G. Schiworski https://orcid.org/0000-0001-9298-004X
P. Schmidt https://orcid.org/0000-0003-1542-1791
S. Schmidt https://orcid.org/0000-0002-8206-8089
R. Schnabel https://orcid.org/0000-0003-2896-4218
K. Schouteden https://orcid.org/0000-0002-5975-585X
E. Schwartz https://orcid.org/0000-0001-8922-7794
M. Scialpi https://orcid.org/0009-0007-6434-1460
J. Scott https://orcid.org/0000-0001-6701-6515
S. M. Scott https://orcid.org/0000-0002-9875-7700
R. M. Sedas https://orcid.org/0000-0001-8961-3855
M. Seglar-Arroyo https://orcid.org/0000-0001-8654-409X
Y. Sekiguchi https://orcid.org/0000-0002-2648-3835
A. S. Sengupta https://orcid.org/0000-0002-3212-0475
E. G. Seo https://orcid.org/0000-0002-8588-4794
J. W. Seo https://orcid.org/0000-0003-4937-0769
M. Serra https://orcid.org/0000-0002-6093-8063
U. S. Shah https://orcid.org/0000-0001-8249-7425
M. A. Shaikh https://orcid.org/0000-0003-0826-6164
L. Shao https://orcid.org/0000-0002-1334-8853
A. K. Sharma https://orcid.org/0000-0003-0067-346X
P. Shawhan https://orcid.org/0000-0002-8249-8070
N. S. Shcheblanov https://orcid.org/0000-0001-8696-2435
H. Shinkai https://orcid.org/0000-0003-1082-2844
D. H. Shoemaker https://orcid.org/0000-0002-4147-2560
D. M. Shoemaker https://orcid.org/0000-0002-9899-6357
H. Siegel https://orcid.org/0000-0001-5161-4617
D. Sigg https://orcid.org/0000-0003-4606-6526
L. Silenzi https://orcid.org/0000-0001-7316-3239
L. Silvestri https://orcid.org/0009-0008-5207-661X
L. P. Singer https://orcid.org/0000-0001-9898-5597
D. Singh https://orcid.org/0000-0001-9675-4584
N. Singh https://orcid.org/0000-0002-1135-3456
A. M. Sintes https://orcid.org/0000-0001-9050-7515
V. Skliris https://orcid.org/0000-0003-0902-9216
B. J. J. Slagmolen https://orcid.org/0000-0002-2471-3828
J. R. Smith https://orcid.org/0000-0003-0638-9670
L. Smith https://orcid.org/0000-0002-3035-0947
R. J. E. Smith https://orcid.org/0000-0001-8516-3324
W. J. Smith https://orcid.org/0009-0003-7949-4911
K. Somiya https://orcid.org/0000-0003-2601-2264
I. Song https://orcid.org/0000-0002-4301-8281
S. Soni https://orcid.org/0000-0003-3856-8534
V. Sordini https://orcid.org/0000-0003-0885-824X
H. Sotani https://orcid.org/0000-0002-3239-2921
F. Spada https://orcid.org/0000-0001-5664-1657
V. Spagnuolo https://orcid.org/0000-0002-0098-4260
A. P. Spencer https://orcid.org/0000-0003-4418-3366
P. Spinicelli https://orcid.org/0000-0001-8078-6047
F. Stachurski https://orcid.org/0000-0002-8658-5753
D. A. Steer https://orcid.org/0000-0002-8781-1273
N. Steinle https://orcid.org/0000-0003-0658-402X
S. Steinlechner https://orcid.org/0000-0003-4710-8548
N. Stergioulas https://orcid.org/0000-0002-5490-5302
S. Sudhagar https://orcid.org/0000-0001-8578-4665
L. Suleiman https://orcid.org/0000-0003-3783-7448
J. Sun https://orcid.org/0009-0008-8278-0077
L. Sun https://orcid.org/0000-0001-7959-892X
J. Suresh https://orcid.org/0000-0003-2389-6666
P. J. Sutton https://orcid.org/0000-0003-1614-3922
B. L. Swinkels https://orcid.org/0000-0002-3066-3601
A. Syx https://orcid.org/0009-0000-6424-6411
M. J. Szczepańczyk https://orcid.org/0000-0002-6167-6149
P. Szewczyk https://orcid.org/0000-0002-1339-9167
M. Tacca https://orcid.org/0000-0003-1353-0441
H. Tagoshi https://orcid.org/0000-0001-8530-9178
S. C. Tait https://orcid.org/0000-0003-0327-953X
H. Takahashi https://orcid.org/0000-0003-0596-4397
R. Takahashi https://orcid.org/0000-0003-1367-5149
A. Takamori https://orcid.org/0000-0001-6032-1330
S. Takano https://orcid.org/0000-0002-1266-4555
H. Takeda https://orcid.org/0000-0001-9937-2557
N. Tamanini https://orcid.org/0000-0001-8760-5421
S. J. Tanaka https://orcid.org/0000-0002-8796-1992
S. Tanioka https://orcid.org/0000-0003-3321-1018
L. Tao https://orcid.org/0000-0003-4382-5507
E. N. Tapia San Martín https://orcid.org/0000-0002-4817-5606
A. Taruya https://orcid.org/0000-0002-4016-1955
J. D. Tasson https://orcid.org/0000-0002-4777-5087
J. G. Tau https://orcid.org/0009-0004-7428-762X
R. Tenorio https://orcid.org/0000-0002-3582-2587
A. Theodoropoulos https://orcid.org/0000-0003-4486-7135
L. M. Thomas https://orcid.org/0000-0003-3271-6436
J. E. Thompson https://orcid.org/0000-0002-0419-5517
E. Thrane https://orcid.org/0000-0002-4418-3895
J. Tissino https://orcid.org/0000-0003-2483-6710
S. Tiwari https://orcid.org/0000-0003-1611-6625
V. Tiwari https://orcid.org/0000-0002-1602-4176
A. M. Toivonen https://orcid.org/0009-0008-9546-2035
K. Toland https://orcid.org/0000-0001-9537-9698
A. E. Tolley https://orcid.org/0000-0001-9841-943X
T. Tomaru https://orcid.org/0000-0002-8927-9014
T. Tomura https://orcid.org/0000-0002-7504-8258
H. Tong https://orcid.org/0000-0002-4534-0485
A. Torres-Forné https://orcid.org/0000-0001-8709-5118
I. Tosta e Melo https://orcid.org/0000-0001-5833-4052
E. Tournefier https://orcid.org/0000-0002-5465-9607
A. Trapananti https://orcid.org/0000-0001-7763-5758
R. Travaglini https://orcid.org/0000-0002-5288-1407
F. Travasso https://orcid.org/0000-0002-4653-6156
M. C. Tringali https://orcid.org/0000-0001-5087-189X
A. Tripathee https://orcid.org/0000-0002-6976-5576
G. Troian https://orcid.org/0000-0001-6837-607X
A. Trovato https://orcid.org/0000-0002-9714-1904
T. Tsang https://orcid.org/0000-0003-3666-686X
S. Tsuchida https://orcid.org/0000-0001-8217-0764
L. Tsukada https://orcid.org/0000-0003-0596-5648
K. Turbang https://orcid.org/0000-0002-9296-8603
M. Turconi https://orcid.org/0000-0001-9999-2027
H. Ubach https://orcid.org/0000-0002-0679-9074
N. Uchikata https://orcid.org/0000-0003-0030-3653
T. Uchiyama https://orcid.org/0000-0003-2148-1694
R. P. Udall https://orcid.org/0000-0001-6877-3278
T. Uehara https://orcid.org/0000-0003-4375-098X
K. Ueno https://orcid.org/0000-0003-3227-6055
V. Undheim https://orcid.org/0000-0003-4028-0054
T. Ushiba https://orcid.org/0000-0002-5059-4033
M. Vacatello https://orcid.org/0009-0006-0934-1014
H. Vahlbruch https://orcid.org/0000-0003-2357-2338
N. Vaidya https://orcid.org/0000-0003-1843-7545
G. Vajente https://orcid.org/0000-0002-7656-6882

J. Valencia https://orcid.org/0000-0003-2648-9759
M. Valentini https://orcid.org/0000-0003-1215-4552
S. A. Vallejo-Peña https://orcid.org/0000-0002-6827-9509
V. Valsan https://orcid.org/0000-0003-0315-4091
M. van Dael https://orcid.org/0000-0002-6061-8131
E. Van den Bossche https://orcid.org/0009-0009-2070-0964
J. F. J. van den Brand https://orcid.org/0000-0003-4434-5353
M. van der Sluys https://orcid.org/0000-0003-1231-0762
J. van Dongen https://orcid.org/0000-0003-0964-2483
H. van Haevermaet https://orcid.org/0000-0003-2386-957X
J. V. van Heijningen https://orcid.org/0000-0002-8391-7513
P. Van Hove https://orcid.org/0000-0002-2431-3381
N. van Remortel https://orcid.org/0000-0003-4180-8199
A. F. Vargas https://orcid.org/0000-0001-8396-5227
V. Varma https://orcid.org/0000-0002-9994-1761
A. Vecchio https://orcid.org/0000-0002-6254-1617
J. Veitch https://orcid.org/0000-0002-6508-0713
P. J. Veitch https://orcid.org/0000-0002-2597-435X
R. C. Venterea https://orcid.org/0000-0003-3299-3804
P. Verdier https://orcid.org/0000-0003-3090-2948
D. Verkindt https://orcid.org/0000-0003-4344-7227
Y. Verma https://orcid.org/0000-0003-4147-3173
S. M. Vermeulen https://orcid.org/0000-0003-4227-8214
A. Veutro https://orcid.org/0009-0002-9160-5808
A. Viceré https://orcid.org/0000-0003-0624-6231
A. D. Viets https://orcid.org/0000-0002-4241-1428
A. Vijaykumar https://orcid.org/0000-0002-4103-0666
V. Villa-Ortega https://orcid.org/0000-0001-7983-1963
E. T. Vincent https://orcid.org/0000-0002-0442-1916
S. Vitale https://orcid.org/0000-0003-2700-0767
H. Vocca https://orcid.org/0000-0002-1200-3917
D. Voigt https://orcid.org/0000-0001-9075-6503
L. Vujeva https://orcid.org/0000-0001-7697-8361
S. P. Vyatchanin https://orcid.org/0000-0002-6823-911X
M. Wade https://orcid.org/0000-0002-5703-4469
K. J. Wagner https://orcid.org/0000-0002-7255-4251
H. Wang https://orcid.org/0000-0002-6589-2738
Y. F. Wang https://orcid.org/0000-0002-2928-2916
G. Waratkar https://orcid.org/0000-0003-3630-9440
M. Was https://orcid.org/0000-0002-1890-1128
T. Washimi https://orcid.org/0000-0001-5792-4907
N. L. Weickhardt https://orcid.org/0000-0002-3923-5806
A. J. Weinstein https://orcid.org/0000-0002-0928-6784
L. Wen https://orcid.org/0000-0001-7987-295X
K. Wette https://orcid.org/0000-0002-4394-7179
J. T. Whelan https://orcid.org/0000-0001-5710-6576
B. F. Whiting https://orcid.org/0000-0002-8501-8669
C. Whittle https://orcid.org/0000-0002-8833-7438
D. Wilken https://orcid.org/0000-0002-7290-9411
D. Williams https://orcid.org/0000-0003-3772-198X
M. J. Williams https://orcid.org/0000-0003-2198-2974
N. S. Williams https://orcid.org/0000-0002-5656-8119
J. L. Willis https://orcid.org/0000-0002-9929-0225
B. Willke https://orcid.org/0000-0003-0524-2925
M. Wils https://orcid.org/0000-0002-1544-7193
G. Woan https://orcid.org/0000-0003-0381-0394
H. T. Wong https://orcid.org/0000-0003-4145-4394
I. C. F. Wong https://orcid.org/0000-0003-2166-0027
M. Wright https://orcid.org/0000-0003-1829-7482
C. Wu https://orcid.org/0000-0003-3191-8845
D. S. Wu https://orcid.org/0000-0003-2849-3751
H. Wu https://orcid.org/0000-0003-4813-3833
Z. Wu https://orcid.org/0000-0002-0032-5257
D. M. Wysocki https://orcid.org/0000-0001-9138-4078
V. A. Xu https://orcid.org/0000-0002-3020-3293
Y. Xu https://orcid.org/0000-0001-8697-3505
N. Yadav https://orcid.org/0009-0009-5010-1065
H. Yamamoto https://orcid.org/0000-0001-6919-9570
K. Yamamoto https://orcid.org/0000-0002-3033-2845
T. S. Yamamoto https://orcid.org/0000-0002-8181-924X
T. Yamamoto https://orcid.org/0000-0002-0808-4822
R. Yamazaki https://orcid.org/0000-0002-1251-7889
K. Z. Yang https://orcid.org/0000-0001-8083-4037
Y. Yang https://orcid.org/0000-0002-3780-1413
Z. Yarbrough https://orcid.org/0000-0002-9825-1136
A. B. Yelikar https://orcid.org/0000-0002-8065-1174
J. Yokoyama https://orcid.org/0000-0001-7127-4808
H. Yuzurihara https://orcid.org/0000-0002-3710-6613
M. Zeeshan https://orcid.org/0000-0002-6494-7303
M. Zeoli https://orcid.org/0009-0007-1898-4844
M. Zevin https://orcid.org/0000-0002-0147-0835
R. Zhang https://orcid.org/0000-0001-8095-483X
C. Zhao https://orcid.org/0000-0001-5825-2401
Z.-C. Zhao https://orcid.org/0000-0001-5180-4496
Y. Zheng https://orcid.org/0000-0002-5432-1331
H. Zhong https://orcid.org/0000-0001-8324-5158
Z.-H. Zhu https://orcid.org/0000-0002-3567-6743
A. B. Zimmerman https://orcid.org/0000-0002-7453-6372
M. E. Zucker https://orcid.org/0000-0002-2544-1596
J. Zweizig https://orcid.org/0000-0002-1521-3397
Jim Palfreyman https://orcid.org/0000-0001-8691-8039
S.B. Araujo Furlan https://orcid.org/0000-0003-4027-4826
S. del Palacio https://orcid.org/0000-0002-5761-2417
G. Gancio https://orcid.org/0000-0003-1282-3031
F. García https://orcid.org/0000-0001-9072-4069
G. E. Romero https://orcid.org/0000-0002-5260-1807
E. Zubieta https://orcid.org/0009-0009-5593-367X

References

Aasi, J., Abbott, B. P., Abbott, R., et al. 2015, CQGra, 32, 074001
Abac, A. G., Abbott, R., Abouelfettouh, I., et al. 2024, ApJ, 977, 255
Abac, A. G., Abbott, R., Abouelfettouh, I., et al. 2025a, ApJ, 985, 183
Abac, A. G., Abbott, R., Abouelfettouh, I., et al. 2025b, ApJ, 983, 99
Abac, A. G., Abouelfettouh, I., Acernese, F., et al. 2025c, PhRvD, 112, 102005
Abac, A. G., Abouelfettouh, I., Acernese, F., et al. 2025d, arXiv e-prints, arXiv:2508.18082
Abac, A. G., Abouelfettouh, I., Acernese, F., et al. 2026a, arXiv e-prints, arXiv:2603.25938
Abac, A. G., Abouelfettouh, I., Acernese, F., et al. 2026b, PhRvD, 113, 082004
Abac, A. G., Abouelfettouh, I., Acernese, F., et al. 2026c, arXiv:2605.27090
Abadie, J., Abbott, B. P., Abbott, R., et al. 2011, PhRvD, 83, 042001
Abbott, B., Abbott, R., Abbott, T., et al. 2017, PhRvL, 119, 18
Abbott, B., Abbott, R., Abbott, T., et al. 2018, PhRvL, 121, 16
Abbott, B. P., Abbott, R., Abbott, T. D., et al. 2017, ApJ, 839, 12
Abbott, B. P., Abbott, R., Abbott, T. D., et al. 2019, ApJ, 879, 10
Abbott, B. P., Abbott, R., Abbott, T. D., et al. 2020, LRR, 23, 3
Abbott, R., Abbott, T. D., Acernese, F., et al. 2021a, PhRvD, 104, 122004
Abbott, R., Abbott, T. D., Acernese, F., et al. 2021b, PhRvD, 104, 102001
Abbott, R., Abbott, T. D., Acernese, F., et al. 2022a, ApJ, 932, 133
Abbott, R., Abbott, T. D., Acernese, F., et al. 2023, PhRvX, 13, 041039
Abbott, R., Abe, H., Acernese, F., et al. 2022b, ApJ, 935, 1

Abbott, R., Abe, H., Acernese, F., et al. 2024, ApJ, 966, 137
Acernese, F., Agathos, M., Agatsuma, K., et al. 2015, CQGra, 32, 024001
Akmal, A., Pandharipande, V. R., & Ravenhall, D. G. 1998, PhRvC, 58, 1804
Akutsu, T., Ando, M., Arai, K., et al. 2021, PTEP, 2021, 05A101
Allen, B., Goetz, E., Keitel, D., et al. 2024, SFT Data Format Version 2–3 Specification LIGO–T040164–v3, LIGO Laboratory https://dcc.ligo.org/T040164-v3/public
Andersson, N., & Kokkotas, K. D. 1998, MNRAS, 299, 1059
Antonopoulou, D., Haskell, B., & Espinoza, C. M. 2022, RPPh, 85, 126901
Ashton, G., Hübner, M., Lasky, P. D., et al. 2019, ApJS, 241, 27
Ashton, G., Keitel, D., Prix, R., Tenorio, R., & Ferrer, M.-A. 2025, PyFstat v2.2.1,
Astone, P., Colla, A., D'Antonio, S., Frasca, S., & Palomba, C. 2014, PhRvD, 90, 042002
Astone, P., D'Antonio, S., Frasca, S., & Palomba, C. 2010, CQGra, 27, 194016
Astone, P., Frasca, S., & Palomba, C. 2005, CQGra, 22, S1197
Baiko, D. A., & Chugunov, A. I. 2018, MNRAS, 480, 5511
Ball, M., & Frey, R. 2025, MNRAS, 545, staf2176
Barr, E. D., Dutta, A., Freire, P. C. C., et al. 2024, Sci, 383, 275
Basu, A., Shaw, B., Antonopoulou, D., et al. 2022, MNRAS, 510, 4049
Behnke, B., Papa, M. A., & Prix, R. 2015, PhRvD, 91, 064007
Bennett, M. F., van Eysden, C. A., & Melatos, A. 2010, MNRAS, 409, 1705
Bransgrove, A., Beloborodov, A. M., & Levin, Y. 2020, ApJ, 897, 173
Brun, R., & Rademakers, F. 1997, NIMPA, 389, 81
Capote, E., Jia, W., Aritomi, N., et al. 2025, PhRvD, 111, 062002
Cheunchitra, T., Melatos, A., Carlin, J. B., & Howitt, G. 2024, MNRAS, 528, 1360
Cordes, J. M., Downs, G. S., & Krause-Polstorff, J. 1988, ApJ, 330, 847
Cutler, C., & Schutz, B. F. 2005, PhRvD, 72, 063006
D'Antonio, S., Palomba, C., Astone, P., et al. 2023, PhRvD, 108, 122001
Davis, D., Neunzert, A., Goetz, E., et al. 2025, Self-gating of O4a h(t) for use in continuous-wave searches LIGO-T2400003, LIGO Laboratory https://dcc.ligo.org/T2400003/public
De Lillo, F., Suresh, J., Depasse, A., et al. 2023, PhRvD, 107, 102001
Dodson, R., Legge, D., Reynolds, J. E., & McCulloch, P. M. 2003, ApJ, 596, 1137
Dodson, R., Lewis, D., & McCulloch, P. 2007, Ap&SS, 308, 585
Douchin, F., & Haensel, P. 2001, A&A, 380, 151
Drago, M., Klimenko, S., Lazzaro, C., et al. 2021, SoftX, 14, 100678
Dreissigacker, C., Prix, R., & Wette, K. 2018, PhRvD, 98, 084058
Dunn, L., Melatos, A., Espinoza, C. M., Antonopoulou, D., & Dodson, R. 2023, MNRAS, 522, 5469
Dupuis, R. J., & Woan, G. 2005, PhRvD, 72, 102002
Echeverria, F. 1989, PhRvD, 40, 3194
Edwards, R. T., Hobbs, G. B., & Manchester, R. N. 2006, MNRAS, 372, 1549
Espinoza, C. M., Antonopoulou, D., Dodson, R., Stepanova, M., & Scherer, A. 2021, A&A, 649, C2
Espinoza, C. M., Lyne, A. G., Stappers, B. W., & Kramer, M. 2011, MNRAS, 414, 1679
Finn, L. S. 1992, PhRvD, 46, 5236
Fuentes, J. R., Espinoza, C. M., Reisenegger, A., et al. 2017, A&A, 608, A131
Ganapathy, D., Jia, W., Nakano, M., et al. 2023, PhRvX, 13, 041021
Gancio, G., Lousto, C. O., Combi, L., et al. 2020, A&A, 633, A84
Glampedakis, K., & Gualtieri, L. 2018, ASSL, 457, 673
Goetz, E., & Riles, K. 2024, Segments used for creating standard SFTs in O4 data LIGO-T2400058-v3, LIGO Laboratory https://dcc.ligo.org/T2400058-v3/public
Harris, C. R., Millman, K. J., van der Walt, S. J., et al. 2020, Natur, 585, 357
Haskell, B. 2018, IAUS, 337, 203
Haskell, B., & Jones, D. I. 2024, APh, 157, 102921
Haskell, B., & Melatos, A. 2015, IJMPD, 24, 1530008
Ho, W. C. G., Jones, D. I., Andersson, N., & Espinoza, C. M. 2020, PhRvD, 101, 103009
Hobbs, G. B., Edwards, R. T., & Manchester, R. N. 2006, MNRAS, 369, 655
Hotan, A. W., van Straten, W., & Manchester, R. N. 2004, PASA, 21, 302
Hunter, J. D. 2007, CSE, 9, 90
Jaranowski, P., & Królak, A. 2010, CQGra, 27, 194015
Jaranowski, P., Królak, A., & Schutz, B. F. 1998, PhRvD, 58, 063001
Jia, W., Xu, V., Kuns, K., et al. 2024, Sci, 385, 1318
Johnson-McDaniel, N. K., & Owen, B. J. 2013, PhRvD, 88, 044004
Jones, D. I. 2010, MNRAS, 402, 2503
Jones, D. I., & Andersson, N. 2001, MNRAS, 324, 811
Jones, D. I., & Andersson, N. 2002, MNRAS, 331, 203
Keer, L., & Jones, D. I. 2015, MNRAS, 446, 865
Keitel, D., & Ashton, G. 2018, CQGra, 35, 205003
Keitel, D., Singh, N., & Ferrer, M.-A. 2025, tCWip - transient continuous-wave investigation pipeline v0.5.5 , doi:10.5281/zenodo.17989858
Keitel, D., Tenorio, R., Ashton, G., & Prix, R. 2021, JOSS, 6, 3000
Keitel, D., Woan, G., Pitkin, M., et al. 2019, PhRvD, 100, 064058
Klimenko, S., Vedovato, G., Drago, M., et al. 2016, PhRvD, 93, 042004
Kokkotas, K. D., & Schmidt, B. G. 1999, LRR, 2, 2
Lackey, B. D., Nayyar, M., & Owen, B. J. 2006, PhRvD, 73, 024021
Large, M. I., Vaughan, A. E., & Mills, B. Y. 1968, Natur, 220, 340
Lattimer, J. M. 2021, ARNPS, 71, 433
Levin, Y., & van Hoven, M. 2011, MNRAS, 418, 659
Link, B., Epstein, R. I., & Lattimer, J. M. 2000, ASSL, 254, 117
Link, B., Epstein, R. I., & van Riper, K. A. 1992, Natur, 359, 616
Lopez, D., Tiwari, S., Drago, M., et al. 2022, PhRvD, 106, 103037
Lopez Armengol, F. G., Lousto, C. O., del Palacio, S., et al. 2019, ATel, 12482, 1
Lousto, C. O., Missel, R., Zubieta, E., et al. 2024, RMxAC, 56, 134
LVK 2025, LVK Algorithm Library - LALSuite, Free software (GPL), doi:10.7935/GT1W-FZ16
Macleod, D. M., Areeda, J. S., Coughlin, S. B., Massinger, T. J., & Urban, A. L. 2021, SoftX, 13, 100657
Macquet, A., Bizouard, M. A., Christensen, N., & Coughlin, M. 2021, PhRvD, 104, 102005
Martini, A., Miani, A., Drago, M., et al. 2026, CQGra, 43, 055016
Melatos, A., Douglass, J. A., & Simula, T. P. 2015, ApJ, 807, 132
Modafferi, L. M., Moragues, J., & Keitel, D. 2021, JPhCS, 2156, 012079
Modafferi, L. M., Tenorio, R., & Keitel, D. 2023, PhRvD, 108, 023005
Moragues, J., Modafferi, L. M., Tenorio, R., & Keitel, D. 2023, MNRAS, 519, 5161
Necula, V., Klimenko, S., & Mitselmakher, G. 2012, JPhCS, 363, 012032
Ng, C. Y., & Romani, R. W. 2008, ApJ, 673, 411
Palfreyman, J. 2024, ATel, 16615, 1
Palfreyman, J., Dickey, J. M., Hotan, A., Ellingsen, S., & van Straten, W. 2018, Natur, 556, 219
Piccinni, O. J., Astone, P., D'Antonio, S., et al. 2019, CQGra, 36, 015008
Pitkin, M. 2022, JOSS, 7, 4568
Pitkin, M., Isi, M., Veitch, J., & Woan, G. 2017, arXiv:1705.08978
Pradhan, B. K., Chatterjee, D., Lanoye, M., & Jaikumar, P. 2022, PhRvC, 106, 015805
Price-Whelan, A. M., Sipőcz, B. M., Günther, H. M., et al. 2018, AJ, 156, 123
Prix, R. 2007, PhRvD, 75, 023004
Prix, R. 2015, The F-statistic and its implementation in ComputeFStatistic_v2 LIGO-T0900149, LIGO Laboratory https://dcc.ligo.org/T0900149/public
Prix, R., Giampanis, S., & Messenger, C. 2011, PhRvD, 84, 023007
Raaijmakers, G., Greif, S. K., Hebeler, K., et al. 2021, ApJL, 918, L29
Radhakrishnan, V., & Manchester, R. N. 1969, Natur, 222, 228
Ransom, S. 2011, PRESTO: PulsaR Exploration and Search TOolkit, Astrophysics Source Code Library, record ascl, ascl:1107.017
Reichley, P. E., & Downs, G. S. 1969, Natur, 222, 229
Riles, K. 2023, LRR, 26, 3
Riley, T. E., Watts, A. L., Ray, P. S., et al. 2021, ApJL, 918, L27
Robitaille, T. P., Tollerud, E. J., Greenfield, P., et al. 2013, A&A, 558, A33
Singh, A. 2017, PhRvD, 95, 024022
Soni, S., Berger, B. K., Davis, D., et al. 2025, CQGra, 42, 085016
Sosa-Fiscella, V., Zubieta, E., del Palacio, S., et al. 2021, ATel, 14806, 1
Speagle, J. S. 2020, MNRAS, 493, 3132
Sun, L., Goetz, E., Kissel, J. S., et al. 2021, arXiv:2107.00129
Sun, L., Melatos, A., & Lasky, P. D. 2019, PhRvD, 99, 123010
Sun, L., Melatos, A., Suvorova, S., Moran, W., & Evans, R. J. 2018, PhRvD, 97, 043013
Sun, L., Goetz, E., Kissel, J. S., et al. 2020, CQGra, 37, 225008
Sutton, P. J., Jones, G., Chatterji, S., et al. 2010, NJPh, 12, 053034
Suvorova, S., Sun, L., Melatos, A., Moran, W., & Evans, R. J. 2016, PhRvD, 93, 123009
Taylor, J. H., & Weisberg, J. M. 1982, ApJ, 253, 908
Tenorio, R., Modafferi, L. M., Keitel, D., & Sintes, A. M. 2022a, PhRvD, 105, 044029
Tenorio, R., Modafferi, L. M., Keitel, D., & Sintes, A. M. 2022b, distromax v1.1.0, doi:10.5281/zenodo.7331554
Vajente, G., Huang, Y., Isi, M., et al. 2020, PhRvD, 101, 042003
van der Walt, S., Schönberger, J. L., Nunez-Iglesias, J., et al. 2014, PeerJ, 2, e453
van Eysden, C. A., & Melatos, A. 2008, CQGra, 25, 225020
van Straten, W., & Bailes, M. 2011, PASA, 28, 1
Vargas, A. F., & Melatos, A. 2023, MNRAS, 522, 4880

Viets, A., & Wade, M. 2021, Subtracting Narrow-band Noise from LIGO Strain Data in the Third Observing Run LIGO-T2100058-v5, LIGO Laboratory https://dcc.ligo.org/T2100058-v5/public
Viets, A., Wade, M., Urban, A., et al. 2018, CQGra, 35, 095015
Virtanen, P., Gommers, R., Oliphant, T. E., et al. 2020, NatMe, 17, 261
Viterbi, A. 1967, ITIT, 13, 260
Wade, M., Betzwieser, J., Bhattacharjee, D., et al. 2025, CQGra, 42, 215016
Warszawski, L., & Melatos, A. 2012, MNRAS, 423, 2058
Was, M., Bizouard, M.-A., Brisson, V., et al. 2010, CQGra, 27, 015005
Was, M., Sutton, P. J., Jones, G., & Leonor, I. 2012, PhRvD, 86, 022003
Wette, K. 2020, SoftX, 12, 100634
Wette, K. 2023, APh, 153, 102880
Wette, K., Owen, B. J., Allen, B., et al. 2008, CQGra, 25, 235011
Wilson, O. H., & Ho, W. C. G. 2024, PhRvD, 109, 083006
Wiringa, R. B., Fiks, V., & Fabrocini, A. 1988, PhRvC, 38, 1010
Yagi, K., & Yunes, N. 2017, PhR, 681, 1
Yim, G., & Jones, D. I. 2020, MNRAS, 498, 3138
Yim, G., & Jones, D. I. 2023, MNRAS, 518, 4322
Yim, G., Shao, L., & Xu, R. 2024, MNRAS, 532, 3893
Yu, M., Manchester, R. N., Hobbs, G., et al. 2013, MNRAS, 429, 688
Zhou, S., Gügercinoğlu, E., Yuan, J., Ge, M., & Yu, C. 2022, Univ, 8, 641
Zimmermann, M., & Szedenits, E. 1979, PhRvD, 20, 351
Zubieta, E., Furlan, S. B. A., Palacio, S. d., et al. 2024a, ATel, 16608, 1
Zubieta, E., García, F., del Palacio, S., et al. 2024b, A&A, 689, A191
Zubieta, E., Missel, R., Araujo Furlan, S. B., et al. 2025, A&A, 698, A72
Zubieta, E., Missel, R., Sosa Fiscella, V., et al. 2023, MNRAS, 521, 4504